Biomass Conversion and Biorefinery (2019) 9:129–182
https://doi.org/10.1007/s13399-019-00370-z

REVIEW ARTICLE

Review on modelling approaches based on computational fluid dynamics for biomass combustion systems

Focus on fixed bed and moving grate systems

Andrea Dernbecher[1] · **Alba Dieguez-Alonso**[2] · **Andreas Ortwein**[3] · **Fouzi Tabet**[1]

Received: 24 July 2018 / Revised: 20 December 2018 / Accepted: 11 January 2019 / Published online: 25 February 2019

Abstract

Biomass combustion is an important pathway of energy generation from renewable resources. Even though biomass combustion is an established conversion process, there is a high potential for further optimization of the used technologies. In particular, the advantage of numerical methods for the improvement of biomass combustion systems is not used to its full extent, because the simulation of these complex systems requires various sub-models for the thermo-chemical conversion of the biomass and sufficient computational resources for the combustion simulation. However, simulations are a valuable tool to enhance the design and operating conditions of biomass combustion systems with regard to high efficiency, low emissions and high flexibility. In addition, comparison of experimental and numerical results leads to a better understanding of the processes involved in biomass combustion. The present study gives a comprehensive overview of simulations of biomass combustion systems based on computational fluid dynamics that are available in the literature. It focusses on systems with fixed bed and covers various technologies (moving bed, pellet boilers, wood log stoves) as well as a wide range of sizes from laboratory reactors to industry scale. Besides woody biomass, also alternative fuels such as straw or municipal solid waste are considered. All relevant sub-models for the thermo-chemical conversion of the fuel on the one hand and for the gas-phase combustion on the other hand are discussed in detail. The recent advances in the concerned research fields are described.

Keywords Biomass · Pyrolysis · Gasification · Combustion · Computational fluid dynamics · Modelling

1 Introduction

1.1 Background

Increasing use of renewable energy is considered to be a key measure towards limiting global warming to 2 °C. While wind and solar energy plants are providing power at relatively low operational costs but with limited reliability, bioenergy can be used for flexible heat, system stabilizing and power provision [1–3].

For dry solid biomass with water content below 50 wt%, conversion to power is usually conducted via thermo-chemical conversion. The main conversion processes include pyrolysis, gasification, combustion and hydrothermal processes [4]. Combustion of solid biomass is an established conversion process with high potential for flexible power generation [5, 6].

Traditionally, the most commonly used solid biomass is wood. It is expected that the use of other types of biomass will increase. This will include a diversity of agricultural residues as well as biogenic waste. Additionally, an increase in residues from biomass material use (e.g. in biorefineries) is to be expected. While currently fuel pretreatment is usually limited to drying, chipping, grinding and pelletizing or briquetting, advanced pretreatment technologies like torrefaction or hydrothermal carbonization may play a more important role in the future.

✉ Andrea Dernbecher
andrea.dernbecher@dbfz.de

[1] DBFZ Deutsches Biomasseforschungszentrum gemeinnützige GmbH, Torgauer Straße 116, 04347 Leipzig, Germany

[2] Institute of Energy Engineering, Chair for Energy Process Engineering and Conversion Technologies for Renewable Energies, Technische Universität Berlin, Fasanenstraße 89, 10623 Berlin, Germany

[3] Hochschule Merseburg, Eberhard-Leibnitz-Str. 2, 06217 Merseburg, Germany

Typical technologies for solid biomass combustion include stoves (especially for wood logs), pellet boilers, grate firings, fluidized bed firings and dust firings [7]. For each of these technologies, there are several challenges to be solved for future applications:

- increasing flexibility in terms of start-up, shut-down and load change
- increasing flexibility for different types of biomass
- improving integration into the local and overall energy system
- increasing efficiency
- reducing emissions

1.2 Structure of a CFD-based model

Parallel to experimental investigation, numerical analysis has gained significant importance to improve biomass combustion systems to meet the aforementioned challenges. Computational fluid dynamics (CFD) support a better understanding and an accelerated development of combustion systems. In the fields of mechanic and process engineering, as well as combustion science, computational methods are already widely used for design and development. For instance, CFD is used for optimization of geometries and operating conditions in power plant technology [8], renewable energy [9], agriculture [10] and combustion engines [11, 12]. However, CFD simulations of biomass combustion systems remain a niche application in practice, even though various studies concerning numerical investigations of the combustion of solid fuels (for example [13–16]) are available in the literature. Biomass is a complex fuel with varying compositions and it is a challenge to describe its thermo-chemical decomposition by numerical methods. This is not covered in full extend by commercial CFD tools, and in most cases, they have to be complemented by self-written code for the fuel bed. However, the development of biomass combustion systems can benefit from increasing use of numerical methods, if suitable models are used for the simulation. CFD-based modelling approaches for biomass combustion systems are composed of the following sub-models:

- The *bed model* describes biomass physical, chemical and thermal properties; biomass drying and pyrolysis, as well as char gasification and combustion; and heat and mass transfer phenomena. Depending on the investigated system, bed models can benefit from the coupling of additional sub-models to account for the presence of gas-phase reactions in the fuel bed, particle/bed shrinkage and formation of pollutants. In Section 2, the theoretical background of the most frequently used sub-models in the simulation of thermo-chemical conversion of biomass is given. Special emphasis is placed on pyrolysis mechanisms. Furthermore, a summary of the latest developments in single particle models and a detailed review of bed models are provided in Section 2.
- The *gas-phase simulation* includes gas-phase reaction mechanisms, turbulence and radiation. Of special relevance is the interaction between mixing and combustion kinetics, described in the combustion models. Widely used models and simulation approaches are described in Section 3.
- *Additional models* are used to describe the formation of NO_x, particulate matter, soot and other pollutants. Frequently used additional models are summarized in Section 4.

Since already many modelling approaches for various technologies and types of biomass are available in the literature, this study gives an overview on ongoing research in the field of biomass combustion and CFD with a focus on fixed bed and moving grate combustion. A selection of comprehensive simulations of biomass combustion systems is given in Section 5.

2 Fuel bed modelling

2.1 Modelling the processes involved in thermo-chemical conversion of biomass

Bed models describe the thermo-chemical conversion of the solid biomass in the fuel bed of the fired combustion system. Modelling of the fuel bed is challenging, because biomass is a natural product with heterogeneous properties. Therefore, it is not probable to find an universally applicable approach that can be used for a broad range of biomass types, as well as firing systems. Most existing modelling approaches are developed for particular cases and differ substantially in level of detail. It is important to choose a suitable bed model for the targeted application, since the products of the solid fuel thermo-chemical conversion, which have to be predicted by the bed model, will be part of the input conditions for the gas-phase model. Besides, solid fuel devolatilization and char conversion kinetics have a strong influence on the overall behaviour of the system. A recent review on fuel bed models was published by Kodaei et al. in 2015 [17].

2.1.1 Fuel properties

Fuel properties have a severe impact on combustion behaviour of the biomass firing system. They vary with biomass type, origin, storage and preparation. Additionally, they continuously change during the thermo-chemical conversion process. Fuel properties can be grouped into

physical, chemical and thermal properties [18]. Physical properties are mainly influenced by fuel type and preparation and include bulk density, true density, particle size and porosity. Chemical properties are determined by the origin of the biomass and include elemental composition, content of moisture, cellulose, hemicellulose, lignin, extractives and inorganic species, and heating value. Thermal properties include thermal conductivity, specific heat and emissivity of the biomass. Thermal properties are determined by physical and chemical properties [4, 7, 18, 19].

2.1.2 Heat transfer

Heat transfer in biomass is influenced by the properties of all present materials and phases (bound water, free water, gas and solid). It depends strongly on the type of biomass, stage of thermo-chemical conversion and temperature. Additionally, biomass is anisotropic and the heat conductivity is different along or perpendicular to the fibres [19–21].

In homogeneous heat transfer models (thermal equilibrium), it is assumed that heat transfer can be described based on lumped properties for the biomass. The temperature of all phases is considered uniform. The overall thermal conductivity of biomass is calculated from conductivity through cell walls and gas phase, convection and radiation in the pores. Parameters for calculation (density of the solid ρ_s, true density ρ_0, porosity ε, thermal conductivity λ and heat capacity c_p) can be found in the literature for frequently used biomasses [19, 20, 22, 23]. The resulting thermal conductivity is in the range of $\lambda = 0.1$ W/(km) to $\lambda = 0.5$ W/(km) [21].

In many bed modelling approaches, heterogeneous heat transfer (thermal non-equilibrium) is assumed. In this case, temperatures of gaseous and solid phases are not equal and separate conservation equations for each phase and an additional equation for heat transfer between phases are necessary (examples: [24–26]).

For the simulation of thermo-chemical conversion of single biomass particles or fuel beds, which are composed of biomass particles, it has to be decided if the particles should be modelled as thermally thin or thick. Small particles are considered to be thermally thin. In this case, the temperature gradient inside the particle is neglected and evaporation, pyrolysis and char combustion are considered to occur consecutively. This assumption is not valid for large biomass particles, where temperature gradients due to heat transport, heat of reaction and enthalpy of phase changes have to be taken into account. To estimate whether the isothermal approach is applicable or not, the Biot Bi number is used [27, 28]:

$$Bi = \frac{h_{rad} l_p}{\lambda} \tag{1}$$

where l_p is the characteristic length of the particle, λ is the thermal conductivity of the biomass and h_{rad} is the heat transfer coefficient from radiation. A biomass particle with Biot number $Bi < 0.2$ can be assumed to be thermally thin. For larger particles, inner-particle heat transfer has to be taken into account and the different conversion stages can overlap [27, 28].

2.1.3 Drying

The first step of thermo-chemical conversion of biomass is drying. In virgin biomass, water is present in the form of liquid water and water vapour in the pores as well as bound water in the solid structure [29]. The moisture evaporates when biomass is introduced to a dry environment and temperature increases. The process is determined by transport of heat, momentum and mass through biomass [30]. Additionally, recondensation of water vapour in cooler regions can be observed.

To describe drying in simulation of biomass conversion, the evaporation rate of moisture is modelled. Three approaches are widely used in the literature: kinetic rate, thermal and equilibrium models [31, 32].

Kinetic rate models describe drying as the reaction of virgin biomass reacting to dry biomass and water vapour (biomass → dry biomass + water). The evaporation rate $\dot{\omega}_{evp}$ is then described by an Arrhenius approach (2) [33]:

$$\dot{\omega}_{evp} = A \cdot exp\left(-\frac{E_a}{RT}\right) \rho_s w_w \tag{2}$$

where T is the temperature in Kelvin, E_a is the activation energy, R is the universal gas constant, A is the pre-exponential factor, ρ_S is the density of the solid and w_w is the current mass fraction of water. The function provides the maximum evaporation rate approximately at the boiling temperature of water. This model can be found in several publications [33–37], since it is easy to implement and has a high computational stability in comparison to the thermal approach. In the kinetic approach, the evaporation rate increases slowly with the temperature. In this way, it avoids abrupt changes and the possibility of overshooting in the modelled system. However, E_a and A have to be determined experimentally and are not transferable to other systems, which limits the applicability of this model.

For the calculation of the evaporation rate with the thermal approach, the process is considered to be thermally controlled. It is based on the assumption that drying starts when the temperature in a moist zone reaches evaporation temperature. All absorbed energy is then used for evaporation and temperature stays constant until drying in this region is completed. In thermally thick particles, this leads to a drying front, which moves through the particle. Pyrolysis starts when the moisture is evaporated. The

thermal approach is widely used [38–40]. One possibility to define the evaporation rate was presented by Peters et al. [40]:

$$\dot{\omega}_{evp}(r) = 0 \qquad \text{for } T_s < T_{evp} \qquad (3)$$

$$\dot{\omega}_{evp}(r) = \frac{\left(T_g - T_{evp}\right)\rho_s c_p}{H_{evp}\delta t} \qquad \text{for } T_s \geq T_{evp} \qquad (4)$$

in which c_p is the heat capacity of dry biomass, H_{evp} is the evaporation enthalpy, δt is the time step and T_g and T_s are the temperatures of the gas phase and the solid phase, respectively. Since $\dot{\omega}_{evp}$ rises abruptly when the boiling temperature T_{evp} = 100°C is reached, this approach may lead to computational instabilities.

Another possibility to model evaporation is the equilibrium approach, especially for temperatures below the boiling point of water [31]. The driving concentration gradient of moisture on the biomass surface and moisture in the surrounding air is taken into consideration (as in Eq. 5). For this reason, the model is also called diffusion model. It is the only approach, which includes evaporation and recondensation [32]. Examples for the application of the model can be found at Zhou et al. [41] or Wurzenberger et al. [42].

A combination of both, diffusion model and thermal approach, is used to cover a broad temperature range. The diffusion model is used for temperatures below the boiling point of water and the thermal approach for temperatures equal or above [43]. Equations 5 to 7 give an example for this approach (according to [44, 45]).

$$\dot{\omega}_{evp} = S_a h_s (c_{w,s} - c_{w,g}) \qquad \text{for } T_s < T_{evp} \qquad (5)$$

$$\dot{\omega}_{evp} = \frac{Q_{cr}}{H_{evp}} \qquad \text{for } T_s \geq T_{evp} \qquad (6)$$

$$Q_{cr} = S_a \left(k_s (T_g - T_s) + \varepsilon_b \sigma_b (T_{env}^4 - T_s^4)\right) \qquad (7)$$

In this set of equations, S_a is the surface area, h_s is the mass transfer coefficient between the solid surface and gas phase, $c_{w,s}$ and $c_{w,g}$ are the concentration of water at the solid surface and in the gaseous phase, Q_{cr} is the heat transferred by convection and radiation, k_s is the convective heat transfer coefficient, ε_b is the bed porosity, σ_b is the Stefan-Boltzmann constant and T_{env} is the temperature of the environment.

2.1.4 Pyrolysis

Pyrolysis is the thermo-chemical decomposition of biomass, usually in the absence of externally supplied oxygen, with the objective of producing either liquid (bio-oil) or solid (charcoal) biofuels [46, 47]. For the former, fast pyrolysis is the most appropriate process, with liquid yields maximization [48], while for the latter, slow pyrolysis is best fitted [49]. Slow pyrolysis is also the process mainly used for biochar production. Moreover, pyrolysis is a key stage in other thermo-chemical conversion processes, such as gasification and combustion [50, 51]. In these processes, the pyrolysis conversion step influences the yields and composition of the volatile fraction, as well as char yields and reactivity, affecting therefore the global process performance [50]. Hence, a deep understanding of the pyrolysis mechanism and its appropriate kinetic description is fundamental to evaluate feasibility, design, scale up, control and optimization of industrial thermo-chemical conversion processes [47, 51–53]. However, this is not an easy task due to the complexity of the involved chemical reactions, their interaction with transport phenomena and the high heterogeneity of biomass feedstock [46, 47, 54–56].

The products of pyrolysis are lumped in:

- *Solid fraction or char.* Its yield is maximized with low conversion temperatures, low heating rates, higher pressure (e.g. atmospheric pressure vs. vacuum) and bigger particle size (thermally thick particles), i.e. those conditions leading to higher residence time of the produced volatiles in the solid matrix [49]. This enhances the presence of heterogeneous secondary reactions and the formation of secondary char [49, 57, 58]. Higher lignin, inorganic species and moisture content also increase the solid fraction yields [49]. However, as important as the yields are the chemical composition and chemical and physical structure of the char, influencing char reactivity [50, 58].
- *Liquid fraction or condensable volatiles at ambient temperature.* Maximization of the liquid fraction yield is achieved through high heating rates, low residence time of volatiles in the reaction zone (e.g. < 2 s) and medium temperatures around 500 °C [48, 59]. Volatile products from pyrolysis consist of a very complex mixture of organic and inorganic compounds. The organic fraction can be classified, according to Evans and Milne [60], in primary oxygenates, secondary hydrocarbons and tertiary compounds. Primary oxygenates are formed by acids, sugars, alcohols, ketones, aldehydes, phenols, guaiacols, syringols, furans and other mixed oxygenates [61]. Tertiary volatiles include polyaromatic compounds (PAC) and BTXs (benzene, toluene, xylene) [60]. Secondary volatiles are the compounds in between, including also potentially BTXs, as well as phenolics, furans and heterocyclic compounds [61]. Besides, water would be also included in this fraction. Other classifications, such as the one offered by Anca-Couce [46] in his detailed pyrolysis review, grouped the liquid fraction components in water vapour, carbonyls and alcohols, heterocyclics, sugars, phenolics, BTXs and PAH (polycyclic aromatic hydrocarbons).
- *Gas fraction*, including permanent gases, light hydrocarbons and minor inorganic species, such as NH_3 [46].

In the last decades, plenty of research has been done in the field to better understand and kinetically describe the pyrolysis mechanism. For this purpose, lignocellulosic biomass can be seen as only one component or as a combination of several components, usually cellulose, hemicellulose and lignin [30, 47, 62], but also extractives and inorganic species.

For the sake of clarity in the present review, pyrolysis mechanisms are classified in:

- One-component single reaction mechanism
- Multi-component parallel single reaction mechanism
- One-component competitive mechanism
- Detailed mechanism

One-component single reaction mechanisms of the form Biomass → Char + Volatiles (Gas and Tar) are the simplest way of understanding biomass decomposition, since it is considered to take place only through one global reaction. This barely qualifies as a mechanism, since it does not provide any knowledge on how this devolatilization may take place. However, due to the number of models based on this approach, it is included in this classification. Antal and Varhegyi [63] reported that the pyrolysis behaviour of pure cellulose with no significant transport limitations (both mass and heat transport) can be described by a single-step, first order model with high activation energy (around 238kJ/mol), as shown in Eq. 8, where α represents the fraction of released volatiles at each time step [63].

$$\frac{-d\alpha}{dt} = A \cdot exp^{\frac{-Ea}{RT}} \cdot (1-\alpha) \tag{8}$$

It is important to take into account that such models can only predict mass loss rate (conversion time) but not product distribution (and composition) depending on process conditions, since it is assumed a fixed ratio between pyrolysis products yields, i.e. volatiles and chars [30, 51, 64]. This approach is often applied to model the solid bed conversion in biomass combustion processes, as shown in Table 1, as well as in Tables 2, 3, 4, 5, and 6, which summarize the solid bed conversion models, although with significant variability in the used kinetic parameters and products yields. A second step for tar cracking in the gas phase can be added, as done for example in [65] and [66] (Table 1), using the kinetic parameters determined by Liden et al. [67] and estimating the composition of the gas produced in secondary cracking reactions based on data from the literature [68]. In Tables 2, 3, 4, 5, and 6, the one-component single reaction mechanism is referred to as *simple one-step* pyrolysis model.

Multi-component parallel single reaction mechanisms, or multi-component devolatilization mechanisms, as named by Di Blasi [47], consist of single devolatilization reactions for each biomass component. They can also predict mass loss rates but not product distribution according to the process conditions [30, 47, 64], as for the one-component global reaction mechanisms. Based on this approach, biomass pyrolysis can be described as the sum of contributions from the devolatilization of each component, considering no interactions between them [46, 47, 63, 64], as it is shown in Eq. 9 [63]. Most often the number of components is three, correspondent to cellulose, hemicellulose and lignin, which are the main macromolecules in biomass. In this case, the term pseudo-component is usually used, instead of component, because the contribution of each of these pseudo-components does not match one-to-one the contribution of the actual macromolecules in the lignocellulosic material [46, 47].

$$\frac{-d\alpha_i}{dt} = A_i exp^{\frac{-Ea_i}{RT}} (1-\alpha_i) \tag{9}$$

The advantage of this approach, in comparison to one-component single reaction mechanisms, is the more accurate description of the biomass devolatilization curves [64]. Gronli et al. [64] could model the devolatilization behaviour of nine different wood species (softwoods and hardwoods) with a five-component parallel reaction mechanism, including two different extractives, cellulose, hemicellulose and lignin, with the same set of activation energies, but varying final product yields and pre-exponential factors. The multi-component parallel single reaction mechanism is referred to in Tables 2, 3, 4, 5, and 6 by naming the components, which are included in the mechanism (for example *cellulose, hemicellulose, lignin*). A variation of the multi-component parallel single reaction mechanisms is the one proposed by Wurzenberger et al. [42]. In this case, the formation of several pyrolysis products is described by independent parallel reactions, while the biomass is treated as a single component (see Table 1).

One-component competitive mechanisms include several competitive reactions leading to the formation of pyrolysis products. As reviewed by Di Blasi [47] and Anca-Couce [46], Shafizadeh and Chin [69] introduced such mechanism, where biomass decomposes through three competitive reactions to combustible volatiles, char and tar (see Fig. 1, mechanism (6)). The latter could further react and contribute to secondary char and combustible volatile formation [69]. The use of such approach should allow in principle the prediction of not only conversion rate but also product yields when coupled with transport phenomena [30, 47]. However, as highlighted by Anca-Couce [46], the use of the kinetic schemes available in the literature leads to very different predictions, suggesting that these kinetic parameters are not widely applicable beyond those conditions under which they were determined [46]. Scattering in the kinetic data

has been also highlighted by Di Blasi [47], with activation energy values (applying fast heating rates or isothermal conditions) in the range of 56 to 174 kJ/mol, attributed to the different heating conditions and biomass properties, potentially including heat and mass transport limitations, as well as to the mathematical data processing [46, 47]. This variability is also shown in Table 1. This approach is also widely used in fuel bed models, as it is shown in Tables 2, 3, 4, 5, and 6. The model is referred to as *Shafizadeh and Chin (one-step)* or *Shafizadeh and Chin (two-step)*, when tar cracking is considered in the model.

Competitive mechanisms have been also widely used to describe the pyrolysis behaviour of cellulose, which is the most investigated component in biomass. In Fig. 1, two of the most extended mechanisms to describe the pyrolysis of cellulose are presented: the Broido-Shafizadeh scheme (1) and the scheme proposed by Piskorz et al. [70] (3). The Broido-Shafizadeh mechanism was developed based on the work of Broido and colleagues (e.g. [71, 72]) and Shafizadeh and colleagues (e.g. [73, 74]). According to this scheme, first, a cellulose depolymerization step takes place to form active cellulose, with no mass variation [74]. Then, the active cellulose reacts further through two possible competitive pathways, leading to the formation of char and gases or tarry volatiles. As later highlighted by Varhegyi et al. [75], this mechanism does not account for the presence of transport limitations, enhancing vapour-solid interactions. Mok and Antal [76] proposed later on a detailed mechanism based on competitive reactions in several stages, to account for the presence of transport limitations with varying pressures and flow rates at experimental level.

An important contribution to the understanding of cellulose pyrolysis was done by Piskorz et al. [70]. In his scheme, active cellulose would decompose through two competitive reactions to form sugars (e.g. levoglucosan) or light volatiles and gas. The latter pathway implies the direct formation of light compounds (e.g. hydroxyacetaldehyde) from primary cellulose ring fragmentation [70, 77], possibly catalyzed by alkaline ions [70]. At the same time, depolymerization of cellulose competes with the formation of char at low temperatures, being the latter also enhanced by the presence of alkaline species. The work of Mamleev et al. [78], partly summarized in the detailed mechanism shown in Fig. 1 (mechanism 4), further confirms the need of a catalyst for the ring fragmentation reactions to take place. According to their understanding of cellulose pyrolysis, transglycosylation reactions do not need a catalyst; therefore, they can proceed producing voids in the solid matrix and filling also these voids with tar. Among the compounds in the tar, volatile acids can then catalyze fragmentation reactions. Alkali species can also contribute. Further reactions in the liquid phase occur leading to the formation of light gases or char following dehydration reactions after ring fragmentation [78].

Detailed mechanisms include, therefore, a more comprehensive description of the chemical reactions involved, considering competitive and parallel reactions and taking also into account the presence of secondary reactions, product of interactions between the vapour and the condensed phases. One of the most promising detailed pyrolysis mechanisms available in the literature, including kinetic parameters, is the one proposed by Ranzi et al. [62] (see Fig. 1, mechanism 5) and its further modifications and adaptations (e.g. [79–81], see also Table 2). Even more interesting is the fact that this detailed scheme, with initially 15 reactions and more than 20 volatile compounds, could be applied with no apparent problem to biomass combustion processes (see Table 1). Anca-Couce et al. [82] developed also an adaptation of Ranzi's mechanism [79] to account for heterogeneous secondary reactions. Further advances require a better characterization of product composition, as well as a deeper understanding and description of the influence of biomass composition and transport limitations on the pyrolysis process.

2.1.5 Combustion and gasification of char

In the last step of thermo-chemical conversion of biomass, char is consumed by the heterogeneous gasification and combustion reactions. During gasification, char reacts with CO_2, H_2O and H_2, or with O_2 in an under-stoichiometric reaction. Char combustion is the reaction of char with O_2 to form CO and CO_2. A review paper on biomass char gasification and combustion was published by Di Blasi in 2009 [50].

Depending on the Thiele modulus, reactions of solids on particle scale are described by a shrinking core or by a reacting core approach [107]. The Thiele modulus Th gives a relation of kinetic to diffusion time scale. For reactions with reaction order $n = 1$, it is defined as follows: [108].

$$Th = l_p \sqrt{\frac{k}{D_p r}} \tag{10}$$

in which k is the reaction rate constant, l_p is the characteristic length of particle, D_p is the diffusion coefficient of the particle and r is the hydraulic radius of the pores. If $Th < 1$, a shrinking core regime is found. Heterogeneous reactions happen on the surface and the gaseous reactants do not diffuse into the solid particle. For $Th > 1$ the reacting core regime is defined. In this regime, gaseous reactants diffuse into the particle and volumetric reactions are observed in the solid [107]. In biomass combustion modelling, a reacting core model is

Table 1 Kinetic schemes used to describe pyrolysis in thermo-chemical conversion of biomass in fixed beds. The detailed mechanisms are adapted from Ranzi et al. [80, 81]

Study	Mechanism	Products	Kinetic scheme
Yang et al. 2003 [45]	One-component single reaction		First-order reaction rates
(packed bed combustion)		Influence of pyrolysis heating rate on combustion behaviour	Very fast devolatil.: $A_1 = 5.16 \times 10^6\ s^{-1}$; $E_1 = 84$ kJ/mol [83]
		Products: Char + Volatiles (CO, CO_2, H_2, C_mH_n,...)	Fast devolatil.: $A_2 = 3.4 \times 10^4\ s^{-1}$; $E_2 = 69$ kJ/mol [84]
		no information on the considered products yields is provided	Medium devolatil.: $A_3 = 7.0 \times 10^4\ s^{-1}$; $E_3 = 83$ kJ/mol [85]
			Slow devolatil.: $A_4 = 3.0 \times 10^3\ s^{-1}$; $E_4 = 69$ kJ/mol [28]
			Very slow devolatil.: $A_4 = 2.98 \times 10^3\ s^{-1}$; $E_4 = 73.1$ kJ/mol [86]
Di Blasi 2000 [65]	One-component single reaction (1) + tar cracking (2)	ν_{char}: (I) 0.33; (II) 0.41; (III) 0.33	First-order reaction rates
(downdraft gasification)		ν_{tar}:(I) 0.19; (II) 0.19; (III) 0.2	$A_1 = 1.516 \times 10^3\ s^{-1}$ [87]
		ν_{gas}: (I) 0.48; (II) 0.4; (III) 0.5	$Ep_1 = 105$ kJ/mol [87]
		CO^1: (I) 7.5%; (II) 5.5%; (III) 11%	$A_2 = 4.28 \times 10^6\ s^{-1}$ (tar cracking) [67]
		CO_2^1: (I) 13%; (II) 10.5%; (III) 11%	$Ep_2 = 107$ kJ/mol (tar cracking) [67]
		H_2^1: (I) 1%; (II) 0.02%; (III) 1%	$\Delta H_1 = -420$ kJ/kg [88]
		CH_4^1: (I) 1.5%; (II) 1%; (III) 2%	$\Delta H_2 = 42$ kJ/kg [88]
		H_2O^1: (I) 25%, (II) 23%; (III) 25%	
		CO^2: (I) 9.5%; (II) 9.5%; (III) 13%	
		CO_2^2: (I) 5.7%; (II) 5.7%, (III) 3%	
		CH_4^2: (I) 3.8%; (II) 3.8%; (III) 4%	
		Gas composition values given as wt.% of dry biomass	
		ν_{char}, ν_{tar}, ν_{gas}: stoichiometric coefficients	
		3 sets of experimental data applied	
		(I) data were obtained from 0.5–1 cm wood chips [65]	
		(II) data were obtained from rice husk [65]	
		(III) data used for parametric investigation of pyrolysis products effects on gasification [65]	
		Composition of secondary gas (2) estimated based on literature data [68]	
		Assuming surface T of 850 K	

Table 1 (continued)

Study	Mechanism	Products	Kinetic scheme
Di Blasi 2004 [66] (updraft gasification)	One-component single reaction (1) + tar cracking (2)	Products: Char, Tar, CO, CO_2, H_2, CH_4, H_2O Products yields determined experimentally ν_{tar}: (I) 0.385; (II) 0.420; (III) 0.450; (IV) 0.480 [90] ν_{char}: (I) 0.350; (II) 0.315; (III) 0.285; (IV) 0.255 [90] (I) data obtained with air feed rate of 1.590 kg/h; fuel feed rate of 1.250 kg/h [90] (II) data obtained with air feed rate of 1.760 kg/h; fuel feed rate of 1.560 kg/h [90] (III) data obtained with air feed rate of 2.160 kg/h; fuel feed rate of 1.950 kg/h [90] (IV) data obtained with air feed rate of 2.460 kg/h; fuel feed rate of 2.340 kg/h [90] Composition of secondary gas (2) estimated based on literature data [68] T (maximum external T) in the range 700 – 850 K, depending on the air and fuel feeding rates ratio $\nu^1_{CO} = 0.045$; $\nu^1_{CO_2} = 0.10$; $\nu^1_{CH_4} = 0.003$; $\nu^1_{H_2} = 0.002$; $\nu^1_{H_2O} = 0.115$ [90] $\nu^2_{CO} = 0.70$; $\nu^2_{CO_2} = 0.18$; $\nu^2_{CH_4} = 0.12$ [68] ν: stoichiometric coefficient	First-order reaction rates $k_1 = 1.516 \times 10^3 \exp(-75549/T_s)\ s^{-1}$ [89] $k_2 = 4.26 \times 10^6 \exp(-12919/T_g)\ s^{-1}$ (tar cracking) [67]
Zhou et al. 2005 [41] (fixed bed combustion)	One-component single reaction	Products: Volatiles + Char Released volatile fraction is assumed to equal the volatile content in biomass Volatiles for gas-phase model: 71.65 wt.% tar ($CH_{1.84}O_{0.96}$) + 28.35 wt. % gas [91] Gas: 63 wt.% CO_2, 28.8 wt.% CO; 3.5 wt.% CH_4, 3.5 wt.% C_mH_n, 1.2 wt.% H_2 [91]	First-order reaction rate $k_{vol} = 1.56 \times 10^{10} \exp(-16600/T_s)\ s^{-1}$

Table 1 (continued)

Study	Mechanism	Products	Kinetic scheme
Galgano et al. 2006 [92] (particle combustion)	One-component single reaction	Products: Volatiles + Char Volatile fraction: $\nu_{volatiles}$ = 0.8 (stoichiometric coefficient) [93] Volatiles for gas-phase model: Y_{CH_4} = 0.062; Y_{CO} = 0.383; Y_{CO_2} = 0.237; Y_{H_2} = 0.006; Y_{H_2O} = 0.312, with Y being the mass fraction. Tars are assumed to decompose in heterogeneous secondary reactions forming CO_2, CO and CH_4 [68, 95]	First-order reaction rate $A_1 = 4.37 \times 10^6$ m s^{-1} [93]; E_1 = 143 kJ/mol [94] ΔH_1 = 430 kJ/kg [93]
Shin and Choi 2000 [96] (fixed bed combustion)	One-component competitive reactions	Products: Char and Volatiles	First-order reaction rates $k_1 = 5.16 \times 10^6 \exp(-10700/T_b)$ (volatiles formation) $k_2 = 2.66 \times 10^{10} \exp(-12800/T_b)$ (char formation)
Porteiro et al. 2006 [38] Porteiro et al. 2007 [98] Porteiro et al. 2009 [99] (particle and fixed bed (boiler) combustion)	One-component competitive reactions	Products: Char, Tar and Gas Species for gas-phase model: CO, CO_2, H_2, H_2O, CH_4, tar (benzene) Species amount determined with elemental species balance and heating value	First-order reaction rates $A_{gas} = 1.44 \times 10^4$ s^{-1}; E_{gas} = 88.6 kJ/mol [97] $A_{tar} = 4.13 \times 10^6$ s^{-1}; E_{tar} = 112.7 kJ/mol [97] $A_{char} = 7.38 \times 10^5$ s^{-1}; E_{char} = 106.5 kJ/mol [97] $\Delta H_{pyrolysis}$ = -610 kJ/kg [100]
Johansson et al. 2007 [101]	One-component competitive reactions	(Products: Char + Tar + Gas) Char yield is assumed to be 25% of dry mass	First-order reaction rates $k_{char} = 1.1 \times 10^7 \exp(-14602/T_s)$ s^{-1} (char formation) [35] $k_{tar} = 2.2 \times 10^8 \exp(-16009/T_s)$ s^{-1} (tar formation) [35] $k_{gas} = 1.3 \times 10^8 \exp(-16875/T_s)$ s^{-1} (tar formation) [35]
Wurzenberger et al. 2002 [42] (moving grate combustion) (particle combustion)	One-component parallel (independent) devolatilization reactions (several products) (1) + tar cracking (2)	Products yields determined experimentally with TGA [102] H_2O [1]: 0.048 kg/kg d.b.	First-order reaction rates $A_{H_2O} = 3.68 \times 10^{13}$ s^{-1}; E_{H_2O} = 149.5 kJ/mol [102]

Table 1 (continued)

Study	Mechanism	Products	Kinetic scheme
		CO_2^1: 0.0724 kg/kg d.b.	A_{CO_2} = 5.23 x 10^9 s^{-1}; E_{CO_2} = 105.0 kJ/mol [102]
		CO^1: 0.0506 kg/kg d.b.	A_{CO} = 9.00 x 10^9 s^{-1}; E_{CO} = 111.0 kJ/mol [102]
		H_2^1: 0.0060 kg/kg d.b	A_{H_2} = 4.73 x 10^4 s^{-1}; E_{H_2} = 92.5 kJ/mol [102]
		CH_4^1: 0.0106 kg/kg d.b	A_{CH_4} = 1.09 x 10^5 s^{-1}; E_{CH_4} = 71.3 kJ/mol [102]
		tar^1: 0.6340 kg/kg d.b	A_{tar} = 2.09 x 10^{10} s^{-1}; E_{tar} = 112.7 kJ/mol [102]
		$char^1$: rest	
		ν^2_{CO} = 0.78 x 0.72222 (tar cracking) [68, 103]	
		$\nu^2_{H_2}$ = 0.78 x 0.02222 (tar cracking) [68, 103]	
		$\nu^2_{CO_2}$ = 0.78 x 0.14222 (tar cracking) [68, 103]	$A_2 = 10^{4.98}$ s^{-1}; E_2 = 93.37 kJ/mol [68]
		$\nu^2_{CH_4}$ = 0.78 x 0.11334 (tar cracking) [68, 103]	
		$\nu^2_{tar_{inert}}$ = 0.22 (tar cracking) [68, 103]	
		ν is here the mass specific coefficient	
		$\nu^2_{H_2}$ = 0.78 x 0.02222 (tar cracking) [68, 103]	
		$\nu^2_{CO_2}$ = 0.78 x 0.14222 (tar cracking) [68, 103]	
		$\nu^2_{CH_4}$ = 0.78 x 0.11334 (tar cracking) [68, 103]	
		$\nu^2_{tar_{inert}}$ = 0.22 (tar cracking) [68, 103]	
		ν is here the mass specific coefficient	
(particle combustion)	Multi-component parallel single reactions	Products: Volatiles (90 wt.% d.b.) + Char and Ash (10 wt.% d.b.) (proximate analysis)	First-order reactions
	Hemicellulose, cellulose, lignin	Volatiles for gas phase (combustion) model: CO, CO_2, H_2O, H_2, light and heavy hydrocarbons (tar)	A_{hemi} = 2.527 x 10^{11} s^{-1}; E_{hemi} = 147 kJ/mol [104]
Mehrabian et al. 2012 [31]	a = mass fraction of biomass component	Light and heavy hydrocarbons (tar) lumped as CH_4 for combustion model	A_{cel} = 1.379 x 10^{14} s^{-1}; E_{cel} = 193 kJ/mol [104]

Table 1 (continued)

Study	Mechanism	Products	Kinetic scheme
	a_{hemi} = 0.26; a_{cel} = 0.64; a_{lig} = 0.10	Mass fraction of each species determined by closure of elemental and energy balances Homogeneous reaction in particle pores neglected	A_{lig} = 2.202 x 10^{12} s^{-1}; E_{lig} = 181 kJ/mol [104]
Mehrabian et al. 2014 [105] (packed bed combustion)	Multi-component parallel single reactions	Products: Volatiles + Char	First-order reaction rates
	Hemicellulose, cellulose, lignin	Volatiles for gas-phase (combustion) detailed models: CO, CO_2, CH_4, H_2, H_2O, N_2, C_2H_2, C_2H_4, C_2H_6, CH_2O	A_{hemi} = 2.527 x 10^{11} s^{-1}; E_{hemi} = 147 kJ/mol [104]
	a = mass fraction of biomass component	Primary tars are assumed to be already converted into secondary products (mainly CO, CH_4 and C_2 hydrocarbons)	A_{cel} = 1.379 x 10^{14} s^{-1}; E_{cel} = 193 kJ/mol [104]
	a_{hemi} = 0.26; a_{cel} = 0.64; a_{lig} = 0.10	Reaction rate of tar secondary conversion (tar cracking) unknown Elemental species and enthalpy conservation equations used to determine composition of pyrolysis products. Extensive literature review is used to determine the mass ratios of the volatile species, as constraints for the conservation equations. For further details, the reader is directed to [105]	A_{lig} = 2.202 x 10^{12} s^{-1}; E_{lig} = 181 kJ/mol [104]

Table 1 (continued)

Study	Mechanism	Products	Kinetic scheme
Ranzi et al. 2011 [80] (travelling grate combustion)	Detailed pyrolysis mechanism [62]	More than 20 different volatile species [62]	[62, 80]
	CELL→ CELLA		$k_{c1} = 8 \times 10^{13} \exp(-46000/RT)\ s^{-1}$; $\Delta H_{c1} = 107$ kcal/kg
	CELLA→ $5H_2O$ + 6char		$k_{c2} = 8 \times 10^{7} \exp(-32000/RT)\ s^{-1}$; $\Delta H_{c2} = -260$ kcal/kg
	CELLA→ 0.95HAA + 0.25GLYOX + $0.2CH_3CHO$ + 0.25HMFU + $0.2C_3H_6O$ + $0.16CO_2$ + 0.23CO + $0.9H_2O$ + $0.1CH_4$ + 0.61char		$k_{c3} = 1 \times 10^{9} \exp(-30000/RT)\ s^{-1}$; $\Delta H_{c3} = 215$ kcal/kg
	CELLA→ LVG		$k_{c4} = 4T \exp(-10000/RT)\ s^{-1}$; $\Delta H_{c4} = 175$ kcal/kg
	HCE→ 0.4HCE1 + 0.6HCE2		$k_{h1} = 1 \times 10^{10} \exp(-31000/RT)\ s^{-1}$; $\Delta H_{h1} = 131$ kcal/kg
	HCE1→ 0.75G(H_2) + $0.8CO_2$ + 1.4CO + $0.5CH_2O$ + $0.25CH_3OH$ + 0.125EtOH + $0.125H_2O$ + $0.625CH_4$ + $0.25C_2H_4$ + 0.675char		$k_{h2} = 3 \times 10^{9} \exp(-27000/RT)\ s^{-1}$; $\Delta H_{h2} = 107$ kcal/kg
	HCE1→ XYLAN		$k_{h3} = 3T \exp(-11000/RT)\ s^{-1}$; $\Delta H_{h3} = 169$ kcal/kg
	HCE2→ $0.2CO_2$ + $0.5CH_4$ + $0.25C_2H_4$ + 0.8G(CO_2) + 0.8(COH_2) + $0.7CH_2O$ + $0.25CH_3OH$ + 0.125EtOH + $0.125H_2O$ + char		$k_{h4} = 1 \times 10^{10} \exp(-33000/RT)\ s^{-1}$; $\Delta H_{h3} = 62$ kcal/kg
	LIG-C→ $0.35LIG_{CC}$ + 0.1COUMARYL + 0.08PHENOL + $0.41C_2H_4$ + H_2O + $0.495CH_4$ + 0.32CO + G(COH_2) + 5.735char		$k_{l1} = 4 \times 10^{15} \exp(-48500/RT)\ s^{-1}$; $\Delta H_{l1} = 144$ kcal/kg
	LIG_{CC} → 0.3pCOUMARYL + 0.2PHENOL + $0.35C_3H_4O_2$ + $0.7H_2O$ + $0.65CH_4$ + $0.6C_2H_4$ + G(COH_2) + 0.8G(CO) + 6.4char		$k_{l2} = 5 \times 10^{6} \exp(-31500/RT)\ s^{-1}$; $\Delta H_{l2} = 69$ kcal/kg
	LIG-H → LIG_{OH} + C_3H_6O		$k_{l3} = 2 \times 10^{13} \exp(-37500/RT)\ s^{-1}$; $\Delta H_{l3} = 125$ kcal/kg
	LIG-O → LIG_{OH} + CO_2		$k_{l4} = 1 \times 10^{9} \exp(-25500/RT)\ s^{-1}$; $\Delta H_{l4} = 122$ kcal/kg
	LIG_{OH} → LIG + H_2O + CH_3OH + $0.45CH_4$ + $0.2C_2H_4$ + 1.4G(CO) + 0.6G(COH_2) + 0.1G(H_2) + 4.15char		$k_{l5} = 3 \times 10^{8} \exp(-30000/RT)\ s^{-1}$; $\Delta H_{l5} = 24$ kcal/kg
	LIG → H_2O + $0.5CO$ + $0.2CH_2O$ + $0.4CH_3OH$ + $0.2CH_3CHO$ + $0.2C_3H_6O$ + $0.6CH_4$ + $0.65C_2H_4$ + G(CO) + 0.5G(COH_2) + 5.5char		$k_{l6} = 1.2 \times 10^{9} \exp(-30000/RT)\ s^{-1}$; $\Delta H_{l6} = -50$ kcal/kg
	LIG → FE2MACR		$k_{l7} = 8T \exp(-12000/RT)\ s^{-1}$; $\Delta H_{l7} = 138$ kcal/kg
	CELL: cellulose; CELLA: active cellulose, HAA: hydroxyl-acetaldehyde; LVG: levoglucosan; GLYOX: glyoxal;		
	HMFU: 5-hydroxymethyl-furfural; HCE: hemicellulose; HCE1: active hemicellulose 1; HCE2: active hemicellulose 2;		
	G(H_2), G(CO), G(COH_2) species trapped in the solid phase and progressively released to the gas phase [62]		

Table 1 (continued)

Study	Mechanism	Products	Kinetic scheme
Ranzi et al. 2014 [81]	Detailed mechanism further adapted from [62, 80]		[62, 80, 81]
(particle and reactor level combustion)	Further adaptation and extension based on validation with experimental data and other literature		
	CELL→ CELLA		$k_{c1} = 4 \times 10^{13} \exp(-45000/RT)\ s^{-1}$; $\Delta H_{c1} = 0$ kJ/kg
	CELLA→ $5H_2O$ + 6char		$k_{c2} = 4 \times 10^{7} \exp(-31000/RT)\ s^{-1}$; $\Delta H_{c2} = -1913$ kJ/kg
	CELLA→ 0.8HAA + 0.2GLYOX + $0.1C_2H_4O$ + 0.25HMFU + $0.3C_3H_6O$ + $0.21CO_2$ + $0.1H_2$ + $0.4CH_2O$ + $0.16CO$ + $0.83H_2O$ + $0.1CH_4$ + 0.02HCOOH + 0.61char		$k_{c3} = 0.5 \times 10^{9} \exp(-29000/RT)\ s^{-1}$; $\Delta H_{c3} = 620$ kJ/kg
	CELLA→ LVG		$k_{c4} = 1.8T \exp(-10000/RT)\ s^{-1}$; $\Delta H_{c4} = 364$ kJ/kg
	HCE→ 0.4HCE1 + 0.6HCE2		$k_{h1} = 0.33 \times 10^{10} \exp(-31000/RT)\ s^{-1}$; $\Delta H_{h1} = 100$ kJ/kg
	HCE1→ $0.025H_2O$ + $0.5CO_2$ + 0.025HCOOH + 0.5CO + $0.8CH_2O$ + $0.125C_2H_5OH$ + $0.1CH_3OH$ + $0.25C_2H_4$ + $0.125G(H_2)$ + $0.275G(CO_2)$ + $0.4G(COH_2)$ + $0.45G(CH_3OH)$ + $0.325G(CH_4)$ + 0.875char		$k_{h2} = 1 \times 10^{9} \exp(-32000/RT)\ s^{-1}$; $\Delta H_{h2} = -92$ kJ/kg
	HCE1→ $0.25H_2O$ + $0.5CO_2$ + 0.05HCOOH + 0.3CO + 0.15G(CO) + $0.25G(CO_2)$ + $1.7G(COH_2)$ + $0.625G(CH_4)$ + $0.375G(C_2H_4)$ + 0.675char		$k_{h2*} = 0.5T \exp(-8000/RT)\ s^{-1}$; $\Delta H_{h2*} = -1860$ kJ/kg
	HCE1→ XYLAN		$k_{h3} = 0.9T \exp(-11000/RT)\ s^{-1}$; $\Delta H_{h3} = 588$ kJ/kg
	HCE2→ $0.2H_2O$ + 0.175CO + $0.275CO_2$ + $0.5CH_2O$ + $0.1C_2H_5OH$ + 0.2HAA + 0.025HCOOH + $0.25G(CH_4)$ + $0.3G(CH_3OH)$ + $0.275G(C_2H_4)$ + $0.4G(CO_2)$ + $0.925G(COH_2)$ + char		$k_{h4} = 0.33 \times 10^{10} \exp(-33000/RT)\ s^{-1}$; $\Delta H_{h4} = 212$ kJ/kg
	LIG-C→ $0.35LIG_{CC}$ + 0.1COUMARYL + 0.08PHENOL + $0.41C_2H_4$ + H_2O + $0.3CH_2O$ + 0.32CO + $0.7G(COH_2)$ + 0.495G(CH_4) + 5.735char		$k_{l1} = 1.33 \times 10^{15} \exp(-48500/RT)\ s^{-1}$; $\Delta H_{l1} = -490$ kJ/kg
	LIG_{CC} → 0.3COUMARYL + 0.2PHENOL + 0.35HAA + $0.7H_2O$ + 0.4CO + $0.65G(CH_4)$ + $0.6G(C_2H_4)$ + $G(COH_2)$ + 0.4G(CO) + 6.75char		$k_{l2} = 1.6 \times 10^{6} \exp(-31500/RT)\ s^{-1}$; $\Delta H_{l2} = -503$ kJ/kg
	LIG-H → LIG_{OH} + C_3H_6O		$k_{l3} = 0.67 \times 10^{13} \exp(-37500/RT)\ s^{-1}$; $\Delta H_{l3} = 100$ kJ/kg

Table 1 (continued)

Study	Mechanism	Products	Kinetic scheme
	LIG-O → LIG_{OH} + G(CO_2)		k_{l4} = 0.33 x 10^9 exp(-25500/RT) s^{-1}; ΔH_{l4} = 446 kJ/kg
	LIG_{OH} → LIG + 0.9H_2O + 0.15G(H_2) + 0.1CH_4 + 0.5CH_3OH + 0.5G(CH_3OH) + 0.05CO_2 + 0.3CO + G(CO) +		k_{l5} = 0.5 x 10^8 exp(-30000/RT) s^{-1}; ΔH_{l5} = -120 kJ/kg
	0.05HCOOH + 0.6G(COH_2) + 0.35G(CH_4) + 0.2G(C_2H_4) + 4.15char		
	LIG_{OH} → 1.5H_2O + 0.5CO + 0.1CH_4 + 0.5G(H_2) + 1.6G(CO) + 3.9G(COH_2) + 1.65G(CH_4) + 0.3G(C_2H_4) +		k_{l5*} = 33 exp(-15000/RT) s^{-1}; ΔH_{l5*} = -1604 kJ/kg
	0.5G(CH_3OH) + 10.15char		
	LIG → 0.95H_2O + CO + 0.2CH_2O + 0.4CH_3OH + 0.05HCOOH + 0.2C_3H_6O + 0.2CH_4 + 0.45G(CO) + 0.5G(COH_2) +		k_{l6} = 0.4 x 10^9 exp(-30000/RT) s^{-1}; ΔH_{l6} = -470 kJ/kg
	0.65G(C_2H_4) + 0.4G(CH_4) + 0.2C_2H_4O + 5.5char		
	LIG → 0.6H_2O + 0.4CO + 0.2CH_4 + 0.4CH_2O + 0.2G(CO) + 0.4G(CH_4) + 0.5G(C_2H_4) + 0.4G(CH_3OH) +		k_{l6*} = 0.083T exp(-8000/RT) s^{-1}; ΔH_{l6*} = -1663 kJ/kg
	2G(COH_2) + 6char		
	LIG → FE2MACR		k_{l7} = 2.4T exp(-12000/RT) s^{-1}; ΔH_{l7} = 686 kJ/kg
	G(CO_2) → CO_2		k_{l8} = 1 x 10^6 exp(-24000/RT) s^{-1}; ΔH_{l8} = -1814 kJ/kg
	G(CO) → CO		k_{l9} = 0.5 x 10^{13} exp(-50000/RT) s^{-1}; ΔH_{l9} = -2000 kJ/kg
	G(COH_2) → CO + H_2		k_{l10} = 5 x 10^{11} exp(-71000/RT) s^{-1}; ΔH_{l10} = 6778 kJ/kg
	G(H_2) → H_2		k_{l11} = 5 x 10^{11} exp(-75000/RT) s^{-1}; ΔH_{l11} = 0 kJ/kg
	G(CH_4) → CH_4		k_{l12} = 0.5 x 10^{13} exp(-71700/RT) s^{-1}; ΔH_{l12} = 0 kJ/kg
	G(C_2H_4) → C_2H_4		k_{l13} = 0.5 x 10^{13} exp(-71700/RT) s^{-1}; ΔH_{l13} = 0 kJ/kg
	G(CH_3OH) → CH_3OH		k_{l14} = 0.2 x 10^{13} exp(-50000/RT) s^{-1}; ΔH_{l14} = 0 kJ/kg
	Secondary gas-phase reactions of the released volatiles are modelled with a general and a detailed kinetic scheme for pyrolysis		
	and combustion of oxygenated fuels and hydrocarbons [106], available at:		
	www.creckmodeling.chem.polimi.it. [81]		
	Tars and other heavy species are grouped in pseudo-components [81]		

Table 2 One-dimensional separate bed models

Author	Biomass and application	Thermal regime	Evaporation	Pyrolysis	Heterogeneous reactions	Homogeneous reactions	Shrinking
Fatehi and Kaviany 1994 [181]	Spherical wood particles, fixed bed bed reactor, model only	Thermally thin particles, thermal equilibrium, radiation between particles	Not modelled	One-step reaction: $biomass + O_2 \rightarrow ash + gas$, variation of kinetics and heat of reaction, diffusion of O_2 to particle surface considered		Not modelled	Not modelled
Bryden and Ragland 1996 [126]	Wood logs, fixed bed combustor, bed model only	Thermally thick particles, thermal non-equilibrium	Combined drying and pyrolysis rate depending on char consumption and thickness of char layer		O_2, CO_2, H_2O, diffusion considered	Eqs. 34, 37, 40 with $m = 1$, $n = 1.522$, $l = 0.0228$; mixing not considered	Drying, pyrolysis and char consumption: ρ_S and ε const.; d_p (of wood logs) decreases, solid fuel moves downwards with velocity v_s.
Fatehi and Kaviany 1997 [24]	Spherical wood particles, fixed bed reactor, bed model only	Thermally thin particles, thermal non-equilibrium, radiation between particles	Not modelled	One-step reaction: $biomass + O_2 \rightarrow gas$ with different kinetic parameters for volumetric and surface reaction, diffusion of O_2 to particle surface considered		$CH_2O + O_2 \rightarrow H_2O + CO_2$	Not modelled
Cooper and Hallet 2000 [25]	Char particles, stationary overfeed packed bed, fixed bed reactor, bed model only	Thermally thin particles, thermal non-equilibrium	Not modelled	Not modelled	O_2, CO_2, diffusion considered	Eq. 34 mixing not considered	Char consumption: ρ_s and ε_B const; decreasing d_p; solid fuel moves downwards with velocity v_s (Eq. 26)
Di Blasi 2000 [65]	Wood chips, rice husk, down draft gasifier, bed model only	Thermally thin particles, thermal non-equilibrium	Diffusion	Simple one -step + tar cracking	O_2, H_2O, CO_2, diffusion considered, unreacting core shrinking particle model	Eq. 33 with $m = 1$, $n = 4$, Eqs. 34, 37, 38, 40 with $m = 1$, $n = 1.522$, $l = 0.0228$; mixing not considered	Drying and pyrolysis: constant volume and ε, decreasing ρ_s. Char consumption : Constant ρ_s and ε, decreasing d_p and v_s (Eq. 26)
Saastamoinen et al. 2000 [26]	Spruce and pine particles with different sizes, fixed bed reactor, bed model only	Thermally thin and thick particles, thermal non-equilibrium in ignition front	Thermal	Thermally controlled	Not modelled	$CH_{2.26}O_{0.99} + AO_2 \rightarrow B_1CO + B_2CO_2 + B_3H_2O + B_4CH_4$, mixing not considered	Not modelled

Table 2 (continued)

Author	Biomass and application	Thermal regime	Evaporation	Pyrolysis	Heterogeneous reactions	Homogeneous reactions	Shrinking
Shin and Choi 2000 [96]	MSW, substitute for experiments: lauan wood with additives, moving grate, fixed bed reactor, bed model only	Thermally thick particles considered as surface area, thermal non-equilibrium	Diffusion	Shafizadeh and Chin (one-step)	O_2, diffusion considered	Eqs. 33, 34, mixing not considered	Shrinkage of volume based on shrinking factor (shrinking factor depends on mass loss) and decrease of ρ_s during combustion process, additionally: change of external surface area
Kær 2001 [197]	Straw, moving grate	Thermally thin particles, thermal non-equilibrium, heat transfer by radiation between particles is considered	Combined mass transfer and thermal	Simple one-step	O_2, diffusion considered	Eqs. 33, 34	
Ryan and Hallett 2002 [117]	Coke particles, overfeed packed bed, fixed bed reactor, bed model only	Thermally thin particles, thermal non-equilibrium, ash considered in heat and mass transfer	Not modelled	Not modelled	O_2, CO_2, diffusion considered	Eq. 34	Char consumption: ρ_s and d_p const., changing ε, solid continuity based on Eq. 26
Thunman and Leckner 2002 [119]	Wood particles, counter current fixed bed, fixed bed reactor, bed model only	Thermally thick particles, thermal non-equilibrium	Kinetic	Simple one-step	O_2, CO_2, H_2O, diffusion considered	Eq. 33 with $m = 1.16$, $n = 4$, Eqs. 34, 37, 38, 40 with $m = 6$, $n = 6.2$, $l = 0.2$, mixing according to Yang et. al [118]	Shrinking of volume, no solid velocity, individual shrinking factor for each conversion phase, decrease of ρ_s
Wurzenberger et al 2002 [42]	Beech wood particles, fixed bed reactor, bed model only (transient 1D + 1D model)	Thermally thick particles, thermal non-equilibrium in bed model, thermal equilibrium in single particles	Diffusion	Independent reaction rate for the formation of each product, secondary reactions for cracking of tar	O_2, CO_2, H_2O, diffusion in reaction rate	Eqs. 32, 34, 37, 38, mixing not considered	Decrease of ρ_s and ε_p during drying, pyrolysis and char consumption on particle scale. Combustion can lead to $\varepsilon_p = 100\%$, to represent shrinking on bed scale.
Yang et al. 2003 [45, 182]	Pine wood cubes, municipal solid waste, fixed bed, bed model only	Thermally thin particles, thermal non-equilibrium	Combined diffusion and thermal	Simple one-step	O_2, diffusion considered	Eqs. 34, 37, 40, mixing considered	v_s in solid continuity (Eq. 26)

Table 2 (continued)

Author	Biomass and application	Thermal regime	Evaporation	Pyrolysis	Heterogeneous reactions	Homogeneous reactions	Shrinking
Di Blasi 2004 [66]	Wood chips, counter current fixed bed gasifier, bed model only	Thermally thin particles, thermal non-equilibrium	Diffusion	Simple one-step + tar cracking	Char modelled as $CH_\alpha O_\beta$,reactions with O_2, H_2O, CO_2, H_2, diffusion considered	Eq. 33 with $m = 1$, $n = 4$, Eqs. 34, 37, 38, 40 with $m = 1$, $n = 1.522$, $l = 0.0228$, mixing not considered	Pyrolysis: d_p, ε const., ρ_s decreases. Char consumption: ρ_s, ε const., d_p decreases, v_s increases (see Eq. 26)
Huttunen et al. 2004 [111]	Wood chips, moving grate, coupling with gas-phase simulation	Thermally thin particles, thermal equilibrium	Thermal	Not modelled, volatiles are released to gas phase at constant rate	O_2, diffusion controlled	Two-step reaction mechanism with products CO_2 and H_2O, mass balance, mixing not considered	Pyrolysis: const. bed height. Char consumption: d_p decreases and leads to decreasing bed height with ρ_s const.
Thunman and Leckner 2005 [198]	Wood particles, counter current fixed bed reactor, bed model only	Thermally thick particles, thermal non-equilibrium	Kinetic	Shafizadeh and Chin (one-step)	O_2, CO_2, H_2O, diffusion considered	Eqs. 33, 34, 37, 38, 39, mixing considered	Shrinking of volume, no solid velocity, individual shrinking factor for each conversion phase, decrease of ρ_s
Yang et al. 2005 [123]	MSW, pine, fixed bed reactor, bed model only	Thermally thin particles, thermal non-equilibrium	Combined diffusion and thermal	Simple one-step	O_2, diffusion considered	Eqs. 34, 35, 37 mixing considered	Decrease of bed volume in each phase related to conversion rates, v_s in continuity (Eq. 26)
Zhou et al. 2005 [41]	Straw, fixed bed reactor (stationary), bed model only	Thermal non-equilibrium, layer model, thermally thin particles	Diffusion	Simple one-step	O_2, diffusion	Eq. 33 with $m = 1$, $n = 4$ (34), (37), (40) with $m = 1$, $n = 1.84$, $l = 0.96$, mixing according to Zwietering model	Effects of volume reduction neglected, decrease of ρ_s
Galgano et al. 2006 [92, 112]	Single wood log, coupling with gas phase at solid/gas interface	Thermal equilibrium, layer model	Thermal	Simple one-step	O_2, H_2O, CO_2, oxidation reaction diffusion controlled	Homogeneous reactions in wood log not modelled	Not modelled
Johansson et al. 2007 [101, 127]	Spherical wood particles, fixed bed reactor, bed model only	Comparison of thermally thin and thick particles, thermal non-equilibrium ([101])	Kinetic	Shafizadeh and Chin (one-step)	O_2, H_2O, CO_2 H_2 diffusion considered	Eq. 33 with $m = 1.16$, $n = 4$, Eqs. 34, 37, 38, 39 with $m = 6$, $n = 6.2$, $l = 0.2$, mixing considered (comparison of three mixing mechanisms in [127])	Linear shrinking of d_p during all phases with different shrinking factors; ρ_s and ε constant during char combustion, ε constant during whole thermo-chemical conversion process

Table 2 (continued)

Author	Biomass and application	Thermal regime	Evaporation	Pyrolysis	Heterogeneous reactions	Homogeneous reactions	Shrinking
Menghini and Marra 2008 [183]	Single wood log, coupling with gas phase simulation at solid/gas interface	Thermal equilibrium, layer model	Combined reaction for drying and pyrolysis: $C_{42}H_{84}O_{35} + 11.4O_2 \rightarrow 15char + 4.6CH_4 + 16.1CO + 3.7H_2 + 6.3CO_2 + 29.1H_2O$		O_2, H_2O, CO_2, diffusion not considered modelled	Homogeneous reactions in wood log not	Not modelled
Porteiro et al. 2009 [99]	Wood pellets, continuous fed bed, two-way coupling with gas-phase simulation	Thermally thick 1-D particles, perfectly stirred reactor model for separate bed calculations	Thermal	Shafizadeh and Chin (one-step)	O_2, diffusion considered	Not modelled	No shrinking, decrease of ρ_s
Bauer et al. 2010 [184]	Wood chips, moving bed, bed model only, simplified differential equations of bed model can be included in comprehensive simulation	Thermally thin particles, thermal equilibrium	Mass balance of water, evaporation rate depends on moisture content of fuel and position on grate	Rate of thermal decomposition (pyrolysis + char consumption) depends on primary air flow rate, position on grate and plant/operation specifications		Not modelled	Not modelled
Girgis and Hallett 2010 [121]	Wood particles, overfeed packed bed, bed model only	Thermally thin particles, thermal non-equilibrium	Thermal + recondensation	Simple one-step	O_2, CO_2, diffusion considered	Not modelled	Pyrolysis: d_p const, ρ_s decreases; Char consumption: ρ_s const. d_p decreasing (based on Eq. 26)
Ranzi et al. 2014 [81] (same model as in [80])	Wood, spherical particles, fixed bed reactor, coupling with gas phase	Thermally thick	Not modelled particles	Cellulose, hemicellulose, lignin; very detailed mechanism	O_2, H_2O	Not modelled	Change of ρ_s, ε and volume on particle and reactor scale during all phases of thermo-chemical combustion

Table 3 Two-dimensional separate bed models

Author	Biomass and application	Thermal regime	Evaporation	Pyrolysis	Heterogeneous reactions	Homogeneous reactions	Shrinking
Van der Lans et al. 2000 [188]	Straw, moving bed, bed model only	Thermally thin particles, thermal equilibrium	Not modelled	Simple one-step	O_2, diffusion considered	Not modelled	Change of ρ_s
Ryu, Shin and Choi 2002 [186]	Municpal solid waste, moving bed, coupling with gas phase	Thermally thin particles, thermal non-equilibrium	Not specified	Simple one-step	O_2, diffusion considered	Eqs. 34, 37, 39, mixing not considered	Change of ρ_s
Yang et al. 2002 [118]	Municipal solid waste, moving bed, bed model only	Thermally thin particles, thermal non-equilibrium, mixing of fuel particles considered	Combined diffusion and thermal	Simple one-step	O_2, diffusion considered	Eqs. 33, 34 mixing considered	Change of ρ_s, solid velocity v_s, moving boundary
Kær 2005 [189]	Straw, moving grate, walking column, bed model only	Thermally thin particles, thermal non-equilibrium	Combined diffusion and thermal	Simple one-step	O_2, diffusion considered	Oxidation of $CH_{1.6}O_{0.8}$ to CO and CO_2	Change of ρ_s, solid velocity v_s, grid adapted to bed height in each time step
Yang et al. 2005 [128]	Municipal solid waste, fixed bed, bed model only	Thermally thick particles, thermal non-equilibrium, separate meshes for gas and solid phase	Combined diffusion and thermal	Simple one-step	O_2, diffusion considered	Eqs. 34, 35 (with $m = 1$, $n = 4$), Eq. 37, mixing considered	Shrinking factor for particle shrinkage in each phase, 0=no shrinking, 1=linear shrinking, in simulation 0.8 used for each phase (based on Peters 2003)
Yang et al. 2007 [124]	Straw, vibrating grate, two-way coupling with gas-phase simulation	Thermally thin particles, thermal non-equilibrium	Combined diffusion and thermal	Simple one-step, release of NH_3	O_2, diffusion considered, reaction of fuel nitrogen to NO	Eqs. 34, 35 (with $m = 1$, $n = 4$), Eq. 37, mixing considered, reactions of NH_3 to NO and N_2	Volume shrinking and change of ρ_s based on mass loss, v_s similar to Eq. 26
Yang et al. 2007 [125]	Municipal solid waste, moving bed, two-way coupling with gas-phase simulation	Thermally thin particles, thermal non-equilibrium	Combined diffusion and thermal	Simple one-step	O_2, diffusion considered	Eqs. 34, 35, 37, mixing considered	Volume shrinking and change of ρ_s based on mass loss, v_s similar to Eq. 26. 3/6 simulation cases with constant bed height

Table 3 (continued)

Author	Biomass and application	Thermal regime	Evaporation	Pyrolysis	Heterogeneous reactions	Homogeneous reactions	Shrinking
Hermansson and Thunman 2011 [129, 191]	Wood char, moving bed, bed model only	Thermally thick particles, thermal non-equilibrium	Not modelled	Not modelled	O_2, CO_2, H_2O, diffusion considered	Eqs. 34, 37, 38, mixing considered	Decrease of ρ_s, ε and volume on particle and bed scale. Additionally collapsing of fuel bed.
Ranzi et al. 2011 [80]	Spherical wood particles, moving grate, coupling with gas-phase simulation	Thermally thick particles	Not modelled	Cellulose, hemicellulose, lignin; very detailed mechanism	O_2, H_2O	Not modelled	Change of ρ_s, ε and volume on particle and reactor scale during all phases of thermo-chemical combustion
Miljković 2013 [135]	Straw, moving bed, bed model only	Thermally thin particles, thermal non-equilibrium	Lewis' semi empirical method	Simple one-step	O_2, diffusion in reaction rate (based on [199])	Eq. 33 with $m = 1$, $n = 4$, Eqs. 34, 37, 40 with $m = 1$, $n = 1.84$, $l = 0.96$, mixing described as diffusion problem	Moving grid, according to bed shrinkage during pyrolysis and char consumption
Duffy 2013 [136]	Wood pellets, moving bed, bed model only	Thermally thin particles, thermal non-equilibrium	Thermal, overheating of solid is possible to ensure computational stability	Shafizadeh and Chin (one-step)	O_2, CO_2, H_2O, diffusion considered	Eq. 33 with n=1, m=4, Eqs. 34, 37, 38, 40, mixing considered (k-ε-model and EDM)	Decrease of ρ_s, ε and volume on particle and bed scale during all phases of thermo-chemical conversion (based on [129]). Additionally collapsing of fuel bed.

Table 4 Three-dimensional separate bed models

Author	Biomass and application	Thermal regime	Evaporation	Pyrolysis	Heterogeneous reaction	Homogeneous reactions	Shrinking
Saidi 2007 [200]	Cellulose material, tobacco, bed model only	Thermally thin particles, thermal non-equilibrium	Kinetic	Independent reaction rate for the formation of each product	O_2, diffusion considered	Not modelled	Not modelled
Buczyński et al. 2012 [196]	ECORET coal, biomass, fixed bed, bed model only	Thermally thin particles, thermal non-equilibrium	Kinetic	Simple one-step	O_2, CO_2, diffusion not considered, specific surface	$C_{1.05}H_{4.22}O_{0.74}N_{0.076} + 1.21O_2 \rightarrow 1.05CO + 2.11H_2O + 0.038N_2$ $CO + 0.5O_2 \leftrightarrow CO_2$ mixing not considered	
Mehrabian et al. 2014 [105]	Pellets, laboratory scale fixed bed reactor, coupling with gas phase	Thermally thick particles, thermal non-equilibrium	Thermal	Cellulose, hemicellulose, lignin	O_2, CO_2, H_2O, H_2, diffusion considered	GRI2.11, DRM22 and Kilpinen97 mechanisms	Decrease of ρ_s and volume on particle scale during pyrolysis and char consumption, bed shrinks according to particles, particle positions recalculated

often applied for drying and pyrolysis, while a shrinking core approach is used for gasification and combustion of char [65].

In the case of shrinking core regime, the diffusion of the gaseous reactants (O_2, CO_2, H_2O and H_2) to the particle surface has to be taken into account, since either diffusion or reaction kinetics can be the rate-limiting step. A common approach to consider diffusion of gaseous reactands is to introduce an effective rate constant k_{eff}, which considers the kinetic rate constant k_{kin} and the mass transfer coefficient for the transport of gaseous components to the particle surface k_m. The gasification rate is then calculated based on k_{eff}, the particle surface area A_p and the particle density number ν_p. ε_p and V_p are the porosity and the volume of the particle respectively [66, 109].

$$k_{eff} = \frac{1}{\frac{1}{k_m} + \frac{1}{k_{kin}}} \tag{11}$$

$$\dot{\omega}_{gasf} = k_{eff} A_p \nu_p \tag{12}$$

$$\nu_p = \frac{(1-\varepsilon_p)}{V_p} \tag{13}$$

Alternatively, diffusion can be accounted for by inclusion of the specific surface of the particle [110] or the amount of unreacted carbon [42] in the intrinsic reaction rate of the heterogeneous reaction. Some models neglect the influence of the kinetic rate and consider the reaction rate of the combustion reaction to be limited by diffusion only [92, 111, 112].

For most of the bed models, char is considered to be 100% carbon. The oxidation is described by the following equations [34, 43]:

$$C + \frac{1}{\phi} O_2 \rightarrow 2\left(1 - \frac{1}{\phi}\right) CO + \left(\frac{2}{\phi} - 1\right) CO_2 \tag{14}$$

$$\phi = \frac{\frac{1}{r_c}}{\frac{1}{2} + \frac{1}{r_c}} \tag{15}$$

$$r_c = \frac{CO}{CO_2} = \alpha exp\left(-\frac{\beta}{T_s}\right) \tag{16}$$

Factor ϕ expresses the dependency of the CO/CO_2 ratio on the temperature of the solid T_s. There are two sets of values for α and β, which are mainly used in the literature [43]. Yang et al. [45] for example used $\alpha = 2500$ and $\beta = 6420$ based on experiments with graphite and char from coal [113]. For their bed models in straw combustion, Zhou et al. [41] and Miltner et al. [109] used the correlation of Pedersen [114]: $\alpha = 12$ and $\beta = 3300$, determined specifically for biomass combustion. A study with commonly used models to predict the CO/CO_2 ratio during combustion of biomass char was performed by Anca-Couce et al. in 2017 [115]. They came to the conclusion that among the tested models, the approach of Pedersen [114] is best suited for the modelling of combustion of biomass char. However, it was

Table 5 Discrete particle bed models

Author	Biomass and application	Thermal regime regime	Evaporation	Pyrolysis	Heterogeneous reactions	Homogeneous reactions	Shrinking
Bruch 2001 [204]	Wood, spherical particles, heat and mass exchange	Heat conduction through particles, radiation between particles	Thermal	Shafizadeh and Chin (one-step)	O_2, H_2O, CO_2	Eqs. 34, 37, tar cracking	
Peters et al. 2002 [40]	Fir wood spheres, moving grate (TAMARA), bed model only	Thermally thick 1-D particles, thermal non-equilibrium	Thermal vs. kinetic, better results with thermal	Simple one-step	O_2, diffusion considered	Eqs. 34, 37	Modelling approach covers kinetic and transport control for reactions of solids. Depending on rate-limiting process decreasing density or particle size is simulated. Shrinking particles lead to shrinking bed. Results show: Particles shrink mainly during combustion
Bruch et al. 2003 [110]	Beech wood spheres, packed bed, bed model only	Thermally thick 1-D particles, thermal non-equilibrium	Thermal	Simple one-step	O_2, specific surface	Not modelled	Particle Scale: Drying, Pyrolysis: d_p const. Char comb.: decreasing ρ_s and d_p; Packed bed scale: During char combustion: recalculation of distribution of particles with const ε. Leads to shrinking bed.
Simsek et al. 2009 [131]	Municipal solid waste, spherical particles, moving bed, two-way coupling with gas-phase simulation	Thermally thin particles, thermal non-equilibrium	Thermal	Simple one-step	O_2, diffusion considered	Not modelled	Drying, Pyrolysis: const. d_p, decreasing ρ_s, char combustion: const. ρ_s, decreasing d_p
Mehrabian et al. 2010 [205]	Softwood pellets, underfeed stoker, coupling with gas-phase simulation	Thermally thin particles, thermal non-equilibrium	Combined diffusion and thermal	Simple one-step	O_2, diffusion considered	Not modelled	Continuity equation similar to Eq. 26. Shrinking not further specified

Table 5 (continued)

Author	Biomass and application	Thermal regime regime	Evaporation	Pyrolysis	Heterogeneous reactions	Homogeneous reactions	Shrinking
Peters et al. 2010 [206]	Spherical fir wood particles, fixed bed and moving bed, bed model only	Thermally thin particles, thermal non-equilibrium	Not modelled	Not modelled	Not modelled	Not modelled	Not modelled
Peters et al. 2011 [207]	Spherical fir wood particles, moving bed, bed model only	Thermally thin particles, thermal equilibrium	Not specified	Shafizadeh and Chin (one-step)	O_2, CO_2, diffusion considered	Not modelled	Not modelled
Brosch et al. 2011 [208]	Municipal solid waste, spherical particles, moving bed, coupling with gas-phase simulation	Thermally thick particles, thermal non-equilibrium	Thermal	Pyrolysis front (thermal)	O_2, diffusion considered	Not modelled	Not modelled
Peters et al. 2014 [209]	Wood particles, packed bed, bed model only	Thermally thin particles, local thermal equilibrium	Thermal	Not modelled	Not modelled	Not modelled	Not modelled
Mahmoudi et al. 2016 [122]	Wood chips, moving grate, validation with fixed bed reactor, coupling with gas-phase simulation	Thermally thick particles, thermal non-equilibrium	Diffusion	Shafizadeh and Chin (two-step)	O_2, CO_2, H_2O, diffusion considered	Eqs. 32, 34, 37, 39 with $m = 6$, $n = 6.2$, $l = 0.2$	Drying, Pyrolysis: const. d_p, decreasing ρ_s, char combustion: const. ρ_s, decreasing d_p

Table 6 Porous medium bed models

Author	Biomass and application	Thermal regime regime	Evaporation	Pyrolysis	Heterogeneous reactions	Homogeneous reactions	Shrinking
Miltner et al. 2006/2007 [109, 210]	Bales of whole crop maize	Thermally thin particles, thermal non-equilibrium	Kinetic	Cellulose, hemicellulose, lignin	O_2, diffusion considered	Eqs. 33, 34, 37 $NH_3 + O_2 \rightarrow NO + H_2O + 0.5H_2$, $NH_3 + NO \rightarrow N_2 + H_2O + 0.5H_2HCN + O_2 \rightarrow NO + CO + 0.5H_2NH_3 + NO \rightarrow N_2 + CO + 0.5H_2$ no additional equations for mixing	Not modelled/specified
Kurz et al. 2012 [202]	Wood chips, moving grate	Thermally thin particles, thermal non-equilibrium, mixing of particles	Thermal	Simple one-step	O_2, H_2O, CO_2, diffusion considered	Eqs. 33, 34, 37, mixing considered	Continuity equation similar to Eq. 26
Chaney et al. 2012 [43]	Wood pellets, underfeed pellet bed	Thermally thin particles, thermal non-equilibrium	Kinetic	Simple one-step	O_2, no additional equation for diffusion	Eqs. 34, 40 with $m = 1.9316$, $n = 5.7543$, $l = 2.3750$, no additional equation for mixing	Not modelled/specified
Collazo 2012 [211]	Wood pellets, fixed bed	Thermally thin particles, thermal equilibrium, steady state	Depends on fuel consumption rate obtained from experiments	Depends on fuel consumption rate obtained from experiments	O_2, depends on fuel consumption rate obtained from experiments	Not modelled	Not modelled/specified
Collazo 2012 [116]	Wood pellets, fixed bed	Thermally thin particles, thermal non-equilibrium	Thermal+ overheating of solid phase	Shafizadeh and Chin (one-step)	O_2, diffusion considered	Eq. 37	Not modelled/specified
Ström et al. 2013 [130]	Wood	Thermally thick particels, thermal non-equilibrium	Thermal	Shafizadeh and Chin (one-step)	Not modelled	Not modelled	Particle scale: Drying, Pyrolysis: reduction of d_p and ρ_s with shrinking factors (based on [119])

Table 6 (continued)

Author	Biomass and application	Thermal regime regime	Evaporation	Pyrolysis	Heterogeneous reactions	Homogeneous reactions	Shrinking
Gómez et al. 2014/15/16 [132, 134, 141]	Wood pellets	Thermally thin particles, thermal non-equilibrium	Thermal	Shafizadeh and Chin (one-step)	O_2, H_2O, CO_2, diffusion considered	Eq. 33 with $m_1 = 6$, $n_1 = 6$, $m_2 = 1$, $n_2 = 4$, Eq. 34, 37, 38, no additional equations for mixing	[132]: Drying, Pyrolysis: decrease of ρ_s; Char consumption: decrease of ρ_s and ε; [134, 141]: Drying: decrease of ρ_s; Pyrolysis, Char consumption: decrease of ρ_s and ε; Additionally for all: bed compaction
Buczyński et al. 2015 [212] (based on [196])	EKORET coal (biomass also possible but not modelled in this publication)	Thermally thin particles, thermal non-equilibrium	Kinetic	Simple one-step	O_2, CO_2, diffusion not considered specific surface	Eq. 34, $C_{1.05}H_{4.22}O_{0.74}N_{0.0761} + 1.21O_2 \rightarrow 1.05CO + 2.11H_2O + 0.038N_2$ no additional equations for mixing	Not modelled/specified
Gómez et al. 2015/2017 [133, 142]	Wood pellets	Thermally thick particles, thermal non-equilibrium	Thermal	Shafizadeh and Chin (one-step)	O_2, H_2O, CO_2, surface reactions (shrinking core)	Not modelled	Char consumption: intra-particle subgrid is a moving grid, which shrinks; compaction of fuel bed

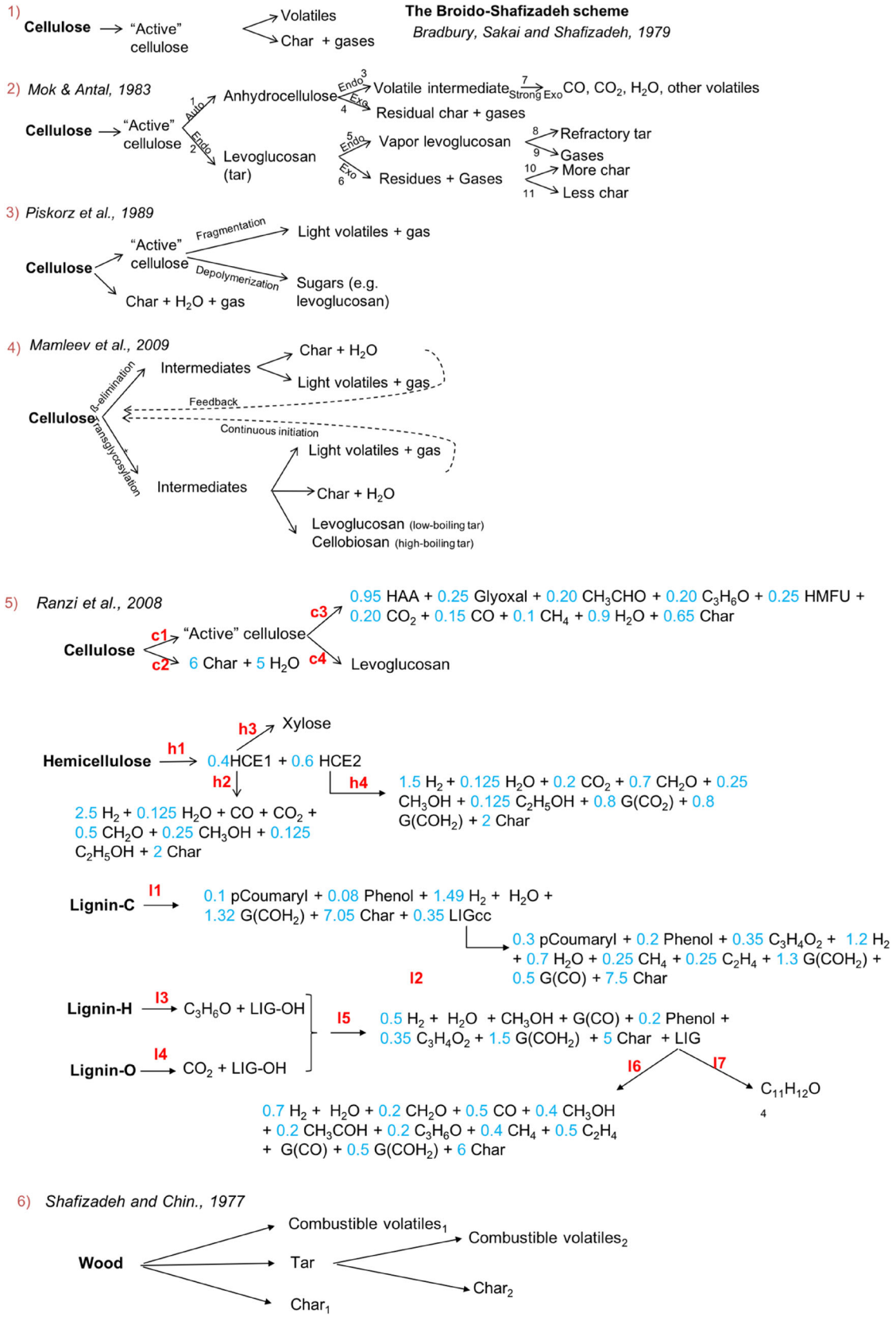

Fig. 1 Several relevant mechanisms for cellulose and wood decomposition. The Broido-Shafizadeh mechanism (1) is adapted from [74], mechanism (2) is adapted from [76], mechanism (3) is adapted from [70], mechanism (4) is adapted from [78], mechanism (5) is adapted from [62] and mechanism (6) is adapted from [69]

determined for a certain feedstock and the applicability to other kinds of biomass char or a different temperature range is limited. Therefore, further investigation of the CO/CO_2 ratio will be necessary, to improve accuracy. The reaction of O_2 with H_2 might compete with heterogeneous reactions of char combustion [34, 38]

Char gasification occurs in addition to char combustion. The following reactions are widely used to model char gasification [34]:

$$C + CO_2 \rightarrow 2CO \quad (17)$$

$$C + H_2O \rightarrow CO + H_2 \quad (18)$$

$$C + 2H_2 \rightarrow CH_4 \quad (19)$$

As char gasification is slower than char combustion, it is often partially or completely neglected in biomass combustion simulations. This can be seen in Tables 2, 3, 4, 5 and 6, where simulation approaches are summarized. Especially, the reaction of carbon with hydrogen (Eq. 19) is slow and thus considered not important for most practical applications [50].

2.1.6 Gas-phase reactions inside the fuel bed

Additionally to drying, pyrolysis and char oxidation reactions, also homogeneous gas-phase reactions can be observed in the fuel bed. Depending on the simulated system and the assumptions made for the bed model, homogeneous gas-phase reactions are described in the modelling approach.

The homogeneous gas-phase reactions include the oxidation of gaseous products from pyrolysis and gasification with oxygen from an external source (e.g. primary air, which flows through the fuel bed) as well as reactions between volatiles from pyrolysis and gasification. The gas-phase reactions are described by single reactions, global reaction mechanisms and detailed reaction mechanisms.

Single reactions describe the complete or partial oxidation of one or more components of the volatile gases. In several bed models, only the oxidation of hydrogen [116], carbon monoxide [25, 117] or both [40] is described. Fatehi et al. [24] used formaldehyde as a representative species for volatile gases and included its oxidation (Eq. 20) in their bed model.

$$CH_2O + O_2 \rightarrow H_2O + CO_2 \quad (20)$$

A reaction to describe the formation of intermediate combustible products was presented by Saastamoinen et al. [26]:

$$CH_{2.26}O_{0.99} + AO_2 \rightarrow B_1CO + B_2CO_2 + B_3H_2O + B_4CH_4 \quad (21)$$

Coefficient A depends on available mass flux of primary air, coefficients B_1 to B_4 are calculated accordingly [26].

Global and detailed reaction mechanisms used for the homogeneous reactions in the fuel bed are the same as for the free board combustion simulation. Details about the mechanisms can be found in Section 3.3. Global reaction mechanisms describe gas-phase combustion with very few overall reactions. In contrast to global reaction mechanisms, detailed mechanisms are composed of elementary reactions, which describe the smallest reaction step in the way they take place on a molecular level [8]. The advantage of global reaction mechanisms is the reduced number of species. Since a separate conservation equation has to be solved for each species in the numerical model, the number of species has direct impact on the computational effort. Therefore, predominantly single reactions or global reaction mechanisms are used in bed models. Only in the bed model presented by Mehrabian et al. in 2014 [105] detailed reaction mechanisms were used.

To predict the reaction rate correctly, not only the reaction kinetics but also mixing of volatiles and oxidizer in the fuel bed have to be considered. The combustion models for homogeneous gas-phase reactions (Section 3.2) are not applicable in the fuel bed, because they are designed for flow in the free board, whereas the fuel bed is considered to be a porous zone. A simplified model (Eq. 22), which is based on the Ergun equation for the pressure drop inside the fuel bed, was used by the groups of Yang [118] and Thunman [119] to describe mixing of volatiles and primary air inside the fuel bed.

$$R_{mix} = 0.83 \left(\frac{150 D_g (1-\varepsilon_b)^{2/3}}{(d^2 \varepsilon_b)} + \frac{1.75 U_g (1-\varepsilon_b)^{1/3}}{d \varepsilon_b} \right) min \left(\frac{C_i}{\Omega_i}, \frac{C_{O_2}}{\Omega_{O_2}} \right) \quad (22)$$

An adapted version of Eq. 22 was used by Johansson et al. in 2007 [101]:

$$R_{mix} = 0.63 \left(\frac{1.75 U_g (1-\varepsilon_b)}{d \varepsilon_b} \right) min(C_i, \Omega_i) \quad (23)$$

in which 0.83 (respectively 0.63) is an empirical mixing-rate constant and the factors 150 and 1.75 are based on the Ergun equation of bed pressure drop. U_g is the superficial velocity of gas, D_g is the molecular diffusion of gas and ε_b is the bed porosity. Ω is the stoichiometric coefficient and C is the molar fraction of the combustible species (index i) or oxygen (index O_2) and d is a length scale of turbulence (assumed equal to the equivalent particle diameter) [119].

Zhou et al. [41] used a different approach to describe mixing of primary air and volatiles, which is based on the Zwietering model. The entrainment of the volatile gases by primary air is described as follows:

$$R_{mix} = \frac{ln(m_{O_2,0}/m_{O_2,\tau_m})}{\tau_m} \quad (24)$$

$$\tau_m = \frac{d_p^2}{2 D_{O_2}} \quad (25)$$

where τ_m is the diffusion time, $m_{O_2,0}$ and m_{O_2,τ_m} are the mass of oxygen at the beginning and end of the diffusion time, D_{O_2} is the oxygen diffusion coefficient and d_p is the particle diameter.

2.1.7 Shrinking

Many bed models include shrinking of the fuel bed, which results from mass loss during drying, pyrolysis and heterogeneous reactions. Depending on the type of bed model and simulated application, shrinking is described on particle or bed scale or a combination of both. The mass loss of biomass can be reflected as decrease of the density of the solid phase, as increase of porosity or decrease of size. If size and porosity of the particle/bed are constant, the decrease of the density of the solid phase corresponds to the reduction of the mass of the solid phase, while the structure of the biomass is not changed. The increase of porosity, while the density of the solid phase and size of the bed/particle are constant, corresponds to the reduction of the volume of the solid phase and a change in the structure. If the size of the bed or particle is reduced without a change of the other properties (solid density, porosity), the conversion of the biomass is limited to its surface. According to Peters [40], shrinking can be described by reduced density (and porosity) in a reacting core regime and by decreasing size in a shrinking core modelling approach (see Section 2.1.5) [107].

A widely used modelling approach is based on the assumption that pyrolysis should be modelled by the reacting core model and char consumption by a shrinking core approach. Consequently, the diameter of fuel particles d_p and height of fuel bed h_b are not reduced during drying and pyrolysis, but density ρ_s decreases and porosity ε increases [120, 121]. Since the porosity ε of a biomass particle or a fuel bed is related to the structure of the biomass, Di Blasi et al. [65, 66] assumed that porosity stays constant during drying and pyrolysis, while the density decreases. Experimental observations, according to which the biomass keeps its structure during drying and pyrolysis, support this approach [65]. Char consumption leads to shrinkage at a particle scale (reduction of d_p) and possibly at a bed scale (reduction of h_b), while density ρ_s and porosity ε_b of the bed are kept constant [25, 65, 111, 122].

For most separate bed models, Eq. 26 [25] or similar formulations are used as continuity equation for the solid phase.

$$\frac{\partial}{\partial t}[(1-\varepsilon_b)\rho_s] + \frac{\partial}{\partial x}(\rho_s v_s) = -S_{sg} \tag{26}$$

Here, ε_b is the porosity of the fuel bed, ρ_s is the density of the solid phase, v_s is the velocity of the solid phase and S_{sg} is the conversion rate of solid to gas. In this continuity equation, the decrease of d_p during char combustion is expressed as increasing velocity of the solid phase v_s, based on the assumption that smaller particles lead to a faster downwards movement of the fuel particles to fill the void spaces. By increasing the number of particles per bed volume, the porosity of the fuel bed is kept constant [25, 65, 66, 117, 121]. Other modelling approaches for separate bed models follow the assumption that the size of particles and bed is only reduced during char consumption, but implement it with different equations [42, 111].

Yang et al. [45, 123–125] described solid mass continuity similar to Eq. 26, but allowed shrinking and change of density ρ_s (and porosity ε) during all phases of thermochemical conversion. Bryden et al. [126] accounted for shrinking in each phase as well. Advanced models enable individual shrinking factors for each step of thermochemical conversion [96, 101, 119, 127–130].

The modelling approach of Peters [40] covered kinetic and transport control for the reactions of the solid phase. Depending on the rate-limiting process, decreasing density (reacting core) or particle size (shrinking particle) was simulated. Their results showed that particle shrinking occurs mainly during combustion. In the bed models of Simsek et al. [131] and Mahmoudi et al. [122], which are based on the discrete particle model (DPM), the assumption of reacting core with decreasing density during pyrolysis and shrinking core with particle shrinkage was followed. The fuel bed shrank according to the particles, due to the discrete particle model.

In the porous medium bed models of Gomez et al. [132–134], which did not account for individual particles in the fuel bed, the reduction of particle size d_p was represented by reduction of porosity of the bed ε_b. The porous medium bed model of Miljkovic et al. [135] modelled shrinking of the bed by a moving grid, which followed the bed shrinkage during pyrolysis and char consumption.

Shrinking in real applications is often accompanied by spontaneous collapsing of the fuel bed. In models of Hermansson et al. [129] and Gomez et al. [132–134], the bed model collapsed when a critical porosity was reached in a computational cell. The content (solid fraction) of the cells above the collapsed area was then distributed to neighbouring cells. The structure and behaviour of the fuel bed was described more realistically by including collapsing in the bed model.

2.1.8 Additional models for the fuel bed

Depending on the simulated case, issues beyond the modelling of heat transfer, drying, pyrolysis, gasification and combustion in the fuel bed may arise. For these issues, additional models have to be defined for the fuel bed. In this section, common approaches are summarized. The

additional fuel bed models can be divided into physical models, considering physical changes in the fuel bed during thermo-chemical conversion, and chemical models, which deal with additional chemical alteration of the fuel besides pyrolysis, gasification and combustion. Especially, the formation of precursors for pollutants formation is described by these models.

Physical models include shrinking, collapsing and channeling. Details about shrinking and collapsing can be found in Section 2.1.7. Channeling can lead to the formation of hot spots and to enhanced emissions. The formation of channels in the fuel bed is described by various authors [129, 136, 137]. Both channeling and collapsing in the fuel bed lead to streak formation in the free board. Since the formation of channels cannot be modelled directly in empirical bed models, Shiehnejadhesar et al. [138] developed a model for streak formation in the free board to extend an empirical bed model.

In combustion systems with moving bed, fuel particles are mixed by the movement of the grate. Yang et al. [139] and Peters et al. [140] included the movement of the particles in the bed model to increase the accuracy. The fuel bed of pellet boilers is quasi stationary, when fuel is consumed by combustion and added by the automatic feeding system. Additionally to fuel consumption and bed shrinking, also, the feeding with new fuel can be described by appropriate models [134, 141, 142]. The formation of large ash particles (fly ash) during the combustion process can have impact on the properties of the fuel bed and should be considered for fuels with high ash content [117]. Porteiro et al. developed a model for small partially or fully burned particles, which are entrained by the flow of primary air through the fuel bed [99].

Chemical models include the formation of precursors for emissions in the biomass bed. Particularly, the precursors of aerosols, soot and NO_x are formed in the biomass bed. For the formation of aerosols, the devolatilization of inorganic salts from the biomass bed is taken into account [143–146]. As the devolatilization of inorganic salts is determined by very fast reactions, this step is often simulated with an equilibrium model in AspenPLUS [147] or FactSage [148]. Additionally the formation of precursors for soot [149] and NO_x [150–152] can be considered in the bed model. For NO_x formation, the release of NH_3 and HCN and the relation of the two precursors have to be modelled.

2.2 Single particle models for pyrolysis

The development of combustion (or gasification) models requires always the implementation of a kinetic model to describe drying, biomass devolatilization and char formation, heterogeneous reactions of char gasification and combustion and gas-phase reactions, including cracking, oxidation and polymerization, of the volatiles released during pyrolysis and char conversion [46, 81]. Of course, such kinetic model needs to be coupled with the relevant transport models within and between the multiple phases considered, as well as with the description of physical properties evolution, such as porosity change, shrinkage and particle breakage. The interaction of the kinetic and transport models in a computational model is often tested and validated for single, thermally thick biomass particles (see Section 2.1.2). Single particle models form an important step in the bed model development, since they offer the opportunity to validate the implemented sub-models with small computational effort and a manageable amount of variables. After validation, single particle models can be used as a starting point for the up-scaling to a full bed model. Various single particle models were developed and validated for the further usage in the simulation of the fuel bed for example as a separate bed model [42, 153], as discrete particle model (DPM) [40, 110] or as porous medium bed model [38]. At the same time, the appropriate description of thermo-chemical conversion processes in fixed bed reactors, where usually thermally thick wood particles are used, should account for the presence of intra-particle phenomena and varying local conditions. This requires the development and implementation of single particle models at the reactor level [81, 154].

For simplification and with regard to the possible implementation of the model in CFD calculations, a one-dimensional approach is chosen for most single particle models. This leads to particles in shapes of spheres, infinite cylinders or infinite plates. More detailed models offer finite cylinders, finite plates or spheres with an additional shape factor (for example [155]).

Detailed reviews on single particle pyrolysis [47] and single particle combustion [154] are available in the literature. It is therefore the objective of the authors in the present work not to repeat such reviews, but to highlight and discuss studies considered of special relevance for the development of comprehensive and detailed CFD models, due to the advanced treatment of the pyrolysis step.

As reviewed by Haberle et al. [154], most single particle models available in the literature include one-component competitive kinetic schemes, multi-component parallel reactions scheme, multi-component competitive schemes or their combinations. These schemes are able to describe the evolution of pyrolysis products lumped mainly in tar, gas and char. Only few include the formation of relevant tar species, necessary for a more accurate modelling of the gas-phase reactions, or good thermochemistry prediction. Most of these particle models are also 1D. Ström and Thunman [130, 156] showed that such approach can reproduce with acceptable accuracy the behaviour of 2D or 3D fixed beds of particles [79]. However, as it will be reviewed in

the following, improvement in such models requires the inclusion of biomass anisotropic properties, leading to 2D or 3D models, although nowadays their implementation in CFD models at reactor level supposes a remarkable challenge.

Park et al. [157] developed a particle model and evaluated three different pyrolysis kinetic mechanisms available in literature. The distinctive thermal regions (endothermic and exothermic behaviour) observed during the pyrolysis of thermally thick spherical wood particles (25.4mm diameter) were investigated. The considered kinetic scheme was the one proposed by Di Blasi in [158], based on the mechanism of Shafizadeh and Chin [69], where the three competitive reactions scheme for biomass pyrolysis was coupled with homogeneous secondary reactions of the primary volatiles. The heats of reaction and kinetic parameters for these secondary reactions were obtained from the literature [35, 67, 94, 120, 159]. The second kinetic scheme considered the separate conversion of the three major macromolecules in wood (cellulose, hemicellulose and lignin). The kinetic parameters were taken from [160] for cellulose decomposition into volatiles and char in two parallel reactions (two components for cellulose); for hemicellulose, the kinetic parameters were taken from [161], considering its decomposition as the competitive formation of tar and an intermediate solid, reacting further to char and gas; the lignin parameters were taken from [162], describing its devolatilization with a single global reaction to produce volatiles and char. In all cases, the amount of char produced was a given parameter. The third kinetic scheme used is the one proposed by Kilzer and Broido in 1965 [163] for cellulose, although extended to wood. The kinetic parameters for the tar production reaction were the same as the ones for tar production in model 1, while the other parameters were obtained by fitting with the experimental data [157]. Upon comparison of the experiments with the numerical results, it was shown that the exothermic behaviour observed in the centre of the particle was not due to the exothermic homogeneous tar cracking reactions or to the exothermic decomposition of lignin, but rather associated to secondary transformation of an intermediate solid to produce char, i.e. to secondary char-forming reactions [157]. Based on the results, a new mechanism was proposed where wood decomposes through three competing reactions to an intermediate solid, tar and gas. The path leading to the formation of the intermediate solid (non-exothermic) is favoured at lower temperatures over the volatile (tar and gas) formation pathways. This intermediate solid reacts further to secondary char in an exothermic reaction. Secondary tar cracking reactions to produce char and gas were also implemented [157]. With this mechanism, a good agreement between experiments and numerical results was achieved, although only temperature evolution and product yields, lumped in tar, gas and char were predicted, not sufficient for detailed combustion modelling. A novelty in this particle model was the inclusion of pressure evolution inside the particle, relevant due to volatile formation and low permeability, leading potentially to particle breakage [157].

Using the detailed pyrolysis mechanism proposed by Ranzi et al. [62] (see Fig. 1), Corbetta et al. [79] developed a single particle model (1D, spherical) with two different approaches: a particle model, including the transport model developed by Park et al. [157], and a multi-phase and multi-scale approach (GASDS code [81]), where kinetics and transport phenomena were combined at particle and reactor level, including secondary reactions of volatiles in the gas phase (reactor level). The kinetic scheme was optimized through comparison with experimental data obtained in kinetically controlled regime (thermogravimetric experiments, TGA) [79], while the particle model was validated with three sets of experimental data [157, 164, 165], varying wood type, particle geometry, heating rate, final temperature and characterized volatile species. The gas-phase model was compared with experimental data from Norinaga et al. [166]. As claimed by the authors [79], the model is partially predictive for thermal aspects and for the characterization of the released species for a wide range of temperatures. However, further improvement of the model would requires the inclusion of heterogeneous secondary reactions, as well as the improvement in physico-chemical aspects such as the anisotropy in the particle properties, a better characterization of the thermochemistry and the inclusion of particle break-up in the model, as highlighted by the authors [79].

Bennadji et al. [164] used also the adaptation made by Corbetta et al. [79] of Ranzi's pyrolysis mechanism [62] to model pyrolysis of hardwood and softwood particles with two different sizes (2.45 and 3.81 cm), comparing temperature in different positions of the particle, mass loss evolution and the online formation of CO, CO_2, CH_4, H_2, CH_3OH, HCOOH, CH_3COOH and CH_2O, all of them species relevant for gas-phase combustion modelling [164]. The authors reported that the main influence of particle size was on the timing of the heating and devolatilization processes, being less important with respect to char and individual gaseous species yields [164]. They suggested that the reduction of some yields with increasing particle size could be related to the presence of intra-particle reactions of pyrolysis products (such as formaldehyde and acetic acid) to form secondary char. Further improvement of the model would require the inclusion of extractives as another biomass component and of intra-particle reactions of tar, as highlighted by the authors [164].

Anca-Couce et al. [167] implemented their adaptation of the Ranzi's scheme (called RAC [82, 167], considering the production of 20 volatile species) in a particle model and compared the simulations with experimental results

for pyrolysis of a spruce cylindrical particles, measuring the release of 14 different species (CO, CO_2, CH_4, ethylene, acetylene, propane, propene, formaldehyde, acetic acid, acetaldehyde, methanol, ethanol, lactic acid). Despite the achieved advances, including a relative good fitting with experimental results, the authors [167] reported that improvements in the pyrolysis mechanism and experimental data were necessary, including the kinetic description of secondary charring reactions, as well as the influence of inorganic species on these reactions; the use of detailed gas-phase mechanisms, able to predict, for example, the formation of polycyclic aromatic hydrocarbons and soot; a better understanding of char devolatization; and a better experimental characterization of the pyrolysis products [167].

There are, therefore, particle models available in literature that implemented detailed pyrolysis kinetic schemes, able to predict, among other relevant properties, a fair amount of volatile products, of significant relevance for the gas-phase reactions. However, such particle models, or even detailed kinetic schemes, are barely used in the modelling and simulation of biomass combustion. To the author's knowledge, only Ranzi et al. [80, 81] (see also Table 1) used a detailed pyrolysis kinetic scheme [62] for modelling of biomass combustion at reactor level, coupling the particle model to the reactor level, and showing that it is possible to use such schemes for complex CFD simulations.

2.3 Modelling approaches for the biomass bed

Bed models are necessary to provide inlet information for the gas-phase simulation in the free board. Besides the usage in comprehensive simulations of combustion systems, advanced bed models are used to enhance the understanding of the processes of thermo-chemical conversion of the fuel bed, aided by mathematical models. The modelling approach depends strongly on the modelled combustion system and of the objective of the simulation. They can be assigned to the groups

- Empirical bed model
- Separate bed model (zero- to three-dimensional)
- Discrete particle method (DPM) based bed model
- Porous medium bed model

For comprehensive simulations of combustion appliances, the computational effort of the bed model is a challenging issue, as gas-phase simulations already demand a lot of resources. Consequently, the level of detail of the bed model tends to be lower in comparison, for example, to single particle models, if the complete combustion process is modelled. In many studies, empirical or separate one- or two-dimensional bed models are used. In modelling approaches which describe the bed model only, a higher complexity is possible. Those models are in many studies tested and improved by comparison with experimental results of laboratory-scale fixed bed reactors. Due to improvement and broader availability of processors, level of detail of bed models increased in the recent years and the inclusion of the bed model into the computational domain of the gas-phase simulation as porous medium bed model has becomes more common.

Several dimensionless numbers can be used to classify the bed model and to simplify the choice of the appropriate model. The Biot number (Eq. 1 in Section 2.1.2) is used to see if fuel particles should be modelled as thermally thin or thick. The Thiele modulus (Eq. 10 in Section 2.1.5) is used to find out about shrinking core or reacting core regime. According to Peters [107], the Damköhler number (Eqs. 27 and 28) of the biomass bed is important to decide, whether the combustion and gasification of char in the fuel bed can be modelled as a well stirred reactor ($Da < 1$), in which reactions occur in any place of the bed at the same time, because reacting agents are available everywhere. Or if a combustion front moves along the bed ($Da > 1$), as the reacting agents flow through the solid and are consumed during the reactions.

$$Da_1 = \frac{S_{Y_{i,g}} l_B}{\vec{v}} \tag{27}$$

$$Da_2 = \frac{S_{Y_{i,g}} l_B^2}{D} \tag{28}$$

$S_{Y_{i,g}}$ is the source term of mass fraction of gaseous species, l_B is the characteristic length of packed bed, $\vec{v}$ is the flow velocity and D is the diffusion coefficient. Da_1 is used when diffusion is negligible and the relation of reaction rate to flow velocity is important to describe the combustion regime ($Pe \gg 1$). Da_2 is suitable for applications in which convection is negligible ($Pe \ll 1$). The Péclet Pe number for mass transfer (29) is used as indication, whether convection or diffusion has more influence on the mass transfer [107].

$$Pe = \frac{l_B \vec{v}}{D} \tag{29}$$

2.3.1 Empirical models

Empirical models represent the most basic form of a bed model. In this approach, the gas-phase simulation is provided with a boundary condition for the inlet, in which the composition of the fuel gas is defined. The fuel gas is formed inside the fuel bed during drying, pyrolysis, gasification and combustion. The composition of the fuel gas can be based on measurements or it can be calculated based on the biomass elemental composition. For the former, pyrolysis experiments are conducted and the composition of the volatiles leaving the fuel at a

certain constant temperature is measured and used for the simulations [18, 168, 169]. The conditions in these experiments deviate from the conditions during combustion, since they are conducted at lower temperature and the presence of oxygen is neglected [170].

Semi-empirical models use calculations based on experimental data to provide information about combustible gases. Different approaches to calculate the composition of volatiles are introduced in several publications [68, 170, 171]. For the widely used approach of Thunman et al. [170], the elemental composition and thermodynamic data of the fuel are required. In addition, it is necessary to measure the ratio of CO to CO_2 and the ratio of light hydrocarbons (C_iH_j) to CO_2 in the pyrolysis gas. By solving the mass and heat balance for any species, the mass fractions of CO_2, CO, H_2O, H_2, light hydrocarbons and heavy hydrocarbons in the pyrolysis gas can be determined. This method is often used, because the calculation can easily be made with only a few measured values and the computational effort is low.

For many combustion systems, the composition of volatiles entering the combustion chamber is not constant during the thermo-chemical conversion of the biomass. Therefore, it might be of interest to apply a concentration profile rather than a constant value. The profile can depend on time, for example for wood log stoves, or on the place on the grate, for example for systems with moving grates. The profiles can be obtained by measurements or as result of a semi-empirical calculation. An example for input profiles is presented by Scharler [172, 173] for a furnace with moving grate. The concentrations, temperature, mass flow and velocity of the devolatilization gas were determined in dependency of the position on the grate. As carbon, which is initially contained in the biomass, decreases, gaseous components are released. Conversion parameters for the formation of CH_4, CO, CO_2, H_2, H_2O and O_2 were calculated based on mass and energy balances. The reduction profile of carbon was determined by experiments and polynomial fitting. The remaining curves were calculated by correlation factors. This approach was further developed by Buchmayr et al. [174, 175]. With spatially resolved measurements above the fuel bed, accuracy of the empirical bed model was improved.

Empirical bed models can be implemented without great effort. They provide reasonable results and do not require additional computational resources for the fuel bed. On the other hand, they need experimental data, which might be difficult to obtain. Also, the measured data are only valid for the investigated combustion system, biomass and operation conditions. Since the empirical bed model is used as an inlet condition, it does not reflect the change of the geometry of the fuel bed and there is no coupling with the gas-phase reactions. Therefore, it is more suitable for stationary simulations. If the empirical model is used to simulate the system it was measured in, it may be more accurate than other bed modelling approaches, but it is not flexible to changes. An empirical bed model can be used for simulations with focus on the gas-phase reactions in the combustion chamber or on additional models. One field of application is the improvement of the design of combustion chambers for certain operation conditions for an existing combustion system.

Semi-empirical models provide more flexibility, but they also need specific data and if the required information is not available, assumptions have to be made. The accuracy of the semi-empirical models depends on the quality of the provided data and of the assumptions.

2.3.2 Separate bed models

The most common modelling approach for biomass combustion systems is the separation of fuel bed and free board. Drying, pyrolysis and consumption of char are simulated in the bed model. Gas-phase combustion is calculated by CFD in the free board. The reactions in the bed model are calculated separately and the resulting gas-phase composition is used as inlet condition for the gas-phase model. One-way or two-way coupling between bed model and gas-phase simulation can be implemented and is based on heat and mass transfer between both regions. Separate bed models can be zero- to three-dimensional.

Separate bed models are summarized in Tables 2, 3 and 4. In these tables, information about the considered biomass and model application is given and the sub-models for drying and pyrolysis are mentioned. The considered heterogeneous and homogeneous reactions in the bed models are specified, as well as the approach to model shrinking of the fuel bed at particle and bed scale.

Zero-dimensional In zero-dimensional models, the calculations based on thermodynamic equilibrium or chemical reaction kinetics are conducted to determine the composition of the combustible gas leaving the biomass bed during decomposition. For calculations based on chemical reaction kinetics, the biomass bed is considered to be a perfectly stirred reactor (PSR) [176] with uniform distribution of concentrations and temperature. The conversion is determined by chemical reactions only, while influences of mixing as well as heat and mass transfer are neglected.

Calculations based on thermodynamic equilibrium can be conducted with the software Aspen PLUS [147], for example. It is mainly used for fluidized bed technology in biomass gasification or combustion. Modelling of a downdraft gasifier with Aspen PLUS was also described in literature [177–179], in which the whole combustion process (bed and free board) was calculated as thermodynamic equilibrium. In the model of Galletti et al. [180], the release of

volatiles was calculated by a zero-dimensional bed model. Three variations for the implementation of the bed model in the combustion simulation of a biomass furnace for a externally fired gas turbine were tested.

One-dimensional One-dimensional models are widely used to simulate the biomass bed, since they provide sound results with low computational effort. Table 2 gives an overview on one-dimensional separate bed models. In these models, gradients along one dimension are described. They are used to model fixed bed laboratory reactors [24–26, 41, 42, 45, 66, 81, 96, 101, 117, 119, 121, 123, 127, 181, 182], single wood logs [92, 112, 183], fixed beds in furnaces with moving beds [111, 184] or packed beds [99].

As preparation for comprehensive coupled models, one-dimensional stand-alone models were developed and validated by experiments in accordingly designed experimental equipment. The focus of these models was on the accurate simulation of the thermo-chemical processes inside the fuel bed [24, 26, 41, 96, 181].

First attempts to model biomass combustion in fixed beds were made to investigate the propagation of the flame front inside the biomass bulk. An early model of this type was developed by Fatehi and Kaviany in 1994 [181] to describe the downward propagation of the flame front in opposite direction to the gas flow. This approach was enhanced towards a model in which gaseous and solid phase are not in equilibrium [24].

A similar model was developed by Saastamoinen et al. in 2000 [26]. The objective of their study was also to investigate the propagation of the flame front. The model was a preparation to examine biomass combustion on a moving grate. Thermally thin and thick particles were described by the model. The influence of parameters on the propagation speed was studied by means of simulations and experiments.

Shin and Choi presented a one-dimensional model for the combustion of waste particles in 2000 [96]. Similar to the previously mentioned models, the propagation of the flame front is investigated by this approach. This model was developed for the simulation of a furnace with moving grate as well.

A comprehensive one-dimensional model for straw combustion was developed by Zhou et al. in 2005 [41]. It includes moisture evaporation, pyrolysis, gasification and combustion. Additionally, gas-phase reactions such as tar cracking are taken into account. Good agreement was observed when compared to experimental results. The model was used to investigate the detailed processes of fixed bed combustion of straw.

The thermo-chemical conversion of a wood log during combustion was modelled by Galgano et al. [112, 183]. They developed a separate bed model, which was coupled to the two-dimensional CFD simulation. The wood log was assumed to have the form of a cylinder and the one-dimensional model represented the thermal gradient in radial direction. The gas-phase combustion was simulated in a two-dimensional domain based on the inlet in7formation of the bed model.

Huttunen et al. [111] introduced the CFD simulation of a furnace with moving grate. The simulation was performed with Ansys Fluent [185] containing a user-defined function (UDF) for the one-dimensional bed model. The spatial variable was orientated in the direction of the grate, which was divided into different zones for drying, pyrolysis and gasification/combustion. The one-dimensional model represented a cross section in the middle of the bed.

The one-dimensional model of Shin and Choi [96] for incineration of solid waste, was further developed and coupled with CFD to simulate waste incineration inside a furnace with moving grate [186]. Simulations based on this one-dimensional model were also performed by Yang et al. [124] and Yin et al. [187]. Yang et al. developed a two-dimensional model for simulation of municipal solid waste on a moving grate in 2002 [118], which was implemented in the in-house code FLIC. Simulations of one-dimensional cases with FLIC were done in [45, 182], to investigate the influence of important parameters as devolatilization rate, moisture content and flow rate of primary air on the processes in the biomass bed numerically.

Two-dimensional Two-dimensional bed models are mainly used to simulate furnaces with a moving grate, where the composition of volatiles varies along the grate [129, 135, 188–191]. In this approach, the first spatial coordinate represents the height of the biomass bed, and the second spatial coordinate correlates with the length of the grate. Among the first to use a two-dimensional bed model were van der Lans et al. in 2000 [188] for the simulation of straw combustion. They proposed to use a one-dimensional transient bed model to calculate the devolatilisation properties and to relate the position on the grate x to the time t based on the transport velocity u_s: $x = u_s t$. This approach is valid when heat transport by conduction in horizontal direction is much smaller than heat transfer by convection in the vertical direction. This assumption can be made, if the Péclet number for heat transfer (30) is larger than 1 ($Pe \gg 1$) [188].

$$Pe = \frac{u_s l_{bed}}{k_{th}/(\rho_s c_{p,s})} \tag{30}$$

where l_{bed} is the length of the bed, k_{th} the effective thermal conductivity, ρ_s the density, and $c_{p,s}$ the heat capacity of the solid material. Kær et al proposed the moving column approach for the modelling of moving grates [189, 190],

Table 7 Examples for modelling of biomass combustion systems with moving grate

Author and year	Biomass	Firing System	Bed model, coupling and volatiles	Turbulence model	Reaction mechanism	Combustion model	Radiation	Additional models
Kim et al. 1996 [232]	MSW	MSW incinerator	Combustion product gases as inlet boundary conditions, properties from measurements not modelled	k-ε model	Not modelled	Combustion not modelled, PDF to quantify mixing	Discrete transfer radiation model (DTRM), grey gases with uniform adsorptivity	Thermal decomposition furan, chlorobenzene and tetrachloride as post-processing
Scharler and Obernberger 2000 [173]	Waste wood	Travelling grate furnace, boiler capacity 440/550 kW_{th}	Empirical model, no coupling, C_mH_n, H_2O, H_2, CO, CO_2, O_2	Realizable k-ε model	$CH_4 + 0.9O_2 \rightarrow CO + 1.2H_2 + 0.8H_2O$; Eqs. 34, 37	Multi-step finite rate/eddy dissipation model	DOM	Euler-Lagrange particle tracking for erosion
Ryu, Shin and Choi 2002 [186]	MSW	Moving bed, 150t/d	2D bed model, inlet gas conditions and radiative heat flux onto the bed, $CH_{2.33}O_{0.76}$, CO, H_2	RNG k-ε model	Irreversible oxidation of volatile component, CO and H_2	Magnussen-Hjertager model	DOM, absorption of CO_2 and H_2O (WSGGM)	
Huttunen et al. 2004 [111]	Wood chips	Moving bed, 1MW	1D bed model, continuity, species mass and fractions energy, CH_nO_m	Standard k-ε model	$CH_yO_z \rightarrow CO + H_2O + 0.8H_2O$; $CO \rightarrow CO_2$	Eddy dissipation combustion model (EDCM)	DOM, WSGGM	
Kær et al. 2004 [192]	Straw	Moving grate, Masnedø boiler ($33MW_{th}$)	2D bed model, inlet gas conditions and radiative heat flux onto the bed, O_2, CO, CO_2, H_2O, volatiles	RNG k-ε model	$C_xH_yO_z + (i_1 + i_2)O_2 \rightarrow xCO + \frac{y}{2}H_2O + i_2O_2$; $\rightarrow xCO_2 + \frac{y}{2}H_2O$; $i_1 = \frac{x}{2} + \frac{y}{4} - \frac{z}{2}$; $i_2 = \frac{x}{2}$	Eddy break-up model	Discrete transfer model	
Kær et al. 2006 [190]	Straw	Moving grate, Masnedø boiler ($33MW_{th}$)	2D bed model, inlet gas conditions and radiative heat flux onto the bed, $CH_{1.6}O_{0.8}$ (based on [189])	RNG k-ε model	Eqs. 34, 40 with $x = 1$, $y = 1.6$, $z = 0.8$	Finite rate/eddy dissipation model	DOM, WSGGM	Ash formation and deposition

Table 7 (continued)

Author and year	Biomass	Firing System	Bed model, coupling and volatiles	Turbulence model	Reaction mechanism	Combustion model	Radiation	Additional models
Yang et al. 2007 [124]	Straw	Vibrating grate, $38MW_{el}$	2D bed model, inlet gas conditions and radiative heat flux onto the bed, CH_4, CO, H_2	Standard k-ε model	Eq. 35 with $x = 1$; Eqs. 37, 38	Finite rate/eddy dissipation model	DOM	NO formation
Yang et al. 2007 [125]	MSW	Moving grate, $25MW_{el}$	2D bed model, inlet and boundary conditions from bed model, C_mH_n, CO, H_2	Standard k-ε model	Eq. 35; Eqs. 37, 38	Not specified	DOM	
Yin et al. 2008 [187]	Wheat straw	Vibrating grate, $108MW_{th}$	Empirical bed/0D model and 2D bed model (from [41]), CO, CO_2, H_2O, O_2, volatiles	Standard k-ε model, realizable k-ε model	Eqs. 33, 34	Finite rate/eddy dissipation model	DOM, WSGGM	
Simsek et al. 2009 [131]	MSW	Moving grate	DPM, heat and mass exchange, convection, radiation, CH_4, C_2H_6, C_2H_4, H_2, CO, H_2O, N_2, H_2S, HCl	Not specified	Not specified	Not specified	Not specified	
Venturini et al. 2010 [193]	Wood chips with water and inert material	Moving grate	2D bed model based on [96], gas temperature, velocity, chemical species from bed top, radiation flux from free board, CH_4, CO, H_2O, CO_2	Low Reynolds k-ε model	GRI-Mech 3.0 truncated to C2-chemistry	Flamelet approach	Not specified	Solid particle transport and deposition formation
Yu et al. 2010 [194]	Rice straw	Moving grate, 200t/d	2D bed model, gas temperature, velocity, chemical species from bed top, radiation flux from free board, CH_4, CO, H_2O, CO_2	RNG k-ε model	Not specified	Not specified	Discrete transfer	NO formation

Table 7 (continued)

Author and year	Biomass	Firing System	Bed model, coupling and volatiles	Turbulence model	Reaction mechanism	Combustion model	Radiation	Additional models
Zhang et al. 2010 [44]	Wood chips	Residential boilers with moving grate, 320kW and 150kW	2D bed model (FLIC), gas temperature, velocity, chemical species from bed top as inlet condition for gas- phase simulation, C_2H_4, CO,O_2, CO_2, NO, HCN	Standard k-ε model	Eq. 33 with n=x, m=y, Eq. 34	Not specified	P1 model	NO formation
Ranzi et al. 2011 [80]	Wood	Travelling grate, 12MW	Separate bed with DPM, heat and mass balance, complex kinetic model for biomass decomposition (>30 species)	Not specified	Kinetic model from CRECK modelling home-page [260]			Dsmoke, BzzMath, reactor network array (RNA) for gas phase
Brosch et al. 2011 [208]	MSW, spherical particles	Moving bed $60MW_{th}$ 23t/h	Coupled DPM bed model	Not specified	Not specified	Not specified	Not specified	
Kurz et al. 2011/2012 [202, 203]	Wood chips (spruce)	Moving grate, 240 kW, 60MW	Porous medium, moving fixed bed, CO, CO_2, H_2O, H_2, C_xH_y	Standard k-ε model with adapted transport equations	Eqs. 34, 35, 37	EDM	DOM	
Yin et al. 2012 [234]	Wheat straw	Moving grate, 88MW	Empirical bed model, profiles of species concentration, temperature and velocity as inlet conditions, H_2O, CO, O_2 N_2, $CH_{2.306}O_{1.031}N_{0.02}$	Standard k-ε model	$CH_{2.306}O_{1.031}N_{0.02} + 0.561O_2 \rightarrow CO + 1.153H_2O + 0.01N_2$; Eq. 34	Finite rate/eddy dissipation model	DOM	
Galletti et al. 2016 [180]	Wood chips	Moving grate, 185kg/h	0D/empirical bed models with 3 different configurations (based on [187]), $C_{1.06}H_{2.24}O_{0.92}N_{0.0028}S_{0.0002}$, CO_2, H_2O, O_2, N_2	Standard k-ε model, realizable k-ε model and k-ω model	$C_{1.06}H_{2.24}O_{0.92}N_{0.0028}S_{0.0002} + 0.63O_2 \rightarrow 1.06CO + 1.12H_2O + 0.0014N_2 + 0.0002SO_2$; Eq. 34	EDM	P1, WSGGM	

Table 8 Pellet boilers

Author and year	Biomass	Firing System	Bed model, coupling and volatiles	Turbulence model	Reaction mechanism	Combustion model	Radiation	Additional models
Klason and Bai 2007 [261]	Wood pellets	Domestic pellet boiler, 8kW to 11kW	2 variations of a semi-empirical bed model with release of fuel N, CH_4, C_xH_y, CO, CO_2, H_2O, O_2, N_2	Standard k-ε model	Eqs. 33, 33 with n=1, m=4, Eqs. 34, 37	EDC	P1	NO formation
Porteiro et al. 2009 [99]	Wood pellets	Domestic pellet boiler, 24kW	UDF, third party mathematical packages, iterative coupling between bed model and free board, CO, H_2, CH_4, CO_2, H_2O, C_6H_6, O_2(based on [170])	Standard k-ε model	Eq. 33 with $n = 1, m = 4$, Eqs. 34, 37, $C_6H_6 + (15/2)\ O_2 \rightarrow 6\ CO_2 + 3H_2O$; $CO_2 \rightarrow CO + 1/2O_2$	Finite rate/eddy dissipation model	DOM	Ejection of biomass particles into free board based on calculations in separate bed model
Mehrabian et al. 2010 [205]	Softwood pellets	Underfeed stoker grate furnace	DPM bed model, CH_4, CO, CO_2, H_2, H_2O, O_2	Realizable k-ε model	Global 4-step mechanism	EDM	DOM	
Chaney et al. 2012 [43]	Biomass pellets	Pellet boiler, 50kW	Porous medium as UDF inside computational domain, discrete devolatilisation zones in fuel bed, $C_{1.93}H_{5.75}O_{2.37}$	k-ε model	Eqs. 34, 39 with n=1.93, m=5.75, l=2.37	Eddy dissipation turbulence interaction	P1	
Collazo et al. 2012 [211]	Wood pellets	Pellet boiler, 18kW	Porous medium inside computational domain, CH_4, C_6H_6, H_2, CO, CO_2, H_2O, O_2, NH_3	Realizable k-ε model	Eq. 33 with n=1, m=4, Eq. 33 with n=6, m=6, Eqs. 34, 37, $CO_2 \rightarrow CO + 1/2O_2$	Finite rate/eddy dissipation	DOM, WSGGM	Ejection of small char particles during combustion, NO formation
Rezeau et al. 2012 [262]	Pellets	Pellet boiler with stair like grate, 250 kW	None	RANS and URANS, realizable k-ε model	Not modelled	Not modelled	Not modelled	
Borello et al. 2013 [195]	Lauan wood chips (as alternative fuel)	Manually fed fixed bed with burner and slope	2D bed model based on [96], H_2O, CO, CO_2, CH_4, O_2, others	Low Reynolds k-ε model	Not specified	Stretched laminar flamelet with finite-rate chemistry	Not specified	Entrained solid particles and deposition
Gomez et al. 2014 [132]	Wood pellets	for fuel Combustor tube, test rig, 24kW	UDF, porous medium, thermally thin spherical equivalent particles, CO, H_2, CH_4, CO_2, H_2O, C_6H_6	Realizable k-ε model	Eq. 33 with n=1, m=4, Eq. 33 with n=6, m=6, Eqs. 34, 37, 38, $CO_2 \rightarrow CO + 1/2O_2$	Finite rate/eddy dissipation model	DOM + DOM in porous medium	Soot formation with Moss-Brooks model

Table 8 (continued)

Author and year	Biomass	Firing System	Bed model, coupling and volatiles	Turbulence model	Reaction mechanism	Combustion model	Radiation	Additional models
Mehrabian et al. 2014 [105]	Spruce pellets	Laboratory scale reactor	3D bed model, fully coupled with gas-phase simulation CO, H_2, CH_4, CO_2, H_2O, N_2, C_2H_2, C_2H_4, C_2H_6, CH_2O (depending on mechanism)	Laminar	DRM22, GRI-mech 2.11, Kilpinen97	No combustion model	DOM, WSGGM	
Buczyński et al. 2015 [212]	ECORET coal, biomass	Domestic retort underfeed boiler, 25kW to 50kW	Porous medium, CO, H_2, CH_4, CO_2, H_2O, C_6H_6	Standard k-ε model	$C_{1.05}H_{4.22}O_{0.74}N_{0.0761} + 1.21O_2 \rightarrow 1.05CO + 2.11H_2O + 0.038N_2$; Eq. 34	EDC	DOM, WSSGM	
Gomez et al. 2015 [141]	Wood pellets	Underfeed pellet boiler 60kW	UDF, porous medium, thermally thin spherical equivalent particles, CO, H_2, CH_4, CO_2, H_2O, C_6H_6	Realizable k-ε model	Eq. 33 with n=1, m=4, Eq. 33 with n=6, m=6, Eqs. 34, 37, 38, $CO_2 \rightarrow CO + 1/2O_2$	Finite rate/eddy dissipation model	DOM + DOM in porous medium	Soot with Moss-Brooks model
Shiehnejadhesar et al. 2015 [138]	Wood pellets	Underfeed pellet furnace 20kW$_{th}$	Empirical bed model, CO, H_2, CH_4, CO_2, H_2O, NH_3, HCN, NO	Realizable k-ε model	Global three-step reaction mechanism, Kilpinen97	EDM, EDC + ISAT, hybrid gas-phase reaction models + ISAT	DOM, WSGGM	Streak formation above fuel bed, NO formation
Buchmayr et al. 2016 [174]	Soft wood chips	Laboratory reactor 50kW$_{th}$	Empirical bed model, CO, H_2, CH_4, CO_2, H_2O, C_7H_{16}, tar	Realizable k-ε model	Eq. 33 with n=1, m=4, Eq. 34, heptane42.che [263]	EDM, EDC, steady flamelet model (SFM)	DOM, WSGGM	
Gomez et al. 2016 [134]	Wood pellets	Pellet-drop-feed boiler, 27kW	UDF, porous medium, thermally thin spherical equivalent particles, CO, H_2, CH_4, CO_2, H_2O, C_6H_6	Realizable k-ε model	Eq. 33 with n=1, m=4, Eq. 33 with n=6, m=6, Eqs. 34, 37, 38, $CO_2 \rightarrow CO + 1/2O_2$	Finite rate/eddy dissipation model	DOM + DOM in porous medium	DPM feeding model, soot with Moss-Brooks model
Gomez et al. 2017 [142]	Wood pellets	Pellet-drop-feed boiler, 27kW	UDF, porous medium, thermally thick spherical equivalent particles, CO, H_2, CH_4, CO_2, H_2O, C_6H_6	Realizable k-ε model	Eq. 33 with n=1, m=4, Eq. 33 with n=6, m=6, Eqs. 34, 37, 38, $CO_2 \rightarrow CO + 1/2O_2$	Finite rate/eddy dissipation model	DOM + DOM in porous medium	DPM feeding model, soot with Moss-Brooks model
Farokhi et al. 2017 [225]	Wood pellets	Laboratory scale reactor 8kW to 11kW	Empirical bed model (based on [261]), C_6H_6, CH_4, CO_2, O_2, H_2O, CO, N_2	Standard k-ε, RNG k-ε, realizable k-ε model	Two global mechanisms: WD and JL, three detailed mechanisms focussed on PAHs and tars (Marinov et al. [244], Ranzi et al. [62] and Richter et al. [245])	EDC, steady flamelet model (SFM), unsteady flamelet model	P1, WSGGM	

Table 9 Biomass combustion systems with wood logs and other batch systems

Author and year	Biomass	Firing System	Bed model, coupling and volatiles	Turbulence model	Reaction mechanism	Combustion model	Radiation	Additional models
Knaus et al. 2009 [224]	Wood logs	Wood log stove with staged combustion, 10kW	Empirical bed model, gasification gases based on measurements	k-ε-, low Re number k-ε- and Reynolds stress turbulence model	$C_mH_n + (m/2 + \alpha n/4)\ O_2 \rightarrow mCO + (m/2 + \alpha n/4)H_2 + \alpha n/2 H_2O$; Eqs. 34, 37	EDC	DOM, Constant absorption coefficient of gas phase (0.2/m)	Modelling of secondary combustion zone, comparison with experiments
Galgano et al. 2006 [92, 112]	Single wood log	Test rig: furnace reactor for a wood log	1D separate bed model, continuity for temperature and gas species mass fractions, heat and mass transfer at solid/gas interface CO, H_2, CH_4, CO_2, H_2O, O_2, N_2	k-ε model, modified for small Re numbers and buoyancy	Eqs. 32, 34, 37, 38	EDC	Discrete transfer method (Lockwood and Shah)	1D bed model, 2D gas-phase comparison of the model with and without gas phase
Menghini et al. 2008 [183]	Single wood log	Test rig: furnace reactor for a wood log	1D separate bed model, continuity for temperature and gas species mass fractions, heat and mass transfer at solid/gas interface, fictitious boundary, CO, H_2, CH_4, CO_2, H_2O, O_2, N_2	Low Reynolds k-ε model	Eqs. 32, 34, 37, 38	EDC	DOM	1D bed model, 2D gas phase
Schütz (PhD) 2012 [257]	Cylindrical wood briquette	Wood log stove, 8kW	Semi-empirical bed model ([170]), CO, H_2, CH_4, CO_2, H_2O	RNG k-ε model	Eqs. 32, 34, 37	EDC	DOM, WSGGM	Soot formation
Sènèchal (PhD) 2013 [258]	Log wood	Wood log stove, 9kW	Porous medium, $C_6H_{11.299}O_{5.17}N_{0.0093}$	SST k-ω model	$C_6H_{11.299}O_{5.17}N_{0.0093} + 3.2395O_2 \rightarrow 6CO + 5.6493H_2O + 0.00465N_2$; Eq. 34	EDC	DOM	Ceramic filter, soot formation
Athanasios et al. 2015 [237]	Beech wood logs	KOMBI kn 30/50 boiler, 32kW, steady state operation	Fuel bed as porous zone with parts of fixed char and wood logs, volatiles and moisture released with Arrhenius rate from outer layer of the logs, O_2, N_2, H_2O, CO, CO_2, $C_{3.43}H_{7.71}O_{3.19}$	Standard k-ε model	Eqs. 34, 40 with n=3.43, m=7.71, l=3.19	Not specified	DOM	

Table 9 (continued)

Author and year	Biomass	Firing System	Bed model, coupling and volatiles	Turbulence model	Reaction mechanism	Combustion model	Radiation	Additional models
Tabet et al. 2016 [233]	Wood logs	Domestic wood log stove 10kW	Porous medium, fuel bed divided into layers for drying, pyrolysis and char combustion, CH_{x_1}, CH_{x_2}, CO, CO_2, H_2O, O_2, N_2	Standard k-ε model	$CH_{x_1} + \frac{x_1-x_2}{4}(O_2 + \Lambda N_2) \rightarrow CH_{x_2} + \frac{x_1-x_2}{2} H_2O + \Lambda \frac{x_1-x_2}{4} N_2$; $CH_{x_2} + \frac{2+x_2}{4} (O_2 + \Lambda N_2) \rightarrow CO + \frac{x_2}{2} H_2O + \Lambda \frac{2+x_2}{4} N_2$; $CO + \frac{1}{2}(O_2 + \Lambda N_2) \rightarrow CO_2 + \frac{\Lambda}{2} N_2$; with $\Lambda = 3.76$	PDF	DOM, WSGGM	

based on the same assumption as van der Lans et al. In this approach the biomass bed was discretized into columns, which moved along the grate.

Miljković et al. developed a two-dimensional model for the biomass bed of a moving grate [135], in which the whole biomass bed was represented by a continuous porous medium. The in-house C++ code showed good results compared to experiments.

In [128, 129, 136] a two-dimensional simulation of a slice of a packed bed model is presented. The models are exceptional among the other approaches, which all relate to moving grates.

Comprehensive simulations with two-dimensional models are presented in publications [187, 190, 192–195]. These comprehensive simulations use bed models, which were described previously in separate publications. Two-dimensional bed models are described in Table 3. The comprehensive simulations are summarized in Tables 7, 8 and 9 in Section 5 and references to the used bed models are given.

Three-dimensional Separate three-dimensional bed models are rare among publications of biomass combustion simulations. Most three-dimensional models are included in the comprehensive simulation as sub-model based on porous medium calculations (see Section 2.3.4). A three-dimensional separate bed model for the simulation of coal and biomass combustion in a domestic small-scale boiler was published by Buczyński et al. [196]. Mehrabian et al. [105] present a coupled model of CFD simulation and porous medium with thermally thick particles, conversion processes in particles are calculated separately in UDF, coupled by source terms and boundary conditions for the fixed bed model.

Separate bed models are more flexible with regard to the used biomass and the simulated system than empirical bed models. The versatile usage of the FLIC model shows that one existing model can be used to simulate several similar combustion systems with only minor changes. The computational effort of separate bed models is low and fuel bed model and gas-phase combustion can be developed independently from each other. Interaction of the fuel bed and the free board can be applied by two-way coupling. However, the change of the geometry of the fuel bed and its influence on the flow in the combustion chamber can only be described by a moving grid in the simulation of the free board. Separate bed models are predominantly used for combustion systems with a fuel bed of bulk material and a continuous operation mode like pellet boilers or systems with moving grate.

2.3.3 Discrete particle method

The discrete particle method (DPM) can be used for the simulation of fuel beds consisting of bulk material like wood

chips or pellets. The biomass particles are represented by Lagrangian particles in these simulations. Their trajectory is calculated based on the forces that apply on the particle, which are the drag by the fluid flow of the gas phase, gravity and interaction with other particles or walls. Mass, size distribution and particle-particle interactions can be assigned to the particles. The thermo-chemical conversion of each fuel particle is calculated individually. Depending on the Biot number (1), particles are treated as thermally thin or thick [40, 110, 131].

Hettel et al. [201] created a program to simulate the pyrolysis of wood pellets. The program PACO calculated the products of pyrolysis for a one-dimensional model. The processes of evaporation, pyrolysis and combustion were considered in the model. Since PACO calculated the thermo-chemical conversion of the particles very fast, it was possible to couple the one-dimensional model with a CFD simulation. A discrete particle model can be coupled with discrete element method (DEM) to enhance the simulation of particle-particle interaction (stickiness, collision, etc.) and particle movement (rotation) [131].

The DPM approach allows a very detailed description of the fuel particles in a bed model. Especially for models of a moving grate, the accurate simulation of the particle movement is interesting. However, it is computationally expensive, as each particle is considered individually.

2.3.4 Porous medium

Increasing computational resources enable the simultaneous simulation of fuel bed and gas-phase reactions. Therefore, the porous medium approach advanced recently in biomass combustion modelling. The biomass bed is modelled as porous medium, which allows the (primary) air to flow through the biomass bed. Heat and mass exchange between solid and gaseous phase are considered. Since the porous zone is modelled as a multi-phase region with two continuous phases, it is also referred to as Euler-Euler approach [202, 203]. A computational cell contains gaseous and solid phase, the relation is defined by the porosity. The necessary parameters for the properties of the porous medium are taken from measurements.

For most simulations with the porous medium approach, particles are assumed to be thermally thin [43, 109, 116, 132, 202]. But there are also models, which account for thermally thick particles by an additional sub-model for intra-particle gradients [133, 142, 156].

In porous medium approaches, no difference is made between gas-phase reactions in the fuel bed and in the free board, as bed and free board are simulated in one domain. Consequently, in Table 6, the mechanisms of the gas-phase reactions are presented.

3 Gas-phase modelling

The simulation of gas-phase combustion includes models for turbulence, interaction of chemical reactions and mixing (combustion model), reaction mechanisms and radiation. Research in combustion simulation is already advanced in various topics and the mainly used models are described in detail elsewhere [8, 213]. This chapter focuses on the modelling approaches used in the examples of comprehensive simulations of biomass combustion systems summarized in Tables 7, 8, 9 and 10.

Gas-phase combustion is grouped into the categories premixed and non-premixed combustion, based on the state of mixture of oxidizer and fuel at the time of ignition. When gaseous fuel and oxidizer are mixed before they enter the combustion chamber, a premixed flame can be observed. In non-premixed flames, mixing and combustion occur simultaneously. Non-premixed flames are also called diffusion flames, since diffusion is in many cases the limiting factor for the combustion reaction. Biomass combustion falls into the category of non-premixed combustion, since the combustible gases from biomass decomposition are mixed with air in the combustion chamber. Premixed as well as non-premixed combustion can occur in laminar or turbulent regime [8, 213].

3.1 Turbulence models

The flow in the free board of biomass combustion systems is predominantly turbulent, although in some applications (for example wood log stoves) laminar regions can be found. Mixing of combustible volatiles and oxidizing air is significantly influenced and improved by turbulence; thus, suitable modelling of turbulence is necessary in the simulation of gas-phase reactions [8].

In computational fluid dynamics, turbulent flow of fluids can be simulated by direct numerical simulation (DNS), by large eddy simulation (LES) and by Reynolds-averaged Navier-Stokes equations (RANS). In DNS, turbulence is not approximated by a model, but simulated directly. Respectively, DNS is very time and CPU demanding. Large data sets are generated by this method and need to be handled. DNS is used in combustion simulation for research and academic purposes. For example, DNS can be used to simulate flames, since they do not require complex geometries. Results of the simulations can be used like experimental data to validate simulation approaches with LES and RANS [214]. The data sets generated with DNS are more comprehensive than experimental data and results are not influenced by the measurement method.

LES provides more accurate results than RANS, since large eddies are considered in the simulation, only small eddies are approximated by models. As well as for RANS,

Table 10 Biomass combustion systems with whole bales of straw

Author and year	Biomass	Firing System	Bed model, coupling and volatiles	Turbulence model	Reaction mechanism	Combustion model	Radiation	Additional models
Miltner et al. 2006/2007 [109, 210]	Baled whole crop maize	PFR; combustor of whole biomass bales	Porous medium, CO, CO_2, H_2O, H_2, C_xH_y	SST k-ω model	Eqs. 33, 34, 37 $NH_3 + O_2 \rightarrow NO + H_2O + 0.5H_2$; $NH_3 * NO \rightarrow N_2 + H_2O + 0.5H_2$; $HCN + O_2 \rightarrow NO + CO + 0.5H_2$; $HCN + NO \rightarrow N_2 + CO + 0.5H_2$	EDC	DOM, WSGGM	NO_x reactions
Djurović 2012 [259]	Soy bean straw	1.56MW boiler with piston feeder for straw bales	Empirical bed model, CH_4, CO_2, CO, O_2, H_2O, N_2, C, based on own measurements	k-ε model with modified parameters	Eq. 33 with n=1, m=4, Eq. 34	Finite rate/eddy dissipation model		

turbulence models are required for the simulation. LES are used for the combustion simulation of simplified application cases (for example 2D geometries or simulation of flames). With increasing CPU availability, the usage of LES becomes more common [215, 216].

Turbulence causes fluctuations in variables, which describe the fluid flow. Those fluctuations are averaged in RANS simulations and are not simulated directly. For engineering applications RANS offers sufficient accuracy in comparatively short calculation times. RANS is widely used to simulate combustion devices like furnaces or internal combustion engines [8]. The system of equations has to be closed by additional equations, which are called turbulence models. In biomass combustion, mainly turbulence models of the k-ε-family are used. These include two transport equations for the closure of the system of equations, one for the turbulent kinetic energy k and one for the dissipation rate ε.

The following turbulence models were used in the various examples in Tables 7, 8, 9 and 10:

- The *standard k-ε model* was introduced in 1972 by Jones and Launder [217]. Due to its simplicity and numerical stability, it is widely used in the simulation of non-reacting and reacting flows for example in furnaces, engines and chemical reactors [8]. Tables 7, 8, 9 and 10 show that the standard k-ε model was used to simulate various biomass combustion systems. Kurz et al. [202] used a modification of the standard k-ε-model to account for the influence of particles on turbulence in a multi-phase flow.
- The *realizable k-ε model* [218] is an improvement of the standard k-ε model, in which a new model equation for the dissipation rate ε and a different non-linear formulation for the eddy viscosity are introduced. It compensates some well-known drawbacks of the standard k-ε-model. It improves the simulation of flows with high strain rates, predicts the spreading rate of jets correctly and leads to better results for rotational flows [218]. It is also widely used among the examples presented in Tables 7, 8, 9 and 10. Yin et al. [187] performed a direct comparison of standard k-ε- and realizable k-ε-model. For their simulated system, the results with realizable k-ε-model were closer to the results measured in experiments.
- The *re-normalization group (RNG) k-ε* model was derived from the Navier-Stokes equations using the re-normalization group theory [219, 220]. Due to this approach, the model constants can be determined by theoretical calculations instead of being based on empirical findings. It provides a more accurate prediction of straining and swirling flows and flows with large anisotropic eddies than the standard k-ε model [221].

- To account for flow with low Reynolds number, numerous *low Reynolds number k-ε models* were developed. A review on popular models was given by Patel et al. in 1985 [222]. Low Reynolds number turbulence models require a finer discretization of the near-wall region, since the logarithmic wall function, which is used to describe the behaviour of the flow near to the wall in the standard k-ε model, is only applicable for highly turbulent flows. Additionally, modifications of the equation for the turbulent kinetic energy k are necessary [223]. Especially for the simulation of wood log stoves, the usage of a low Reynolds number k-ε model should be considered.
- The *k-ω model* with $\omega = k/\varepsilon$ is known to have a better performance in the near-wall region than the k-ε model, whereas the k-ε model is preferred for the simulation of the core flow. The *shear stress transport (SST) k-ω model* uses the k-ε model for the core flow and the k-ω model for the near-wall region to combine the advantages of both models [223]. The k-ω model was used by Galletti et al. [180] for the simulation of a wood chip combustion with moving grate. In comparison with other turbulence models, the k-ω model had a slightly weaker performance. The SST k-ω model was only used by Miltner et al. [210] for the simulation of the combustion of a full bale of straw.
- The above-mentioned two-equation models are based on the assumption that the turbulence of the flow is isotropic. For many practical applications, this assumption is not applicable. The *differential Reynolds stress model (RSM)* can be used for flows with anisotropic turbulence. However, it leads to six additional differential equations and an increasing computational effort [223, 224]. Therefore, the RSM model is not widely used in combustion simulation, even though it may lead to more accurate results than a two-equation model.

A comparison of simulations with k-ε-, low Reynolds number k-ε and Reynolds stress turbulence model and experimental results was published by Knaus et al. in 2000 [224]. They conducted simulations of a wood log stove with the in-house code AIOLOS. The best agreement between simulation and experimental results were produced with the low Reynolds number k-ε-turbulence model. Since they expected regions with low Reynolds number in the investigated stove, this turbulence model was the most suitable for their simulation case. Galletti et al. [180] performed simulations with the standard k-ε model, the realizable k-ε model and the k-ω model for a biomass combustion system for wood chips with a moving grate. They found that the results with the standard k-ε model showed a slightly better agreement with measured values with regard to temperature profiles and CO_2 concentrations than the other models.

Farokhi et al. [225] simulated the free board of a pellet boiler. They compared various possibilities for the turbulence model, combustion model and reaction mechanism. They performed simulations with the standard k-ε model, the RNG k-ε model and the realizable k-ε model. The RNG k-ε model achieved the best results with both tested combustion models (steady flamelet model and eddy dissipation concept), even though the simulation results differed not significantly from each other.

From the mentioned direct comparisons [180, 187, 224, 225], it can be concluded that there is no ideal turbulence model, which is applicable for all biomass combustion systems. In fact, the choice of the turbulence model depends on the given geometry, the flow regime and the other models used in the simulation. The flow in wood log stoves is possibly not fully turbulent. The results of the other models used in the gas-phase simulation are highly influenced by turbulence. Therefore, the turbulence model should be chosen with care and results need to be compared to experimental results.

3.2 Combustion models

The velocity of turbulent combustion is determined by mixing of fuel and oxidizer on the one hand and by the kinetics of the chemical reactions on the other hand. To describe the interaction of turbulence and kinetics, combustion models are used. Based on the given boundary conditions, a suitable combustion model has to be chosen. Combustion models can be divided into eddy break-up models and models based on mixture fraction [213, 226].

The eddy break-up (EBU) model assumes infinitely fast reactions and calculates combustion velocity based on turbulent mixing. The EBU model can be used, when the expression “mixed is burned” is valid. It was developed to describe the combustion of turbulent premixed flames. [8, 213]. To account for turbulent non-premixed flames, the EBU was modified by Magnussen and Hjertager [226] to a model, which is known as eddy dissipation model (EDM). The EDM assumes that the combustion is limited by the mixing of fuel and oxidizer in non-premixed flames. It calculates a combustion rate based on the variables ε and k, which are determined by the turbulence model (see Section 3.1) and on the smaller (and therefore limiting) local concentrations of fuel or oxidizer. This model should only be used with global reaction mechanisms with one or maximum two steps, since the influence of partial reactions or radicals can not be considered in the EDM [185]. The finite rate/eddy dissipation model (FR-ED) is widely used in the simulation of biomass combustion system, as Tables 7 to 10 show. In this model, the Arrhenius rates and the eddy dissipation rates are calculated and the lower of both is used [116].

The eddy dissipation concept (EDC) developed by Magnussen [227] is a further improvement of the EDM. It assumes that the reaction of oxidizer and fuel takes place, when both are mixed on a molecular level. The fine structures, in which the reaction of fuel and oxidizer take place, have a very small volume compared to the rest of the fluid. The combustion reaction is limited by the mass transport from the surrounding fluid to the fine structures. The EDC can be used with complex reaction mechanisms [227], but it can lead to long calculation times, when large mechanisms are used [185].

Usage of in situ adaptive tabulation (ISAT) [228] can reduce calculation time for large reaction mechanisms significantly. ISAT is a method to tabulate the possible results of the chemical reactions in situ during the simulation based on the given conditions. Due to the in situ tabulation, it can be avoided to pre-tabulate states, which are not realizable in the current simulation.

The above-mentioned combustion models were developed based on the assumption of a fully turbulent flow. They are all linked to the turbulence model by the variables ε and k, which are used to determine the mixing in the combustion model. As already mentioned in Section 3.1, in some biomass combustion systems, the assumption of full turbulence is not applicable. In these cases, the combustion model has to account for regions with low Reynolds number as well as the turbulence model. Shiehnejadhesar et al. [229] proposed a combustion model, which is suitable for low and high turbulence regions. It is based on EDC and the finite rate kinetic model. They achieved good results for the simulation of flames with the combustion model, various reaction mechanisms and a modified k-ε turbulence model [229]. In the next step, they applied the new combustion model to the simulation of a pellet burner and compared it with EDM and EDC + ISAT [138].

The above-mentioned combustion models are eddy break-up models. They are widely used for the simulation of biomass combustion, as it is shown in Tables 7, 8, 9 and 10. In the field of non-premixed turbulent combustion, models based on mixture fraction are common [8, 213, 230]. However, they are rarely used for biomass combustion [174]. The mixture fraction ξ is defined as [8]:

$$\xi = \frac{Z_i - Z_{i2}}{Z_{i1} - Z_{i2}} \tag{31}$$

in which Z_{i1} and Z_{i2} are the element mass fractions of the two streams oxidizer and fuel. The definition of ξ is based on the assumption that the diffusivities of all scalars are equal and that all species mix alike [8]. For pure oxidizer, ξ is zero, and for pure fuel, ξ is unity. For the mixture of both, ξ takes values between zero and unity. Since the calculation of the mixture fraction is based on the mass fractions of elements, it is not influenced by chemical reactions and is therefore a conserved scalar [230].

For infinitely fast chemical reactions and adiabatic combustion, all relevant scalars (mass fractions of species, temperature etc.) can be expressed as function of the mixture fraction. The distribution of the mixture fraction can be described by a probability density function (PDF) [213]. There are various possibilities to obtain a suitable PDF. In a widely used approach, the PDF is created from the Favre-averaged mixture fraction $\tilde{\xi}$ and its variance $\widetilde{\xi''^2}$. The other scalars can be calculated based on their relation to the mixture fraction, which is determined by equilibrium chemistry, for instance. Therefore, only two additional conservation equations for $\tilde{\xi}$ and $\widetilde{\xi''^2}$ have to be solved, instead of one for each chemical species. This reduces computation time significantly in comparison to combustion models based on eddy break-up models. However, this approach is only suitable for infinitely fast chemistry and adiabatic combustion. This constrains the usage, especially in terms of modelling CO, NO_x or soot emissions, which are the products of slow reactions [8].

To account for finite rate chemistry in turbulent non-premixed combustion an often used approach is flamelet modelling. Flamelet models are based on the assumption that a turbulent flame can be approximated by small laminar flames, which are called flamelets. This assumption allows the separate calculation of turbulent mixing and chemistry [213, 231]. In a pre-processing step, chemical reactions are tabulated and the tables are looked up during the CFD simulation. As look-up variables, the mixture fraction ξ and the scalar dissipation rate χ are used. Advanced versions of the flamelet approach allow the consideration of ignition and extinction.

Combustion models based on mixture fraction are not common among the examples of biomass combustion system presented in Tables 7, 8, 9 and 10, even though the application of the flamelet approach could lead to reduced calculation time when using large reaction mechanisms. The PDF approach was used by Kim et al. [232] to quantify mixing, but they did not simulate combustion in their model. Tabet et al. [233] used a PDF for the comprehensive simulation of a wood log stove. The flamelet approach was used in several approaches to account for finite chemistry. Venturini et al. [193] and Borello et al. [195] used a flamelet approach and detailed chemistry to simulate the combustion of wood chips. Buchmayr et al. [174] simulated the combustion in a pellet boiler with a flamelet approach to create a computationally inexpensive tool for the reactor development. Farokhi et al. [225] compared steady flamelet model (SFM), unsteady flamelet model (UFM), EDC and a modified EDC for the simulation of a laboratory pellet reactor. They used various turbulence models and reaction mechanisms to investigate the influence of different

models on the computational results. They showed that the combustion model has a considerable impact on the results. The flamelet-based combustion models offered a good prediction of temperature and most species distributions in moderate calculation time. However, they did not predict the formation of species from slow (non-equilibrium) reactions like CO correctly. The best results for the distribution of CO was achieved with the modified EDC. It has to be emphasized that calculation times with EDC were considerably longer than with SFM or UFM especially for large reaction mechanisms, even though ISAT tabulation was used.

3.3 Reaction mechanisms for homogeneous gas-phase reactions

The main reactions in the gas-phase simulation of biomass combustion are the oxidation of hydrocarbons, which were produced during thermo-chemical conversion of biomass in the fuel bed. As well as homogeneous gas-phase reactions in the fuel bed (Section 2.1.6), they can be described by a simple one-step reaction by a global reaction mechanism or by a detailed reaction mechanism. In this section, widely used approaches to describe the chemical reactions in the freeboard are addressed.

As discussed in the previous Section 3.2, calculation of chemical reactions can be time consuming in CFD simulations, if many species are involved. Therefore, global reaction schemes with only few reactions are mainly used for simulations of comprehensive firing systems (see Tables 7, 8, 9 and 10). The reactants of the homogeneous gas-phase reactions have to match with the species released by the bed model. The composition of the combustible gas is therefore often simplified to one or more gaseous hydrocarbons, carbon monoxide, carbon dioxide, hydrogen and water. Light hydrocarbon gas is in most cases represented by methane. The simple one-step reaction for combustion of methane is described by Eq. 32.

$$CH_4 + 2O_2 \rightarrow CO_2 + 2H_2O \tag{32}$$

Benzene C_6H_6 is used to represent heavier gases and tar [99]. Another approach is the usage of a pseudo-gas with the molecular formula $C_xH_yO_z$ to describe the hydrocarbon gas produced in the biomass bed. The parameters x, y and z are calculated from balances of the elements contained in the biomass [43]. Buczynski et al.[196, 212] and Yin et al. [234] added also nitrogen and Galletti et al. [180] added nitrogen and sulphur to the molecular formula of the hydrocarbon gas to account for the formation of nitrogen and sulphur dioxide.

The most popular global reaction schemes for the combustion of hydrocarbons are the ones presented by Westbrook and Dryer in 1981 [235] (WD) and Jones and Lindstedt in 1988 [236] (JL). The WD reaction mechanism describes the two-step oxidation of a hydrocarbon with carbon monoxide as intermediate product [235]:

$$C_xH_y + \left(\frac{x}{2} + \frac{y}{4}\right) O_2 \rightarrow xCO + \frac{y}{2}H_2O \tag{33}$$

$$CO + \frac{1}{2}O_2 \rightarrow CO_2 \tag{34}$$

The JL mechanism is a four-step reaction mechanism with carbon monoxide and hydrogen as intermediate products [236]:

$$C_xH_{2x+2} + x/2O_2 \rightarrow xCO + (x+1)H_2 \tag{35}$$

$$C_xH_{2x+2} + xH_2O \rightarrow xCO + (2x+1)H_2 \tag{36}$$

$$H_2 + \frac{1}{2}O_2 \rightleftharpoons H_2O \tag{37}$$

$$CO + H_2O \rightleftharpoons CO_2 + H_2 \tag{38}$$

Various variations and combinations of both reaction mechanisms have been used in the examples in Tables 7, 8, 9 and 10. To account for pseudo-gas with the molecular formula $C_mH_nO_l$, Eqs. 39 and 40 are used in various publications, for instance [41, 43, 101, 126, 237].

$$C_xH_yO_z + \left(\frac{x}{2} - \frac{z}{2}\right) O_2 \rightarrow xCO + \frac{y}{2}H_2 \tag{39}$$

$$C_xH_yO_z + \left(\frac{x}{2} + \frac{y}{4} - \frac{z}{2}\right) O_2 \rightarrow xCO + \frac{y}{2}H_2O \tag{40}$$

A comparison of WD and JL reaction mechanisms was presented by Yin et al. in 2010 [238] for the co-combustion of straw. Only small difference between the results of both reaction mechanisms were found.

Besides global reaction mechanisms, detailed mechanisms can be used to describe the combustion reactions in the gas phase. Complex reaction mechanisms enhance the accuracy of the prediction of temperatures and exhaust gas compositions. The simulation of pollutants is also improved with complex reaction mechanisms, as intermediate products and products of non-complete combustion are considered. However, the large number of species and reactions tend to slow down simulations significantly. To avoid long CPU times, large reaction mechanisms are used in combination with fast combustion models like the flamelet approach, when they are used in comprehensive simulations of biomass combustion systems.

The most popular mechanism for the combustion of hydrocarbons is GRI-mech 3.0 [239]. It was developed for the combustion of natural gas and is widely used for the oxidation of methane. Besides oxidation of methane, GRI-mech includes reactions to account for oxidation of C2 and C3 hydrocarbons, since ethane and propane can be present in natural gas. However, only small concentrations are expected and the reactions for C2 and C3 chemistry are reduced to a minimum. GRI-mech 2.11 includes 49 species and 277 reactions, GRI-mech 3.0 has 53 species and 325 reactions [239]. DRM22 is a reduced mechanism, which

was derived from GRI-mech. It includes 22 species and 104 reactions.

Development and validation of detailed reaction mechanisms are conducted with simplified test cases and matching experimental data. The investigation of flames, shock tubes or flow reactors allows the analysis of the kinetic model independently from the influence of other models (for example from turbulent mixing or radiation) [240]. Based on existing reaction mechanisms for the combustion of gaseous hydrocarbons or solid fuels, mechanisms for biomass combustion were derived. They were tested and adapted for conditions, which are typical for biomass grate firings [241]. Additional branches for the detailed description of NO_x chemistry [240, 242] or PAH combustion [62, 243] were added. Some mechanisms include chemistry for higher hydrocarbons than methane to account for the variety of gaseous products from pyrolysis and gasification of biomass.

Mehrabian et al. [105] and Shiehnejadhesar [138] used the C-H-O subset of the Kilpinen97 reaction mechanism for their comprehensive simulations. It is based on methane oxidation and includes 12 species and 25 reactions, of which two reactions are Eqs. 35 and 36 of JL global mechanism. The other reactions are a skeletal reaction mechanism derived from Kilpinen97 for the oxidation of the intermediate products H_2 and CO [242]. The NO_x chemistry, which played a major role in the Kilpinen97 mechanism, was omitted for the reduced mechanism.

Farokhi et al. [225] compared 5 reaction mechanisms including the global mechanisms WD and JL. The other three were focussed on the reactions of PAHs and tars (Marinov et al.[244], Ranzi et al. [62] and Richter et al. [245]). Simulations were conducted with EDC combustion model for the global reaction mechanisms and with SFM for the detailed reaction mechanisms. The results show large differences between the global mechanisms (with EDC) and the detailed mechanisms (with SFM) regarding consumption of CH_4 and C_6H_6 and production of CO and CO_2. Due to the simulation cases selected for comparison, it is not possible to say, if the differences can be attributed to the combustion model or the reaction mechanism. The influence of the combustion model is considered to be larger than the influence of the reaction mechanism. Results of both approaches deviate from measured values, but show the same trend as the experiments. The simulations with SFM and detailed chemistry showed significantly lower CO concentrations, which was explained by the authors with the limitation of SFM to predict slow chemistry correctly [225].

As discussed in Section 3.2, the combustion model and the reaction mechanism have to harmonize for the simulations. EDM can only handle global one- or two-step reaction mechanisms, EDC can handle larger mechanisms, but needs long calculation times for detailed chemistry. Flamelet models are fast, but have difficulties to predict slow chemistry correctly.

3.4 Radiation

Heat transfer by radiation has an important impact on the combustion simulation, since the radiative heat flux due to the flame is large compared to heat transfer by convection or conduction. If radiation of the flame to the walls of the reactor is not considered in the calculations, temperatures in the combustion chamber will not be calculated correctly. Furthermore, radiation accounts for the largest share in heat transfer from free board to the biomass bed. The accurate description of radiation is therefore important for the coupling of bed model and gas-phase combustion.

Radiative heat transfer is described by the radiative transfer equation (RTE). It contains terms for adsorption, emission and scattering of the medium, through which the radiation passes [185, 246].

Widespread radiation models for combustion simulation are the discrete ordinate radiation model (DOM) and the P1 model. DOM is based on the solution of the RTE for a finite number of discrete angles. Therefore, it is computationally expensive, when a fine discretization is chosen. The P_N model is based on the assumption that the radiation intensity can be expressed by spherical harmonics. The simplest case of the P_N model is the P1 model, in which the RTE is simplified to a elliptical partial differential equation. The computational costs of P1 model are lower in comparison with DOM, but DOM is known to obtain more accurate results [247, 248].

The emissivity of the gases, through which the heat is transferred, is needed to calculate their absorption coefficient. In many engineering applications, the total emissivity of the gases is calculated by the weighted-sum-of-gray-gases model (WSSGM) [185, 247].

In the examples listed in Tables 7, 8, 9 and 10, predominantly DOM and DOM in combination with WSGGM are used. The P1 model is only used in several examples.

An extensive study on radiative heat transfer in biomass furnaces with fixed bed was conducted by Klason et al. in 2008 [247]. They explained the commonly used models in detail and analyzed the influence of the radiation model on the gas-phase temperature and on the heat transfer from free board to the biomass bed for two examples. They used a 10-kW laboratory furnace and a 50-MW industrial furnace for their investigation. They came to the conclusion that the P1 model achieves fairly good results with low computational effort for the simulation of radiation in the combustion chamber. However, it is not suitable to calculate the radiation from the flame to the bed and should therefore not be used in simulations with a coupled bed model [247].

4 Additional models

In many cases, the objective of CFD simulations is the reduction of emissions from biomass combustion. Therefore, a detailed description of the formation processes of emissions is necessary and additional models are added to the CFD simulation. The models are based on established theories for the formation processes and often derived from experimental investigations. An recent overview about the mechanisms of pollutant formation from biomass combustion was presented by William et al. [249].

4.1 NO_x

Three different pathways for NO_x formation are known in combustion science and can be considered in CFD simulations. In high temperature ranges, NO_x is formed from atmospheric nitrogen (thermal NO_x). The presence of hydrocarbon-radicals can promote other reactions to form NO_x from atmospheric nitrogen (prompt NO_x). Finally, NO_x can be formed from nitrogen-containing species produced during thermo-chemical conversion of fuel (fuel NO_x). In biomass combustion, NO_x is predominantly formed by nitrogen from the fuel, as the conditions which are necessary for the other formation routes are not given in biomass combustion. In biogenic fuels, nitrogen is contained in amines and proteins and released during thermo-chemical conversion [7]. The formation route for fuel NO_x can be described by additional reactions in the reaction scheme for the gas-phase combustion [250]. Extensive reviews about nitrogen chemistry in solid fuels and in the gas phase were published by Glarborg et al. in 2003 and in 2018 [151, 251].

It has to be taken into account that NO_x chemistry is slow in comparison with combustion reactions. Therefore, a combustion model, which can handle finite rate chemistry, has to be used. An alternative is the calculation of NO_x in a post-processing step. Zahirovic et al [252] investigated the prediction of NO_x formation of six reaction mechanisms in three different flames. They came to the conclusion that the results for the combustion (temperature distribution and CO concentration) depended strongly on the turbulence and combustion models, due to the mixing-limited behaviour of the combustion. Contrary to that, they found the results of the NO_x formation were influenced by the used reaction mechanism, since the formation of thermal and fuel NO_x was kinetically dominated. The use of a reaction mechanism with a more detailed N subset led to more accurate results, but also to higher computational costs.

4.2 Particulate emissions

Particulate emissions from biomass combustion systems are produced following various routes, which lead to different properties of the particles. Coarse particles are formed from ash and wood particles, which are entrained by the flow of flue gases during combustion. They can be described by Lagrangian particles in the CFD simulation, which are released from the biomass bed with a certain size distribution and carried by the fluid flow [99]. The formation of inorganic particles and soot particles should be distinguished, when modelling particulate emissions. Formation of inorganic aerosols is linked to the release of inorganic components (K, S, Cl, Na, Zn, Pb) during thermochemical decomposition of biomass. The formation process was described in detail for example by Niu et al. [253]. Aerosols develop, when gaseous precursors react and particles are formed in the cooling gas stream above the flame. The processes nucleation, coagulation, agglomeration and condensation are involved in aerosol formation. Additionally, mechanisms for precipitation of particles on surfaces have to be considered. The mentioned processes are described by equations and can be implemented into a CFD simulation in this way [254]. Another model for the formation and growth of aerosols was presented by Niu et al. [255]. Even though it was developed for coal combustion, the underlying models for particle formation are alike for both fields.

Similar mechanisms are present during the formation of soot particles. Formation and consumption of soot can be described by various models. Widely used and installed in most commercial software is the model of Brookes and Moss [256]. In this model two new species (soot and radical nuclei) are defined and an additional continuity equation is solved for each of them. The soot formation rate in this model depends on temperature and concentration of precursors like acetylene.

4.3 Emission of pollutants

Kim et al. [232] modelled the decomposition of pollutants (dioxin, furan, chlorobenzene, chloroform etc.) based on mixing (PDF) and residence time. A new factor β described the thermal decomposition of a pollutant along its trajectory. An Arrhenius-type reaction with empirical parameters was integrated along the trajectory to describe the state of conversion of the pollutant, since it was assumed that the decomposition of the pollutants depends on temperature and residence time. The trajectories of the pollutants from the place of their release at the grate to the outlet of the furnace were defined by the particle tracking method.

5 Comprehensive simulations of biomass combustion systems

In this section, comprehensive simulations of biomass combustion systems are summarized. They are grouped

according to the technology of the investigated firing system: combustion systems with moving grate, pellet boilers, wood log stoves and whole bales of straw.

5.1 Moving grate

The largest group of publications is related to firing systems with moving grate (see Table 7). This technology is used over a wide range of power outputs from large scale to industry scale (240 kW to 108 MW). Fuel is fed continuously and transported along the grate until the thermo-chemical conversion of the fuel is completed. The mainly used biomass types are wood chips, straw and municipal solid waste (MSW). Empirical, two-dimensional separate and DPM-based bed models are used to describe the fuel bed. CFD simulations are used to predict temperatures inside the combustion chamber and emission of CO, NO_x, ash and pollutants. They are compared with measurements, wherever experimental results are available.

5.2 Pellet boilers

An overview over comprehensive simulations of pellet boilers is given in Table 8. Publications about numerically investigated pellet boilers include laboratory to medium scale boilers for domestic firing systems (8 kW to 250 kW). They are operated continuously with various feeding systems. Either underfeed systems, where the fuel is fed from below the pellet burner or pellet-drop systems, where pellets are transported above the bed and fall down onto the pellet burner are used in the presented publications. For CFD simulations, predominantly empirical or porous medium bed models are used.

5.3 Wood log stoves

Wood log stoves (Table 9) are used for domestic heating. In many cases, they are used as additional heat source and are designed to heat only one room. The power output of the examples in Table 9 is in the region of 32 kW. A particular challenge in CFD simulations of wood log stoves are the various time scales during combustion of the wood. On the one hand, the transient process of wood combustion in the batch fed combustion chamber has to be taken into account. The combustion of the wood logs takes approximately 30 min to 1 h and undergoes various stages of combustion. On the other hand, chemical reactions of combustion are very fast and need to be simulated with small time steps to prevent numerical problems. To avoid this conflict, some authors limit their simulation to the almost stationary phase of combustion and use a stationary simulation approach. For example, Athanasios et al. [237] used a simplified bed model and simulated only the phase of combustion, which can be assumed to be stationary. In the examples in Table 9, the transient process of wood combustion is modelled in one-dimensional separate, empirical or porous medium bed models. Since regions with low turbulence may occur in wood log stoves, a low Reynolds number k-ε model was used by Knaus et al. [224], by Galgano et al. [92] and by Menghini et al. [183]. The combustion reactions were represented by global reaction mechanisms in all examples. Predominantly, the eddy dissipation concept was used as combustion model. The DOM was used in all examples to account for radiation. Schütz [257] and Sènèchal [258] included soot formation in their models.

5.4 Whole bales of straw

The combustion of whole bales of straw is grouped separately in Table 10, since the technology and therefore also the used sub-models are different from the other comprehensive simulations. Miltner et al. [109, 210] considered the straw inside the combustion domain and used a porous medium bed model for this. Djurović [259] focused on the gas-phase combustion in their two-dimensional CFD study and used an empirical bed model to simulate release of volatiles.

6 Conclusions

A comprehensive review on CFD-based models for the simulation of biomass combustion systems and the required sub-models was conducted in the present study. The most important features of the models were compared in tables. Modelling approaches for various combustion systems with fixed bed and moving grate were selected and grouped according to the simulated technology.

Various approaches for the simulation of biomass combustion are already available in the literature. In most of the discussed examples, the models are tailor made to describe specific biomass combustion systems and types of biomass. The modelling approaches constantly evolve and include important sub-models to describe most aspects of biomass combustion.

The choice of the models for the CFD simulation of biomass combustion depends mainly on the simulated application and the research question. However, it might be limited by the available information about the boundary conditions and the available computational resources. Therefore, it is difficult to draw a general conclusion, which models are most suitable for the simulation of biomass combustion. The listings of examples sorted by simulated technology in combination with the detailed description of the models can be a good starting point for the set-up of new simulations. Since many different models are available and

simplifications as well as assumptions have to be made to simulate a complete combustion system, simulation results should be always validated with experimental data.

Further development of simulation tools for biomass combustion is on the one hand needed to increase the accuracy of sub-models. In particular, the sub-models for pyrolysis, release of precursors for pollutants and specific reaction mechanisms for biomass combustion are in the focus of the current research in this field. Not all of theses processes are yet exactly understood and can be completely described by models. Additionally, the improvements, which are made in the sub-models, have to be transferred to comprehensive CFD simulations. On the other hand, developments, which lead to higher computational efficiency, are also needed. This would create the possibility to reduce the number of experiments significantly and to conduct optimizations. Another important issue is the description of operation conditions, which deviate from the normal state (stationary and full load). Emissions are especially high during ignition and burnout of combustion systems and future CFD simulations should be able to describe these phases. The flexibility of fuel bed models has to be increased, to broaden their applicability to combustion systems with different types of biomass and flexible operation conditions.

Funding information This research work is kindly supported by the German Federal Ministry of Food and Agriculture (BMEL).

Abbreviations BTX, benzene, toluene, xylene; CFD, computational fluid dynamics; CPU, central processing unit; DEM, discrete element method; DNS, direct numerical simulation; DOM, discrete ordinate model; DPM, discrete particle model; DTRM, discrete transfer radiation model; EBU, eddy break-up model; EDC, eddy dissipation concept; EDCM, eddy dissipation combustion model; EDM, eddy dissipation model; FR-ED, finite rate/eddy dissipation model; FTIR, Fourier transform infrared spectroscopy; GC-TCD, gas chromatography–thermal conductivity detector; GRI, gas research institute; ISAT, in situ adaptive tabulation; JL, Jones and Lindstedt; LES, large eddy simulation; MSW, municipal solid waste; PAC, polyaromatic compounds; PAH, polycyclic aromatic hydrocarbons; PDF, probability density function; PFR, plug flow reactor; RANS, Reynolds-averaged Navier-Stokes equations; RNA, reactor network array; RNG, re-normalization group (k-ε model); RSM, differential Reynolds stress model; RTE, radiative ransfer equation; SFM, steady flamelet model; SST, shear stress transport (k-ω model); TGA, thermogravimetric analysis; UDF, user-defined function; UFM, unsteady flamelet model; WD, Westbrook and Dryer; WSSGM, weighted-sum-of-gray-gases model.

References

1. Thrän D (ed) (2015) Smart bioenergy: Technologies and concepts for a more flexible bioenergy provision in future energy systems. Springer International Publishing, Cham
2. Szarka N, Scholwin F, Trommler M, Jacobi FH, Eichhorn M, Ortwein A, Thrän D (2013) Energy 61:18. https://doi.org/10.1016/j.energy.2012.12.053
3. Thrän D, Dotzauer M, Lenz V, Liebetrau J, Ortwein A (2015) Energy Sustain Soc 5(1):21. https://doi.org/10.1186/s13705-015-0062-8
4. Pollex A, Ortwein A, Kaltschmitt M (2012) Biomass convers. Biorefin 2(1):21. https://doi.org/10.1007/s13399-011-0025-z
5. Lenz V, Ortwein A (2017) Chem Eng Technol 40(2):313. https://doi.org/10.1002/ceat.201600188
6. Ortwein A, Lenz V (2015). In: Thrän D (ed) Smart Bioenergy,. Springer International Publishing, Cham, pp 49–66. https://doi.org/10.1007/978-3-319-16193-8_4
7. Kaltschmitt M, Hartmann H, Hofbauer H (2016) Energie aus Biomasse, Springer, Berlin. https://doi.org/10.1007/978-3-662-47438-9
8. Warnatz J, Maas U, Dibble RW (2006) Combustion: physical and chemical fundamentals, modeling and simulation, experiments, pollutant formation, 4th. Springer, Berlin
9. Wu B (2013) Comput Electron. Agr. 93:195. https://doi.org/10.1016/j.compag.2012.05.008
10. Lee IB, Bitog JPP, Hong SW, Seo IH, Kwon KS, Bartzanas T, Kacira M (2013) Comput Electron Agric 93:168. https://doi.org/10.1016/j.compag.2012.09.006
11. Kong SC, Reitz RD (2002) Proc Combust Inst 29(1):663. https://doi.org/10.1016/S1540-7489(02)80085-2
12. Rutland CJ (2011) Int J Engine Res 12(5):421. https://doi.org/10.1177/1468087411407248
13. Williams A, Pourkashanian M, Jones JM (2000) Proc Combust Inst 28(2):2141. https://doi.org/10.1016/S0082-0784(00)80624-4 http://linkinghub.elsevier.com/retrieve/pii/S0082078400806244
14. Yin C, Rosendahl LA, Kær SK (2008) Prog Energy Combust Sci 34(6):725. https://doi.org/10.1016/j.pecs.2008.05.002
15. Jones JM, Lea-Langton AR, Ma L, Pourkashanian M, Williams A (2014) Pollutants generated by the combustion of solid biomass fuels. Springerbriefs in applied sciences and technology. Springer, London
16. Tabet F, Gökalp I (2015) Renewable Sustainable Energy Rev 51:1101. https://doi.org/10.1016/j.rser.2015.07.045. http://linkinghub.elsevier.com/retrieve/pii/S1364032115006929
17. Khodaei H, Al-Abdeli YM, Guzzomi F, Yeoh GH (2015) Energy 88:946. https://doi.org/10.1016/j.energy.2015.05.099
18. Ragland KW, Aerts DJ, Baker AJ (1991) Bioresour Technol 37(2):161. https://doi.org/10.1016/0960-8524(91)90205-X
19. Grønli MG (1996) A theoretical and experimental study of the thermal degradation of biomass. Ph.D. thesis, Norwegian University of Sience and Technology, Trondheim
20. Melaaen MC (1996) Numerical heat transfer. Part A: Applications 29(4):331. https://doi.org/10.1080/10407789608913796
21. Thunman H, Leckner B (2002) Biomass Bioenergy 23(1):47. https://doi.org/10.1016/S0961-9534(02)00031-4
22. Plötze M, Niemz P (2011) Eur J Wood Prod 69(4):649. https://doi.org/10.1007/s00107-010-0504-0
23. Dupont C, Chiriac R, Gauthier G, Toche F (2014) Fuel 115:644. https://doi.org/10.1016/j.fuel.2013.07.086
24. Fatehi M, Kaviany M (1997) Int J Heat Mass Transfer 40(11):2607. https://doi.org/10.1016/S0017-9310(96)00282-7
25. Cooper J, Hallett W (2000) Chem Eng Sci 55(20):4451. https://doi.org/10.1016/S0009-2509(00)00097-X
26. Saastamoinen JJ, Taipale R, Horttanainen M, Sarkomaa P (2000) Combust Flame 123(1-2):214. https://doi.org/10.1016/S0010-2180(00)00144-9
27. Bryden KM, Ragland KW, Rutland CJ (2002) Biomass Bioenergy 22(1):41. https://doi.org/10.1016/S0961-9534(01)00060-5

28. Pyle DL, Zaror CA (1984) Chem Eng Sci 39(1):147. https://doi.org/10.1016/0009-2509(84)80140-2
29. Siau JF (1984) Transport processes in wood. Springer, Berlin
30. Di Blasi C (1998) Chem Eng Sci 53(2):353
31. Mehrabian R, Zahirovic S, Scharler R, Obernberger I, Kleditzsch S, Wirtz S, Scherer V, Lu H, Baxter LL (2012) Fuel Process Technol 95:96. https://doi.org/10.1016/j.fuproc.2011.11.021
32. Jalili M (2015) Multi-scale modeling of fixed-bed drying of woody fuel particles. Ph.D. thesis, TU Berlin
33. Di Blasi C, Branca C, Sparano S, La Mantia B (2003) Biomass Bioenergy 25(1):45. https://doi.org/10.1016/S0961-9534(02)00180-0
34. Thunman H, Leckner B, Niklasson F, Johnsson F (2002) Combust Flame 129(1-2):30. https://doi.org/10.1016/S0010-2180(01)00371-6
35. Chan WCR, Kelbon M, Krieger BB (1985) Fuel 64(11):1505. https://doi.org/10.1016/0016-2361(85)90364-3
36. Sreekanth M, Sudhakar DR, Prasad B, Kolar AK, Leckner B (2008) Fuel 87(12):2698. https://doi.org/10.1016/j.fuel.2008.02.005
37. Bryden KM, Hagge MJ (2003) Fuel 82(13):1633. https://doi.org/10.1016/S0016-2361(03)00108-X
38. Porteiro J, Míguez JL, Granada E, Moran JC (2006) Fuel Process Technol 87(2):169. https://doi.org/10.1016/j.fuproc.2005.08.012
39. Saastamoinen J, Richard JR (1996) Combust Flame 106(3):288. https://doi.org/10.1016/0010-2180(96)00001-6
40. Peters B (2002) Combust Flame 131(1-2):132. https://doi.org/10.1016/S0010-2180(02)00393-0
41. Zhou H, Jensen A, Glarborg P, Jensen P, Kavaliauskas A (2005) Fuel 84(4):389. https://doi.org/10.1016/j.fuel.2004.09.020
42. Wurzenberger JC, Wallner S, Raupenstrauch H, Khinast JG (2002) AIChE J 48(10):2398. https://doi.org/10.1002/aic.690481029
43. Chaney J, Liu H, Li J (2012) Energy Convers Manage 63:149. https://doi.org/10.1016/j.enconman.2012.01.036
44. Zhang X, Chen Q, Bradford R, Sharifi V, Swithenbank J (2010) Fuel Process Technol 91(11):1491. https://doi.org/10.1016/j.fuproc.2010.05.026
45. Yang YB, Yamauchi H, Nasserzadeh V, Swithenbank J (2003) Fuel 82(18):2205. https://doi.org/10.1016/S0016-2361(03)00145-5
46. Anca-Couce A (2016) Prog Energy Combust Sci 53:41. https://doi.org/10.1016/j.pecs.2015.10.002
47. Di Blasi C (2008) Prog Energy Combust Sci 34(1):47. https://doi.org/10.1016/j.pecs.2006.12.001
48. Czernik S, Bridgwater AV (2004) Energy & Fuels 18(2):590. https://doi.org/10.1021/ef034067u
49. Antal MJ, Grønli M (2003) Ind Eng Chem Res 42(8):1619. https://doi.org/10.1021/ie0207919
50. Di Blasi C (2009) Prog Energy Combust Sci 35(2):121. https://doi.org/10.1016/j.pecs.2008.08.001
51. White JE, Catallo WJ, Legendre BL (2011) J Anal Appl Pyrolysis 91(1):1. https://doi.org/10.1016/j.jaap.2011.01.004
52. Şensöz S, Can M (2002) Energy Sources 24(4):347. https://doi.org/10.1080/00908310252888727
53. Raveendran K, Ganesh A, Khilar KC (1996) Fuel 75(8):987. https://doi.org/10.1016/0016-2361(96)00030-0
54. Di Blasi C (1996) Ind Eng Chem Res 35(1):37. https://doi.org/10.1021/ie950243d
55. Anca-Couce A (2012) Multi-scale approach to describe fixed-bed thermo-chemical processes of biomass. Ph.D. thesis, TU Berlin
56. Peters B, Schröder E, Bruch C (2003) J Appl Pyrolysis 70(2):211. https://doi.org/10.1016/S0165-2370(02)00133-X
57. Dieguez-Alonso A, Anca-Couce A, Zobel N (2013) J Anal Appl Pyrol 102:33. https://doi.org/10.1016/j.jaap.2013.04.005
58. Anca-Couce A, Dieguez-Alonso A, Zobel N, Berger A, Kienzl N, Behrendt F (2017) Energy & Fuels 31(3):2335. https://doi.org/10.1021/acs.energyfuels.6b02350
59. Lédé J (2013) Oil Gas Sci Technol - Rev IFP Energies Nouvelles 68(5):801. https://doi.org/10.2516/ogst/2013108
60. Evans RJ, Milne TA (1987) Energy Fuels 1(2):123. https://doi.org/10.1021/ef00002a001
61. Milne TA, Evans RJ, Abatzaglou N Biomass gasifier "tars": their nature, formation, and conversion. https://doi.org/10.2172/3726.NREL/TP-570-25357
62. Ranzi E, Cuoci A, Faravelli T, Frassoldati A, Migliavacca G, Pierucci S, Sommariva S (2008) Energy Fuels 22(6):4292. https://doi.org/10.1021/ef800551t
63. Antal MJ Jr, Várhegyi G (1995) Ind Eng Chem Res 34(3):703. https://doi.org/10.1021/ie00042a001
64. Grønli MG, Várhegyi G, Di Blasi C (2002) Ind Eng Chem Res 41(17):4201. https://doi.org/10.1021/ie0201157
65. Di Blasi C (2000) Chem Eng Sci 55(15):2931. https://doi.org/10.1016/S0009-2509(99)00562-X
66. Di Blasi C (2004) AIChE J 50(9):2306. https://doi.org/10.1002/aic.10189
67. Liden AG, Berruti F, Scott DS (1988) Chem Eng Commun 65(1):207. https://doi.org/10.1080/00986448808940254
68. Boroson ML, Howard JB, Longwell JP, Peters WA (1989) AIChE J 35(1):120. https://doi.org/10.1002/aic.690350113
69. Shafizadeh F, Chin PPS (1977) In: Goldstein IS (ed) Wood technology: chemical aspects. American Chemical Society, Washington, DC, pp 57–81
70. Piskorz J, Radlein DS, Scott DS, Czernik S (1989) J Anal Appl Pyrolysis 16(2):127. https://doi.org/10.1016/0165-2370(89)85012-0
71. Broido A, Nelson MA (1975) Combust Flame 24:263. https://doi.org/10.1016/0010-2180(75)90156-X
72. Broido A (1976) In: Shafizadeh F, Sarkanen KV, Tillman DA (eds) Thermal uses and properties of carbohydrates and lignins. Academic Press, New York, pp 19–36. https://doi.org/10.1016/B978-0-12-637750-7.50006-6
73. Shafizadeh F, Bradbury AGW (1979) J Appl Polym Sci 23(5):1431. https://doi.org/10.1002/app.1979.070230513
74. Bradbury AGW, Sakai Y, Shafizadeh F (1979) J Appl Polym Sci 23(11):3271. https://doi.org/10.1002/app.1979.070231112
75. Várhegyi G, Szabó P, Mok WSL, Antal MJ (1993) J Anal Appl Pyrolysis 26(3):159. https://doi.org/10.1016/0165-2370(93)80064-7
76. Mok WSL, Antal MJ (1983) Thermochim Acta 68(2-3):165. https://doi.org/10.1016/0040-6031(83)80222-6
77. Richards GN (1987) J Anal Appl Pyrolysis 10(3):251. https://doi.org/10.1016/0165-2370(87)80006-2
78. Mamleev V, Bourbigot S, Le bras M, Yvon J (2009) J Anal Appl Pyrolysis 84(1):1. https://doi.org/10.1016/j.jaap.2008.10.014
79. Corbetta M, Frassoldati A, Bennadji H, Smith K, Serapiglia MJ, Gauthier G, Melkior T, Ranzi E, Fisher EM (2014) Energy Fuels 28(6):3884. https://doi.org/10.1021/ef500525v
80. Ranzi E, Pierucci S, Aliprandi PC, Stringa S (2011) Energy Fuels 25(9):4195. https://doi.org/10.1021/ef200902v
81. Ranzi E, Corbetta M, Manenti F, Pierucci S (2014) Chem Eng Sci 110:2. https://doi.org/10.1016/j.ces.2013.08.014
82. Anca-Couce A, Mehrabian R, Scharler R, Obernberger I (2014) Energy Convers Manage 87:687. https://doi.org/10.1016/j.enconman.2014.07.061
83. Thurner F, Mann U (1981) Ind Eng Chem Process Des Dev 20(3):482. https://doi.org/10.1021/i200014a015
84. Nunn TR, Howard JB, Longwell JP, Peters WA (1985) Ind Eng Chem Process Des Dev 24(3):836. https://doi.org/10.1021/i200030a053

85. Alves SS, Figueiredo JL (1988) J Anal Appl Pyrolysis 13(1-2):123. https://doi.org/10.1016/0165-2370(88)80052-4
86. Font R, Marcilla A, Verdu E, Devesa J (1990) Ind Eng Chem Res 29(9):1846. https://doi.org/10.1021/ie00105a016
87. Roberts AF (1970) Combust Flame 14(2):261. https://doi.org/10.1016/S0010-2180(70)80037-2
88. Di Blasib C (1996) Chem Eng Sci 51(7):1121. https://doi.org/10.1016/S0009-2509(96)80011-X
89. Roberts A, Clough G (1963) Symp (Int) Combust 9(1):158. https://doi.org/10.1016/S0082-0784(63)80022-3
90. Di Blasi C, Signorelli G, Portoricco G (1999) Ind Eng Chem Res 38(7):2571. https://doi.org/10.1021/ie980753i
91. Bassilakis R, Carangelo R, Wójtowicz M (2001) Fuel 80(12):1765. https://doi.org/10.1016/S0016-2361(01)00061-8
92. Galgano A, Di Blasi C (2006) Prog Comput Fluid Dyn 6(4/5):287. https://doi.org/10.1504/PCFD.2006.010037
93. Galgano A, Di Blasi C (2003) Ind Eng Chem Res 42(10):2101. https://doi.org/10.1021/ie020939o
94. Di Blasi C, Branca C (2001) Ind Eng Chem Res 40(23):5547. https://doi.org/10.1021/ie000997e
95. Adams T (1980) Combust Flame 39(3):225. https://doi.org/10.1016/0010-2180(80)90020-6
96. Shin D, Choi S (2000) Combust Flame 121(1-2):167. https://doi.org/10.1016/S0010-2180(99)00124-8
97. Hagge MJ, Bryden KM (2002) Chem Eng Sci 57(14):2811. https://doi.org/10.1016/S0009-2509(02)00167-7
98. Porteiro J, Granada E, Collazo J, Patiño D, Morán JC (2007) Energy Fuels 21(6):3151. https://doi.org/10.1021/ef0701891
99. Porteiro J, Collazo J, Patiño D, Granada E, Moran Gonzalez JC, Míguez JL (2009) Energy Fuels 23(2):1067. https://doi.org/10.1021/ef8008458
100. Saastamoinen J, Richard J (1988) In: Bridgwater AV, Kuester JL (eds) Res. Thermochem. Biomass Convers. Springer, Netherlands, pp 221–235. https://doi.org/10.1007/978-94-009-2737-7_18
101. Johansson R, Thunman H, Leckner B (2007) Combust Flame 149(1-2):49. https://doi.org/10.1016/j.combustflame.2006.12.009
102. Seebauer V (1999) Experimentelle Untersuchung zur Pyrolyse von Kohle und Holz. Ph.D. thesis Graz University of Technology
103. Rath J, Wolfingera MG, Steiner G, Krammer G, Barontini F, Cozzani V (2003) Fuel 82(1):81. https://doi.org/10.1016/S0016-2361(02)00138-2
104. Branca C, Albano A, Di Blasi C (2005) Thermochim Acta 429(2):133. https://doi.org/10.1016/j.tca.2005.02.030. http://linkinghub.elsevier.com/retrieve/pii/S0040603105001541
105. Mehrabian R, Shiehnejadhesar A, Scharler R, Obernberger I (2014) Fuel 122:164. https://doi.org/10.1016/j.fuel.2014.01.027
106. Ranzi E, Frassoldati A, Grana R, Cuoci A, Faravelli T, Kelley A, Law C (2012) Prog Energy Combust Sci 38(4):468. https://doi.org/10.1016/j.pecs.2012.03.004
107. Peters B (1999) Combust Flame 116(1-2):297. https://doi.org/10.1016/S0010-2180(98)00048-0
108. Thiele EW (1939) Eng Ind Chem 31(7):916. https://doi.org/10.1021/ie50355a027
109. Miltner M, Makaruk A, Harasek M, Friedl A (2006) In: Witt PJ, Schwarz MP (eds) Proceedings of the 5th international conference on computational fluid dynamics in the process industries. CSIRO Australia, Clayton, pp 1–6
110. Bruch C, Peters B, Nussbaumer T (2003) Fuel 82(6):729. https://doi.org/10.1016/S0016-2361(02)00296-X
111. Huttunen M, Kjäldman L, Saastamoinen J (2004) IFRF combustion journal (article number 200401)
112. Galgano A, Di Blasi C, Horvat A, Sinai Y (2006) Energy Fuels 20(5):2223. https://doi.org/10.1021/ef060042u
113. Arthur JR (1951) Trans Faraday Soc 47:164. https://doi.org/10.1039/tf9514700164
114. Pedersen K (2003) The product ratio of CO/CO_2 in the oxidation of biomass char. Master thesis Technical University of Denmark
115. Anca-Couce A, Sommersacher P, Shiehnejadhesar A, Mehrabian R, Hochenauer C, Scharler R (2017) Energy Procedia 120:238. https://doi.org/10.1016/j.egypro.2017.07.170
116. Collazo J, Porteiro J, Patiño D, Granada E (2012) Fuel 93:149. https://doi.org/10.1016/j.fuel.2011.09.044
117. Ryan JS, Hallett WLH (2002) Chem Eng Sci 57(18):3873. https://doi.org/10.1016/S0009-2509(02)00235-X
118. Yang YB, Goh YR, Zakaria R, Nasserzadeh V, Swithenbank J (2002) Waste Manage 22(4):369. https://doi.org/10.1016/S0956-053X(02)00019-3
119. Thunman H, Leckner B (2002) Proc Combust Inst 29(1):511. https://doi.org/10.1016/S1540-7489(02)80066-9
120. Di Blasi C (1993) Combust Sci Technol 90(5):315. https://doi.org/10.1080/00102209308907620
121. Girgis E, Hallett WLH (2010) Energy Fuels 24(3):1584. https://doi.org/10.1021/ef901206d
122. Mahmoudi AH, Besseron X, Hoffmann F, Markovic M, Peters B (2016) Chem Eng Sci 142:32. https://doi.org/10.1016/j.ces.2015.11.015
123. Yang Y, Ryu C, Khor A, Yates N, Sharifi V, Swithenbank J (2005) Fuel 84(16):2116. https://doi.org/10.1016/j.fuel.2005.04.023
124. Yang YB, Newman R, Sharifi V, Swithenbank J, Ariss J (2007) Fuel 86(1-2):129. https://doi.org/10.1016/j.fuel.2006.06.023
125. Yang YB, Sharifi VN, Swithenbank J (2007) Waste Manage 27(5):645. https://doi.org/10.1016/j.wasman.2006.03.014
126. Bryden KM, Ragland KW (1996) Energy Fuels 10(2):269. https://doi.org/10.1021/ef950193p
127. Johansson R, Thunman H, Leckner B (2007) Energy Fuels 21(3):1493. https://doi.org/10.1021/ef060500z
128. Yang YB, Sharifi VN, Swithenbank J (2005) Process Saf Environ Prot 83(6):549. https://doi.org/10.1205/psep.04284
129. Hermansson S, Thunman H (2011) Combust Flame 158(5):988. https://doi.org/10.1016/j.combustflame.2011.01.022
130. Ström H., Thunman H (2013) Combust Flame 160(2):417. https://doi.org/10.1016/j.combustflame.2012.10.005
131. Simsek E, Brosch B, Wirtz S, Scherer V, Krüll F (2009) Powder Technol 193(3):266. https://doi.org/10.1016/10.1016/j.powtec.2009.03.011
132. Gómez MA, Porteiro J, Patiño D, Míguez JL (2014) Fuel 117:716. https://doi.org/10.1016/j.fuel.2013.08.078
133. Gómez MA, Porteiro J, Patiño D, Míguez JL (2015) Energy Convers Manage 105:30. https://doi.org/10.1016/j.enconman.2015.07.059
134. Gómez MA, Porteiro J, de La Cuesta D, Patiño D, Míguez JL (2016) Fuel 184:987. https://doi.org/10.1016/j.fuel.2015.11.082
135. Miljković B, Pešenjanski I, Vićević M (2013) Fuel 104:351. https://doi.org/10.1016/j.fuel.2012.08.017
136. Duffy NT, Eaton JA (2013) Combust Flame 160(10):2204. https://doi.org/10.1016/j.combustflame.2013.04.015
137. Yang YB, Nasserzadeh V, Goodfellow J, Swithenbank J (2003) Chem Eng Res Des 81(2):221. https://doi.org/10.1205/026387603762878683
138. Shiehnejadhesar A, Scharler R, Mehrabian R, Obernberger I (2015) Fuel Process Technol 139:142. https://doi.org/10.1016/j.fuproc.2015.07.029
139. Yang YB, Lim CN, Goodfellow J, Sharifi VN, Swithenbank J (2005) Fuel 84(2-3):213. https://doi.org/10.1016/j.fuel.2004.09.002
140. Peters B, Džiugys A, Hunsinger H, Krebs L (2005) Chem Eng Sci 60(6):1649. https://doi.org/10.1016/j.ces.2004.11.004

141. Gómez MA, Porteiro J, Patiño D, Míguez JL (2015) Energy Convers Manage 101:666. https://doi.org/10.1016/j.enconman.2015.06.003
142. Gómez MA, Porteiro J, de La Cuesta D, Patiño D, Míguez JL (2017) Energy Convers Manage 140:260. https://doi.org/10.1016/j.enconman.2017.03.006
143. Blander M, Milne TA, Dayton DC, Backman R, Blake D, Kühnel V, Linak W, Nordin A, Ljung A (2001) Energy Fuels 15(2):344. https://doi.org/10.1021/ef0001181
144. Nutalapati D, Gupta R, Moghtaderi B, Wall TF (2007) Fuel Process Technol 88(11-12):1044. https://doi.org/10.1016/j.fuproc.2007.06.022
145. Lindberg D, Backman R, Chartrand P, Hupa M (2013) Fuel Process Technol 105:129. https://doi.org/10.1016/j.fuproc.2011.08.008
146. Brunner T, Jöller M, Obernberger I, Frandsen FJ (2002) In: 12th European conference and technology exhibition on biomass for energy industry and climate projection
147. Aspen Technology Inc Chemical process optimization software - chemical process design – aspen plus. http://www.aspentech.com/products/engineering/aspen-plus/
148. Bale CW, Bélisle E, Chartrand P, Decterov SA, Eriksson G, Gheribi AE, Hack K, Jung IH, Kang YB, Melançon J, Pelton AD, Petersen S, Robelin C, Sangster J, Spencer P, Van Ende MA (2016) Calphad 54:35. https://doi.org/10.1016/j.calphad.2016.05.002
149. Ross AB, Jones JM, Chaiklangmuang S, Pourkashanian M, Williams A, Kubica K, Andersson JT, Kerst M, Danihelka P, Bartle KD (2002) Fuel 81(5):571. https://doi.org/10.1016/S0016-2361(01)00157-0
150. Salzmann R, Nussbaumer T (2001) Energy Fuels 15(3):575. https://doi.org/10.1021/ef0001383
151. Glarborg P, Jensen AD, Johnsson JE (2003) Prog Energy Combust Sci 29(2):89. https://doi.org/10.1016/S0360-1285(02)00031-X
152. Anca-Couce A, Sommersacher P, Evic N, Mehrabian R, Scharler R (2018) Fuel 222:529. https://doi.org/10.1016/j.fuel.2018.03.003
153. Yang YB, Sharifi VN, Swithenbank J, Ma L, Darvell LI, Jones JM, Pourkashanian M, Williams A (2008) Energy Fuels 22(1):306. https://doi.org/10.1021/ef700305r
154. Haberle I, Skreiberg Ø, Łazar J, Haugen NEL (2017) Prog Energy Combust Sci 63:204. https://doi.org/10.1016/j.pecs.2017.07.004
155. Lu H, Robert W, Peirce G, Ripa B, Baxter LL (2008) Energy Fuels 22(4):2826. https://doi.org/10.1021/ef800006z
156. Ström H, Thunman H (2013) Appl Energy. https://doi.org/10.1016/j.apenergy.2012.12.057
157. Park WC, Atreya A, Baum HR (2010) Combust Flame 157(3):481. https://doi.org/10.1016/j.combustflame.2009.10.006
158. Di Blasi C (2002) AIChE J 48(10):2386. https://doi.org/10.1002/aic.690481028
159. Park W (2008) A study of pyrolysis of charring materials and its application to fire safety and biomass utilization in mechanical engineering. Ph.D. thesis, University of Michigan, Ann Arbor
160. Capart R, Khezami L, Burnham AK (2004) Thermochim Acta 417(1):79. https://doi.org/10.1016/j.tca.2004.01.029
161. Várhegyi G, Antal MJ, Szekely T, Szabó P (1989) Energy Fuels 3(3):329. https://doi.org/10.1021/ef00015a012
162. Chan RWC, Krieger BB (1981) J Appl Polym Sci 26(5):1533. https://doi.org/10.1002/app.1981.070260510
163. Kilzer JF, Broido A (1965) Pyrodynamics 2:151
164. Bennadji H, Smith K, Shabangu S, Fisher EM (2013) Energy Fuels 27(3):1453. https://doi.org/10.1021/ef400079a
165. Gauthier G, Melkior T, Grateau M, Thiery S, Salvador S (2013) J Anal Appl Pyrolysis 104:521. https://doi.org/10.1016/j.jaap.2013.05.017
166. Norinaga K, Shoji T, Kudo S, Hayashi JI (2013) Fuel 103:141. https://doi.org/10.1016/j.fuel.2011.07.045
167. Anca-Couce A, Sommersacher P, Scharler R (2017) J Anal Appl Pyrol 127:411. https://doi.org/10.1016/j.jaap.2017.07.008
168. Di Blasi C, Branca C, Santoro A, Gonzalez Hernandez E (2001) Combust Flame 124(1-2):165. https://doi.org/10.1016/S0010-2180(00)00191-7
169. Adánez J, Gayán P, de Diego LF, García-Labiano F, Abad A (2003) Ind Eng Chem Res 42(5):987. https://doi.org/10.1021/ie020605z
170. Thunman H, Niklasson F, Johnsson F, Leckner B (2001) Energy Fuels 15(6):1488. https://doi.org/10.1021/ef010097q
171. Prakash N, Karunanithi T (2009) Asian J Sci Res 2(1):1. https://doi.org/10.3923/ajsr.2009.1.27
172. Scharler R (2001) Entwicklung und Optimierung von BIomasse-Rostfeuerungen durch CFD-Analyse. Ph.D. thesis Graz, University of Technology
173. Scharler R, Obernberger I (2000) In: Reis A (ed) Industrial furnaces and boilers, pp 1–17. INFUB, Rio Tinto, Portugal
174. Buchmayr M, Gruber J, Hargassner M, Hochenauer C (2016) Energy Convers Manage 115:32. https://doi.org/10.1016/j.enconman.2016.02.038
175. Buchmayr M, Gruber J, Hargassner M, Hochenauer C (2016) Biomass Bioenergy 95:146. https://doi.org/10.1016/j.biombioe.2016.10.004
176. Lee DH, Yang H, Yan R, Liang DT (2007) Fuel 86(3):410. https://doi.org/10.1016/j.fuel.2006.07.020
177. Paviet F, Chazarenc F, Tazerout M (2009) Int J Chem React Eng, 7(1), https://doi.org/10.2202/1542-6580.2089
178. Nikoo MB, Mahinpey N (2008) Biomass Bioenergy 32(12):1245. https://doi.org/10.1016/j.biombioe.2008.02.020
179. Doherty W, Reynolds A, Kennedy D (2009) Biomass Bioenergy 33(9):1158. https://doi.org/10.1016/j.biombioe.2009.05.004
180. Galletti C, Giomo V, Giorgetti S, Leoni P, Tognotti L (2016) Appl Therm Eng 96:372. https://doi.org/10.1016/j.applthermaleng.2015.11.085
181. Fatehi M, Kaviany M (1994) Combust Flame 99(1):1. https://doi.org/10.1016/0010-2180(94)90078-7
182. Yang Y, Sharifi V, Swithenbank J (2004) Fuel 83(11-12):1553. https://doi.org/10.1016/j.fuel.2004.01.016
183. Menghini D, Marra FS (2008) In: 16th European Biomass Conference & Exhibition, pp 1407–1414
184. Bauer R, Gölles M, Brunner T, Dourdoumas N, Obernberger I (2010) Biomass Bioenergy 34(4):417. https://doi.org/10.1016/j.biombioe.2009.12.005
185. Ansys fluent theory guide, release 15.0. http://www.ansys.com
186. Ryu C, Shin D, Choi S (2002) J Air Waste Manage Assoc 52(2):189. https://doi.org/10.1080/10473289.2002.10470769
187. Yin C, Rosendahl L, Kær SK, Clausen S, Hvid SL, Hille T (2008) Energy Fuels 22(2):1380. https://doi.org/10.1021/ef700689r
188. van der Lans R, Pedersen LT, Jensen A, Glarborg P, Dam-Johansen K (2000) Biomass Bioenergy 19(3):199. https://doi.org/10.1016/S0961-9534(00)00033-7
189. Kær SK (2005) Biomass Bioenergy 28(3):307. https://doi.org/10.1016/j.biombioe.2004.08.017
190. Kær SK, Rosendahl L, Baxter L (2006) Fuel 85(5-6):833. https://doi.org/10.1016/j.fuel.2005.08.016
191. Hermansson S, Thunman H (2011) Energy Fuels 25(4):1387. https://doi.org/10.1021/ef101473b
192. Kær SK (2004) Fuel 83(9):1183. https://doi.org/10.1016/j.fuel.2003.12.003
193. Venturini P, Borello D, Iossa C, Lentini D, Rispoli F (2010) Energy 35(7):3008. https://doi.org/10.1016/j.energy.2010.03.038

194. Yu Z, Ma X, Liao Y (2010) Renew Energy 35(5):895. https://doi.org/10.1016/j.renene.2009.10.006
195. Borello D, Venturini P, Rispoli F, Rafael SG (2013) Appl Energy 101:413. https://doi.org/10.1016/j.apenergy.2012.04.031
196. Buczyński R., Weber R, Szlek A, Nosek R (2012) Energy Fuels 26(8):4767. https://doi.org/10.1021/ef300676r
197. Kær SK (2001) Numerical investigation of ash deposition in straw-fired boilers - using CFD as the framework for slagging and fouling predictions. Ph.D. thesis, Aalborg University, Denmark
198. Thunman H, Leckner B (2005) Proc Combust Inst 30(2):2939. https://doi.org/10.1016/j.proci.2004.07.010
199. Peters B, Bruch C (2001) Chemosphere 42(5-7):481. https://doi.org/10.1016/S0045-6535(00)00220-4
200. Saidi MS, Hajaligol MR, Mhaisekar A, Subbiah M (2007) Appl Math Model 31(9):1970. https://doi.org/10.1016/j.apm.2006.08.003
201. Hettel M, Seidelt S, Haußmann M, Bockhorn H (2011) In: 25. Deutscher Flammentag, VDI-Berichte, vol 2119 (VDI-Verl., Düsseldorf), pp 87–93. VDI-Berichte
202. Kurz D, Schnell U, Scheffknecht G (2012) Combust Theor Model 16(2):251. https://doi.org/10.1080/13647830.2011.610903
203. Kurz D, Schnell U, Scheffknecht G (2011) In: 25. Deutscher Flammentag, VDI-berichte, vol 2119 (VDI-verl., Düsseldorf), pp 183–188. VDI-Berichte
204. Bruch C (2001) Beitrag zur Modellierung der Festbettverbrennung in automatischen Holzfeuerungen. Ph.D. thesis ETH Zürich
205. Mehrabian R, Scharler R, Weissinger A, Obernberger I (2010) In: Proceedings of the 18th European biomass conference & exhibition, ed. by ETA-renewable energies (Italy)
206. Peters B, Džiugys A, Navakas R (2010) In: Modern building materials, structures and techniniques
207. Peters B (2011) In: 25. Deutscher Flammentag, VDI-Berichte, vol 2119 (VDI-Verl., Düsseldorf), pp 147–152. VDI-Berichte
208. Brosch B, Wirtz S, Scherer V, Waldner MH (2011) In: 25. Deutscher Flammentag, VDI-Berichte, vol 2119 (VDI-Verl., Düsseldorf), pp 159–166. VDI-Berichte
209. Peters B, Besseron X, Estupinan A, Hoffmann F, Michael M, Mahmoudi A (2014) Industrial combustion (Article Number 201402)
210. Miltner M, Miltner A, Harasek M, Friedl A (2007) Appl Therm Eng 27(7):1138. https://doi.org/10.1016/j.applthermaleng.2006.02.048
211. Collazo J, Porteiro J, Míguez JL, Granada E, Gómez MA (2012) Energy Convers Manage 64:87. https://doi.org/10.1016/j.enconman.2012.05.020
212. Buczyński R, Weber R, Szlek A (2015) J Energy Inst 88(1):53. https://doi.org/10.1016/j.joei.2014.04.006
213. Poinsot T, Veynante D (2001) Theoretical and numerical combustion. Edwards, Philadelphia, PA
214. Trisjono P, Pitsch H (2015) Flow, Turbul Combust 95(2-3):231. https://doi.org/10.1007/s10494-015-9645-x
215. Gicquel L, Staffelbach G, Poinsot T (2012) Prog Energy Combust Sci 38(6):782. https://doi.org/10.1016/j.pecs.2012.04.004
216. Ma L, Roekaerts D (2016) Combust Flame 165:402. https://doi.org/10.1016/j.combustflame.2015.12.025
217. Jones W, Launder B (1972) Int J Heat Mass Transfer 15(2):301. https://doi.org/10.1016/0017-9310(72)90076-2
218. Shih TH, Liou WW, Shabbir A, Yang Z, Zhu J (1995) Comput Fluids 24(3):227. https://doi.org/10.1016/0045-7930(94)00032-T
219. Yakhot V, Orszag SA (1986) J Sci Comput 1(1):3. https://doi.org/10.1007/BF01061452
220. Yakhot V, Orszag SA, Thangam S, Gatski TB, Speziale CG (1992) Phys Fluids A 4(7):1510. https://doi.org/10.1063/1.858424
221. Han Z, Reitz RD (1995) Combust Sci Technol 106(4-6):267. https://doi.org/10.1080/00102209508907782
222. Patel VC, Rodi W, Scheuerer G (1985) AIAA J 23(9):1308. https://doi.org/10.2514/3.9086
223. Laurien E, Oertel H (2011) Numerische Strömungsmechanik: Grundgleichungen und Modelle – Lösungsmethoden – Qualität und Genauigkeit, 4th edn. (Vieweg+Teubner Verlag / Springer Fachmedien Wiesbaden GmbH Wiesbaden, Wiesbaden). https://doi.org/10.1007/978-3-8348-8121-2
224. Knaus H, Richter S, Unterberger S, Schnell U, Maier H, Hein K (2000) Exp Thermal Fluid Sci 21(1-3):99. https://doi.org/10.1016/S0894-1777(99)00059-X
225. Farokhi M, Birouk M, Tabet F (2017) Energy Convers Manage 143:203. https://doi.org/10.1016/j.enconman.2017.03.086
226. Magnussen BF, Hjertager BH (1977) Symp (Int) Combust 16(1):719. https://doi.org/10.1016/S0082-0784(77)80366-4
227. Magnussen BF (1981) In: Aerospace sciences meetings, ed by AIAA American institute of aeronautics and astronautics, https://doi.org/10.2514/6.1981-42
228. Pope SB (1997) Combust Theory Modell 1(1):41. https://doi.org/10.1088/1364-7830/1/1/006
229. Shiehnejadhesar A, Mehrabian R, Scharler R, Goldin GM, Obernberger I (2014) Fuel 126:177. https://doi.org/10.1016/j.fuel.2014.02.040. http://linkinghub.elsevier.com/retrieve/pii/S0016236114001793
230. Veynante D, Vervisch L (2002) Prog Energy Combust Sci 28(3):193. https://doi.org/10.1016/S0360-1285(01)00017-X
231. Peters N (1986) In: 21st Symposuim (international) on combustion, vol 21, ed. by Combustion Institute, vol 21, pp 1231–1250
232. Kim S, Shin D, Choi S (1996) Combust Flame 106(3):241. https://doi.org/10.1016/0010-2180(95)00190-5
233. Tabet F, Fichet V, Plion P (2016) J Energy Inst 89(2):199. https://doi.org/10.1016/j.joei.2015.02.003
234. Yin C, Rosendahl LA, Clausen S, Hvid SL (2012) Energy 41(1):473. https://doi.org/10.1016/j.energy.2012.02.050
235. Westbrook CK, Dryer FL (1981) Combust Sci Technol 27(1-2):31. https://doi.org/10.1080/00102208108946970
236. Jones WP, Lindstedt RP (1988) Combust Flame 73(3):233. https://doi.org/10.1016/0010-2180(88)90021-1
237. Athanasios N, Nikolaos N, Nikolaos M, Panagiotis G, Kakaras E (2015) Fuel Process Technol 137:75. https://doi.org/10.1016/j.fuproc.2015.04.010
238. Yin C, Kær SK, Rosendahl L, Hvid SL (2010) Bioresour Technol 101(11):4169. https://doi.org/10.1016/j.biortech.2010.01.018
239. Smith GP, Golden DM, Frenklach M, Moriarty NW, Eiteneer B, Goldenberg M, Bowman CT, Hanson R, Song S, Gardiner WC, Lissianski V, Qin Z GRI-Mech 3.0. http://www.me.berkeley.edu/gri-mech/
240. Skreiberg Ø, Kilpinen P, Glarborg P (2004) Combust Flame 136(4):501. https://doi.org/10.1016/j.combustflame.2003.12.008
241. Løvås T, Houshfar E, Bugge M, Skreiberg Ø (2013) Energy Fuels 27(11):6979. https://doi.org/10.1021/ef400949h
242. Zahirović S, Scharler R, Kilpinen P, Obernberger I (2011) Combust Theory Modell 15(5):645. https://doi.org/10.1080/13647830.2011.557441
243. Debiagi PEA, Gentile G, Pelucchi M, Frassoldati A, Cuoci A, Faravelli T, Ranzi E (2016) Biomass Bioenergy 93:60. https://doi.org/10.1016/j.biombioe.2016.06.015
244. Marinov NM, Pitz WJ, Westbrook CK, Vincitore AM, Castaldi MJ, Senkan SM, Melius CF (1998) Combust Flame 114(1-2):192. https://doi.org/10.1016/S0010-2180(97)00275-7
245. Richter H, Howard JB (2002) Phys Chem Chem Phys 4(11):2038. https://doi.org/10.1039/b110089k

246. Chandrasekhar S (1960) Radiative transfer, dover ed., 1. publ. in 1960, an unabridged and slightly rev. version of the work orig. publ. 1950 edn. Dover Publications, New York
247. Klason T, Bai XS, Bahador M, Nilsson TK, Sundén B (2008) Fuel 87(10-11):2141. https://doi.org/10.1016/j.fuel.2007.11.016
248. Modest MF (2013) Radiative heat transfer, 3rd. Academic Press, New York. http://site.ebrary.com/lib/alltitles/docDetail.action?docID=10661889
249. Williams A, Jones JM, Ma L, Pourkashanian M (2012) Prog Energy Combust Sci 38(2):113. https://doi.org/10.1016/j.pecs.2011.10.001. http://linkinghub.elsevier.com/retrieve/pii/S0360128511000530
250. Zhou H, Jensen A, Glarborg P, Kavaliauskas A (2006) Fuel 85(5-6):705. https://doi.org/10.1016/j.fuel.2005.08.038
251. Glarborg P, Miller JA, Ruscic B, Klippenstein SJ (2018) Prog Energy Combust Sci 67:31. https://doi.org/10.1016/j.pecs.2018.01.002
252. Zahirović S, Scharler R, Kilpinen P, Obernberger I (2010) Combust Theory Modell 15(1):61. https://doi.org/10.1080/13647830.2010.524312
253. Niu Y, Tan H, Hui S (2016) Prog. Energy Combust. Sci 52:1. https://doi.org/10.1016/j.pecs.2015.09.003, http://linkinghub.elsevier.com/retrieve/pii/S0360128515300216
254. Jöller M, Brunner T, Obernberger I (2007) Fuel Process Technol 88(11-12):1136. https://doi.org/10.1016/j.fuproc.2007.06.013
255. Niu Y, Wang S, Shaddix CR, Hui S (2016) Combust Flame 173:195. https://doi.org/10.1016/j.combustflame.2016.08.021
256. Brookes S, Moss J (1999) Combust Flame 116(4):486. https://doi.org/10.1016/S0010-2180(98)00056-X
257. Schütz D (2012) Numerische simulation und messtechnische evaluierung der schadstoffemissionen aus stückholzfeuerungen. Ph.D. thesis, Universität Stuttgart. http://elib.uni-stuttgart.de/opus/volltexte/2012/7062/
258. Sènèchal U (2013) Holzverbrennung in Kaminöfen mit Keramikfilter - experimentelle Untersuchungen und mathematische Modellierung. Ph.D. thesis, TU Dresden
259. Djurović D, Nemoda S, Dakić D, Adzić M, Repić B (2012) Int J Heat Mass Transfer 55(15-16):4312. https://doi.org/10.1016/j.ijheatmasstransfer.2012.03.079
260. CRECK Modeling group. http://creckmodeling.chem.polimi.it
261. Klason T, Bai XS (2007) Fuel 86(10-11):1465. https://doi.org/10.1016/j.fuel.2006.11.022
262. Rezeau A, Ramírez JA, Díez LI, Royo J (2012) Comput Fluids 69:45. https://doi.org/10.1016/j.compfluid.2012.08.024
263. Bui-Pham M, Seshadri K (1991) Combust Sci Technol 79(4-6):293. https://doi.org/10.1080/00102209108951771